

THE UNIVERSITY OF MANITOBA

USE OF SINGLE-POLE AUTO-RECLOSURE ON EHV  
LONG DISTANCE AC TRANSMISSION LINES

by

JARNAIL SINGH

A THESIS

SUBMITTED TO THE FACULTY OF GRADUATE STUDIES  
IN PARTIAL FULFILMENT OF THE REQUIREMENTS FOR THE DEGREE OF  
MASTER OF SCIENCE

DEPARTMENT OF ELECTRICAL ENGINEERING

WINNIPEG, MANITOBA

JULY, 1979

USE OF SINGLE-POLE AUTO-RECLOSURE ON EHV  
LONG DISTANCE AC TRANSMISSION LINES

BY

JARNAIL SINGH

A dissertation submitted to the Faculty of Graduate Studies of  
the University of Manitoba in partial fulfillment of the requirements  
of the degree of

MASTER OF SCIENCE

✓  
© 1979

Permission has been granted to the LIBRARY OF THE UNIVER-  
SITY OF MANITOBA to lend or sell copies of this dissertation, to  
the NATIONAL LIBRARY OF CANADA to microfilm this  
dissertation and to lend or sell copies of the film, and UNIVERSITY  
MICROFILMS to publish an abstract of this dissertation.

The author reserves other publication rights, and neither the  
dissertation nor extensive extracts from it may be printed or other-  
wise reproduced without the author's written permission.



- To my wife NARINDER -

ABSTRACT

Most faults on transmission lines are single line to ground (SL-G). For such faults single-pole reclosing would result in an improvement of transient stability over the alternative of three-pole reclosing. The arcing faults which are maintained by the capacitive coupling from the other two energized conductors, tend to sustain current in the original fault arc path, thereby lengthening the time required for arc deionization. An increase in dead time is, therefore, required which decreases the net improvement. A promising remedy consists of neutralizing the capacitive coupling by shunt reactors, which are, generally, required on EHV lines for compensation of normal charging current. This thesis presents different compensation schemes, for transposed and untransposed lines, to reduce dead time following single-pole switching. A number of system parameters of representative magnitudes are considered and their influence on the effectiveness of these schemes is investigated.

ACKNOWLEDGEMENTS

*The author would like to express his deepest gratitude to his supervisor, Professor M.Z. Tarnawecy, for his esteemed guidance in the preparation of this thesis, as well as his encouragement throughout the period of coursework.*

*A very special word of thanks is reserved for Dr. R.M. Mathur for his contagious enthusiasm as a scholar and educator. The author has benefited immensely from his association with Dr. Mathur and will appreciate such a relationship for many years to come.*

*Appreciation is also expressed to Dr. V. Balarama Murty, visiting Scientist with the Department of Electrical Engineering, University of Manitoba, and N.S. Dhaliwal, Senior Plant Engineer, Manitoba Hydro, for their valuable guidance and assistance in every possible way.*

*Special appreciation is due to Mrs. Valerie Ring for her untiring effort in expertly typing the manuscript.*

TABLE OF CONTENTS

	PAGE
ABSTRACT	i
ACKNOWLEDGEMENTS	ii
NOMENCLATURE	vi
DEFINITION OF TERMS	x
LIST OF FIGURES	xii
CHAPTER	
I    INTRODUCTION	1
1.1    High Speed Auto-Reclosing	1
1.2    Extinction of Secondary Arc Current	3
1.3    Intent of Investigation	5
II   METHODS OF COMPENSATION	7
2.1    The Basic Problem	7
2.2    Inductive Method of Reducing Capacitive Coupling Effect	11
2.2.1    Recovery Voltage	14
2.2.2    Secondary Arc Current	14
2.3    Capacitance Method of Reducing Capacitive Coupling Effect	15
2.4    The Method of Using Discharge Resistors	17
III  REPRESENTATION OF TRANSMISSION LINES	20
3.1    System Representation	20
3.2    Representation of Transposed Lines	23
3.2.a    3-Phase Representation	23
3.2.b    Representation by Components	23
3.2.c    Conditions for Component Network Interconnections	24
3.3.2    Line to Ground Fault Through a Resistance R	26
3.3    Use of Simple Four-Legged Reactors	28
3.4    Use of Capacitors	28
3.5    Methods of Solution	31
3.5.1    Mesh Analysis	32
3.5.2    Two-Port Network Analysis	34

CHAPTER	PAGE	
3.6	Modification of the Basic Circuit	38
3.6.1	Shunt Reactor Connections at Line Ends	39
3.6.2	Shunt Reactor Connections at Mid Point	39
3.6.3	Connection of Discharge Resistors Between the Faulted Phase and Ground	39
3.6.4	Connection of Capacitors Across Circuit Breakers	41
3.7	Representation of Untransposed Lines	41
3.7.1	Modified Four-Legged Reactor Bank	41
3.7.2	System Equivalent	45
3.7.3	Useful Shunt Reactor Arrangements	48
3.8	Study on Digital Computer	50
IV	NUMERICAL ANALYSIS AND RESULTS	51
4.1	System Studied	51
4.2	Summary of Cases Studied - Base Case	52
4.3.1	Variation of $X_{OS}$ for Constant $X_{OS}$	67
4.3.2	Unequal Source Reactances at the Two ends	67
4.3.3	Variation of $r_o$ and $\frac{l_o}{l_1}$	69
4.4	Effect of Compensation Factor	74
4.5	Effect of Deviation from Optimum Values of Shunt Reactors - Sensitivity	74
4.6	Use of Discharge Resistors for Minimizing $V_{ff}$	78
4.7	Capacitance Method for Minimizing $V_{ff}$	81
V	DISCUSSION OF RESULTS	83
5.1	Threshold Level of Self-Sustaining Secondary Arc Current	83
5.2.1	Influence of Line Length	85
5.2.2	Influence of Power Angle	87
5.2.3	Influence of $X_1$ and $\frac{X_o}{X_1}$ Ratio	89
5.2.4	Influence of Ratio $\frac{V_S}{V_R}$	91

CHAPTER		PAGE
	5.2.5 Influence of Higher System Voltage	91
	5.2.6 Influence of Degree of Shunt Compensation	92
	5.3 Comparison of Shunt Compensation Methods for Both Transposed and Untransposed Lines	93
	5.4 Comparison of Shunt Reactor Methods with Other Methods	94
VI	CONCLUSIONS	96
	REFERENCES	101
	APPENDIX A	105
	APPENDIX B	109
	APPENDIX C	114



## NOMENCLATURE

Most of the symbols are explained in the text when these are used for the first time. Subscripts or superscripts have been used to identify the symbols with the appropriate quantities. For quick reference, a list of important symbols is given below. Units are converted to per unit values when applicable. For the voltage and currents, the capital letters represent the vectors and the corresponding small letters represent the magnitudes.

- $B_1, B_0$  - Positive and zero sequence capacitive susceptances of a transmission line.
- $B'_1, B'_0$  - Positive and zero sequence inductive susceptances of simple four-legged reactors.
- $B_g$  - Inductive susceptance of each grounded reactor of a 6-reactor scheme.
- $B_{ST}$  - Inductive susceptance of simple four-legged reactor bank (phase-to-neutral) for transposed lines.
- $B_{SNT}$  - Neutral susceptance of simple bank for transposed lines.
- $C_S, C_R$  - Capacitors connected across the breakers of the faulted phase at the sending and receiving ends.
- $E_{HV}$  - Extra high voltage - above 230 KV.
- $E_{QS}, E_{QR}$  - Sending and receiving end source voltages.
- $F$  - Degree of shunt compensation.
- $I, i$  - Healthy phase currents (at the middle of line).
- $I_a$  - Average load current through the healthy phases.

- $I_C$  - Capacitive component of  $I_f$ .
- $I_f$  - Secondary arc current.
- $I_\ell$  - Inductive component of  $I_f$ .
- $L$  - Line length.
- $P$  - Power flow.
- $Q_{RST}$  - Total MVAR capacity of the simple reactors for a transposed line.
- $Q_{RSU}, Q_{RMU}$  - Total MVAR capacity of simple and modified four-legged reactors for an untransposed line.
- $R_1, L_1, C_1$  - Positive sequence resistance, inductance and capacitance of the transmission line for a given length.
- $R_0, L_0, C_0$  - Zero sequence resistance, inductance and capacitance of the transmission line for a given length.
- (Note: Per km magnitudes of the above quantities are represented by small case letters, viz.,  $r_1, \ell_1$ , etc.)
- $R_{FS}, R_{FR}$  - Discharge resistors at sending and receiving ends.
- $V, v$  - Healthy phase voltages (in the middle of the line).
- $V_{ff}$  - Recovery voltage on opened phase at fault location.
- $V_S, V_R$  - Voltages at the line terminals.
- $V_{SNT}$  - Neutral voltage for simple four-legged reactor for transposed line.
- $V_{SNU}, V_{MNU}$  - Neutral voltages for simple and modified four-legged reactors, for untransposed lines.
- $X_{\alpha S}, X_{\alpha R}$  -  $\alpha$  component source reactance at sending and receiving ends.
- $X_{0S}, X_{0R}$  - 0 component source reactance at sending and receiving ends.
- (Note: Sometimes 'source  $X_1$ ' and 'Source  $X_0$ ' have been used in place of  $X_{\alpha S}, X_{\alpha R}$  and  $X_{0S}, X_{0R}$  respectively).

- $X_{h,k}$  - Total line inter-phase mutual reactances between the healthy phases.
- $X_M$  - Modified reactor bank reactance.
- $X_{ST}$  - Shunt reactance of simple four-legged reactor banks (phase-to-neutral) for a transposed line.
- $X_{SU}, X_{MU}$  - Shunt reactances of simple and modified banks (phase-to-neutral) for an untransposed line.
- $X_{SNT}$  - Neutral reactance of the simple bank for a transposed line.
- $X_{SNU}, X_{MNU}$  - Neutral reactances of the simple and modified banks for an untransposed line.
- $Y_M, Y_{MN}$  - Modified shunt and neutral reactor admittances.
- $Y_C$  - Line capacitive admittance.
- $Y_{ST}$  - Shunt reactor admittance of simple bank (phase-to-neutral) for a transposed line.
- $Y_{SU}, Y_{MU}$  - Shunt reactor admittances of the simple and modified banks (phase-to-neutral) for an untransposed line.
- $Y_{SNT}$  - Neutral reactor admittance of simple bank for a transposed line.
- $Y_{SNU}, Y_{MNU}$  - Neutral reactor admittances of simple and modified banks for an untransposed line.
- $Z_{tf}$  - Thevenin impedance of the system as seen from the fault terminals.
- $\alpha$  - Phase angle difference between the current and the voltage in the middle of a line.
- $\beta$  - Phase angle of a healthy phase voltage at the middle of a line.
- $\gamma$  - Phase angle of a healthy phase current at the middle of the line.

$\delta$  - Phase angle difference between  $V_S$  and  $V_R$ .

**SUPERSCRIPTS**

*a* - Average value.

*i* - Faulted phase

*h,k* - Healthy phases.

*g* - Ground.

## DEFINITION OF TERMS

The following terms are specifically defined for use throughout the thesis:

- Power System - An electric power transmission network comprising ac and dc transmission lines, generators, and loads.
- Tie Line - Any interconnecting transmission line between the two power systems.
- Stability - The ability of power system or interconnected power systems to maintain synchronism.
- Power Angle - Phase angle between ac voltage vectors at each end of an ac transmission line.
- Transient Stability - The ability of power systems at each end of an ac tie-line to maintain synchronism through the first power angle swing across the tie-line following a major system disturbance.
- Auto-Reclosure - Circuit breaker with auto-reclose device that opens following a temporary fault and then recloses after the dead time.
- Dead Time - Time interval between the opening and reclosing of the circuit breaker.
- Single-Pole Auto-Reclosing - Following a single line to ground fault (SL-G), the only pole of the circuit breaker in the faulty phase opens, and then recloses after the dead time.

Recovery Voltage

- The power frequency-phase-earth voltage of the switched phase at the location of the fault subsequent to the extinction of the secondary arc.

Secondary Arc Current

- The power frequency current which would flow in the residual fault path of the switched phase following SL-G faults.

LIST OF FIGURES

FIGURE		PAGE
2.1	Basic System	8
2.2	Basic System - Transmission Line in Lumped System	8
2.3	Equivalent Circuit for Basic System	9
2.4	Possible Connections of Shunt Reactors	12
2.5	Equivalent Circuit for Shunt Reactor Method	12
2.6	Equivalent Circuit for the Capacitance Method	16
2.7	Equivalent Circuit for Discharge Resistance Method	18
2.8	Sequence of the Line Breaker and Discharge Resistance Switching	18
3.1	Single-Line Representation of the System	21
3.2	3-Phase Representation of the System	21
3.3	$\alpha$ , $\beta$ , 0 Component Representation of Single-Pole Switching	22
3.4.1	Open Breaker	25
3.4.2	Interconnection of Component Networks	25
3.5.1	Line to Ground Fault Through Resistance R	27
3.5.2	Interconnection of Component Networks	27
3.6.1	3-Phase Representation of the System Using Simple Four-Legged Reactors	29
3.6.2	Simple Four-Legged Reactor Bank	29
3.7.1	3-Phase Representation of the System Using Capacitors	30
3.7.2	Open Breaker - Actual Interconnection of Component Networks	30
3.8	Mesh Analysis	33

FIGURE	PAGE
3.9 Two-Port Network	35
3.10 Actual Interconnection	35
3.11 Simplified Circuit of Fig. 3.10 - Using Principle of Superposition	37
3.12 Simplified Circuit of Fig. 3.11	37
3.13 Shunt Reactors at the End of the Line	40
3.14 Shunt Reactors at the Line Mid-Point	40
3.15 Modified Four-Legged Reactor Bank	42
3.16 A System Diagram with a Simple and a Modified Four-Legged Shunt Reactor Bank	44
3.17 System Equivalent and Vector Diagrams for an Untransposed Transmission Line	46
3.18 Shunt Reactor Arrangement on Untransposed Transmission Lines	49
4.1.1 Base Case; $V_{ff}$ As a Function of Fault Location	55
4.1.2 Profile of $V_{ff}$ for Two Values of Source $X_1$	56
4.1.3 Effect of source $X_1$ Variation	57
4.1.4 Profile of $V_{ff}$ for Two Values of Source $X_o/X_1$	58
4.1.5 Effect of Source $X_o/X_1$	59
4.1.6 Profile of $V_{ff}$ for Two Values of $\frac{V_S}{V_R}$	60
4.1.7 Effect of Variation of $\frac{V_S}{V_R}$	61
4.1.8 Profile of $V_{ff}$ for two Values of $\delta$	62
4.1.9 Effect of Variation of $\delta$	63
4.1.10 Profile of $V_{ff}$ for Two Values of Line Length	64
4.1.11 Effect of Variation of Line Length for Same Initial Loading	65
4.1.12 Effect of Variation of Line Length for Same Initial $\delta$	66



FIGURE	PAGE
4.2.1 Effect of Source $X_1$ Variation (Constant Source $X_0$ )	68
4.2.2 Effect of Unequal Source Reactances at the Two Ends - Case 2.2	70
4.2.3 Effect of Unequal Source Reactances at the Two Ends - Case 2.3	71
4.2.4 Profile of $V_{ff}$ - Two Values of $\frac{r_0}{r_1}$ Ratio	72
4.2.5 Profile of $V_{ff}$ - Two Values of Line $\frac{l_0}{l_1}$ Ratio	73
4.3.1 Maximum Value of Secondary Arc Current Versus Compensation Factor	75
4.3.2 Effect of Variation of the Degree of KVAR Compensation on Recovery Voltage	76
4.3.3 Effect of Compensation on Neutral Voltages	77
4.4 Sensitivity of the Optimum Values of the Shunt Reactors	79
4.5.1 Profile of $V_{ff}$ - Discharge Resistance Method	80
4.5.2 Effect of Variation of Discharge Resistance Magnitudes	80
4.6.1 Profile of $V_{ff}$ - Capacitance Method	82
4.6.2 Effect of Variation of Line Length for the Same Initial Loading	82
5.1 Profile of $V_{ff}$ - Base Case	84
5.2 A $\pi$ Section of the Transmission Line Model	88
A.1 Interconnection of $\alpha$ and 0 Component Networks	106
A.2 $\beta$ Component Representation	106

## CHAPTER I

### INTRODUCTION

#### 1.1 HIGH SPEED AUTO-RECLOSING

Application of high speed reclosing in High Voltage Transmission systems for the purpose of improving transient stability is well known and has been reported in technical literature since 1937.<sup>1,2,3</sup> These papers were concerned with experiences of some of the utilities in applications of high speed reclosing, and therefore were not of a general nature. Crary, et al<sup>4</sup>, carried out a detailed study of high speed reclosing as a means of improving transient stability, considering a number of variables, e.g., line length, source characteristics, time interval before reclosing, etc. This study was made on an A.C. Network Analyser and considered typical (those that were ordinarily obtained in a power system) values of variables mentioned above. This gave a reasonably complete picture of high speed reclosing and its merits.

In the above-mentioned study, the 'dead' time (the time interval between the opening and reclosing of the breaker contacts) was varied over a range of values, mindful of the fact that under practical conditions, arc deionization time could vary over a wide range. It was observed that for equal duration of arc deionization time, single-phase reclosing increased the stability limit by 50 percent over that of 3-phase reclosing. On the other hand, if the arc deionization time for the

single-phase case was assumed to be 50 percent longer than that required for the 3-phase case, then the increase in the stability limit is only 35 percent. Peterson<sup>5</sup> explained that the de-energized phase, in the case of single-phase reclosing, is capacitively coupled to the energized phases.

An IEEE working group has reviewed available technical literature, and has prepared an exhaustive bibliography on the subject of arc deionization time, as it affects the 'dead' time in high speed reclosing. In conclusion, the working group among other things, observed that arc deionization time is affected by the following factors:

- 1) Magnitude and duration of fault current.
- 2) Magnitude and duration of capacitive and magnetic coupling current which may flow due to induced voltage from adjacent unfaulted conductor that remains energized. This current is proportional to both length and voltage of the line.

The above work shows a particular importance for single-pole reclosing. It has also significance for 3-pole reclosing of 1 circuit on a double circuit line. At the present state of the art, high speed relaying and 2 cycle breakers can keep the fault current duration to a low value. If a way can be found to eliminate or substantially reduce the capacitive and magnetic coupling, as mentioned above, with the attendant reduction of 'dead' time, then high speed, automatic, single-pole reclosing can result in increased power limits. This is especially true because single-line to ground, non-permanent

faults cause most of the breaker operations (as high as 90 percent depending on the geographic conditions).

## 1.2 EXTINCTION OF THE SECONDARY ARC

Subsequent to a single-line to ground fault and to the opening of circuit breaker poles associated with the faulted phase, the fault arc is no longer supported by direct metallic contact with the system. Instead, it is supported by capacitive and magnetic coupling from the two unfaulted phases, which are still energized at approximately normal circuit voltage and carrying load current. This arc is known as the secondary arc, and the current through it as the Secondary Arc Current. The coupling has led to the consideration of two factors which are of great importance for arc extinction, namely,

- 1) The magnitude and rate of rise of recovery voltage.
- 2) The magnitude of the current to be interrupted, i.e., the current in the secondary arc.

The extinction of secondary arc depends on its current, recovery voltage, length of arc path and wind velocity, etc. Recovery voltage and length of arc path both increase with the circuit voltage level. Here again, the healthy phases determine the restriking voltage transient and recovery voltage. These, together with the dielectric properties of the residual fault path, will resolve whether a further restrike may take place.

The secondary arc is important if single-phase switching is to be utilized, since successful reclosing of the open phase cannot occur until the secondary arc is extinguished. The secondary arc is understood to be inherently unstable; that is, if given sufficient time the arc will extinguish itself. The time necessary for the arc self extinction, is a function of secondary arc current, and it is desirable to minimize its magnitude thus reducing the dead time and increasing the probability of a successful reclosure.

Capacitive coupling is important, regardless of line length and pre-fault loading (line loading prior to fault and switching operations). Its importance increases with the increase of circuit voltage. Inductive coupling is sensitive to both the line length and loading. Various methods have been proposed to minimize the magnitude of secondary arc current and recovery voltage. Knudsen<sup>8</sup> and Kimbark<sup>9</sup> proposed a four-legged reactor scheme for transposed lines. The four-legged reactor scheme consists of phase reactors connected between each phase and a neutral point, and a neutral reactor connected between the neutral point and ground. This scheme effectively compensates the capacitive coupling between the energized and de-energized phases, but has less effect on the inductive coupling.

The simple four-legged reactor scheme, as discussed above, will not sufficiently reduce the secondary arc current on long untransposed lines because of unequal interphase

capacitances. For these lines a modified four-legged reactor scheme has been suggested by Shperling, et al<sup>10</sup>. This scheme at one end, in conjunction with a conventional four-legged reactor at the other end, effectively compensates the capacitive coupling between the faulted and the two healthy phases of the long untransposed transmission line.

Peterson, et al<sup>11</sup> has suggested, for nullifying the capacitive coupling, a capacitor to be connected across terminals of each breaker pole, proportional to the particular line. Jahn, et al<sup>12</sup>, has shown that the use of ACSR ground wires can help reduce magnetic coupling. Forced extinction of the secondary arc by shunting with jets of a conducting salt solution ( $\text{NH}_4\text{Cl}$ ), was tried on a French 220 KV system and is described by Miller, et al<sup>13</sup>. A modification of the above idea, where discharge resistors are connected through switches at the two ends of the faulted conductor, has also been suggested. Heinemann<sup>14</sup> describes how this could also be used to reduce switching surge over voltages during reclosing.

### 1.3 INTENT OF INVESTIGATION

This thesis investigates the usefulness of conventional and switchable four-legged reactors, for transposed and untransposed lines to reduce 'dead' time in single-pole reclosing as a function of the following system parameters:

- 1) Source positive sequence inductive reactance value.
- 2) Source zero sequence to positive sequence inductive

reactance ratio.

3) Sending end to receiving end voltage ratio.

4) Power angle between sending and receiving ends.

5) Length of transmission line.

6) Transmission line zero sequence to positive sequence inductive reactance ratio.

7) Transmission line zero sequence resistance to inductive reactance ratio.

For some of the cases analysed, results will be compared with the alternatives of using capacitors or discharge resistors.

## CHAPTER II

### METHODS OF COMPENSATION

In this chapter some of the basic concepts are explained and discussed to help to understand the problems associated with single-pole reclosing. In order to keep the analysis simple, assumptions are made without affecting the validity of the analysis.

#### 2.1 THE BASIC PROBLEM

Consider the system shown in Fig. 2.1 when a 3-phase transmission line is connected to an ideal source at one end and the other end remaining open. A single line to ground (SL-G) fault occurs, and the breaker in phase A is opened to clear the fault. Representing the transmission line in lumped capacitances (neglecting the line inductance and resistance), as seen from the source, the system is now represented by Fig. 2.2.  $C_1$  is the positive sequence capacitance and  $C_0$  is the zero sequence capacitance for the line length under consideration. Using the Thevenin's Theorem, the system of Fig. 2.2 can be simplified to that in Fig. 2.3, while retaining the identity of the SL-G fault (represented by switch 'S' in closed position) and the open breaker in phase A. Any capacitances which are directly across the source voltages are of no interest and are not shown.



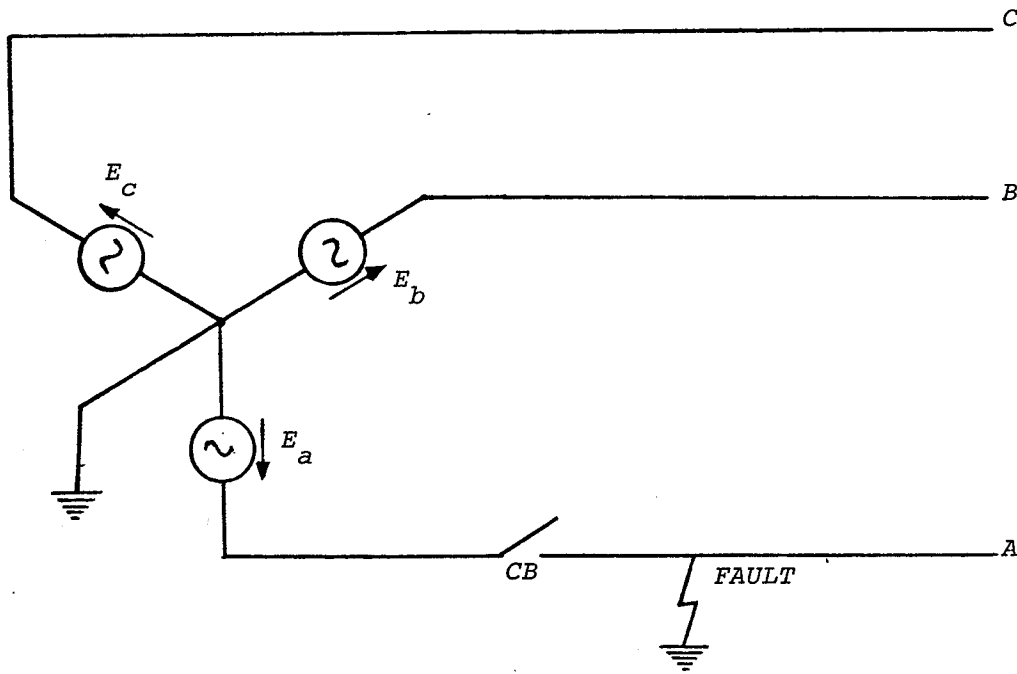


FIG. 2.1 - BASIC SYSTEM

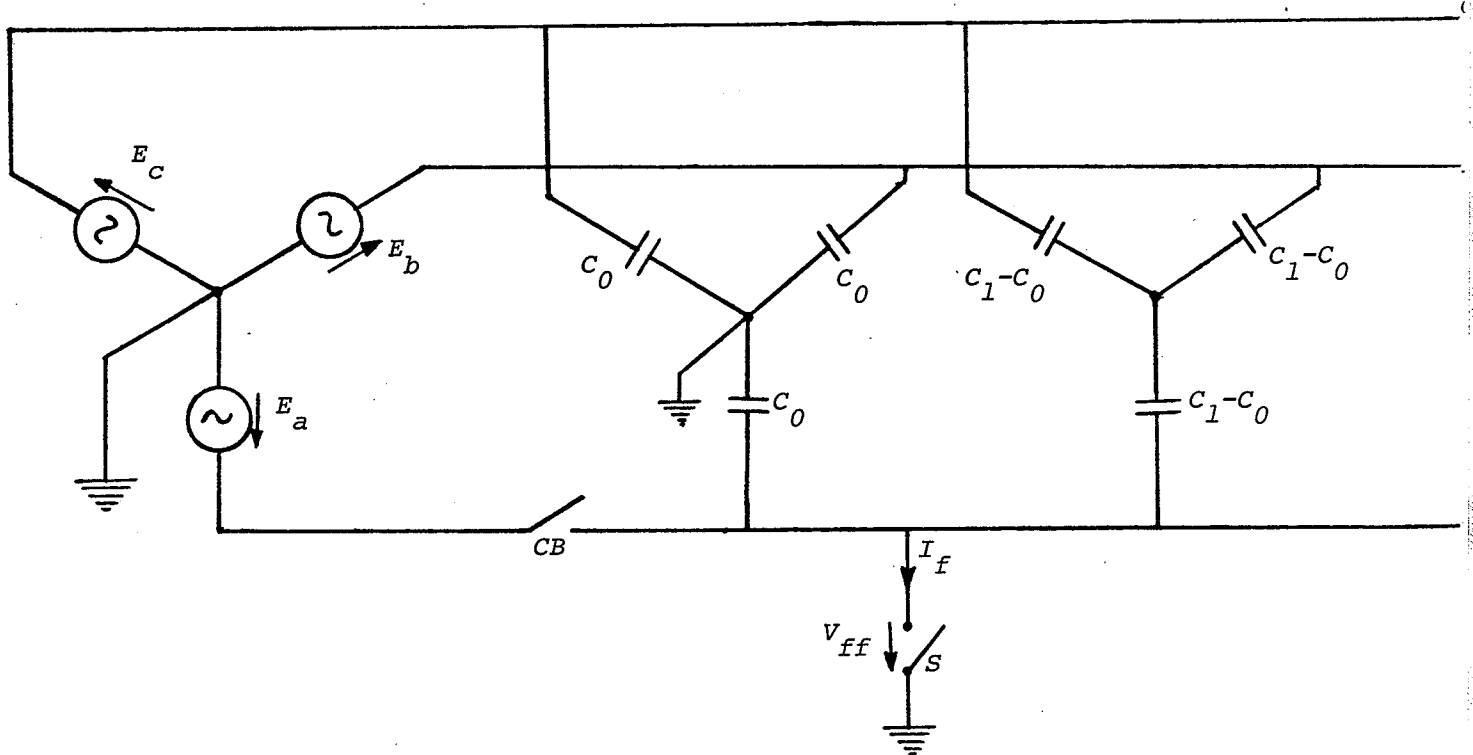


FIG. 2.2 - BASIC SYSTEM - TRANSMISSION LINE IN LUMPED CAPACITANCES

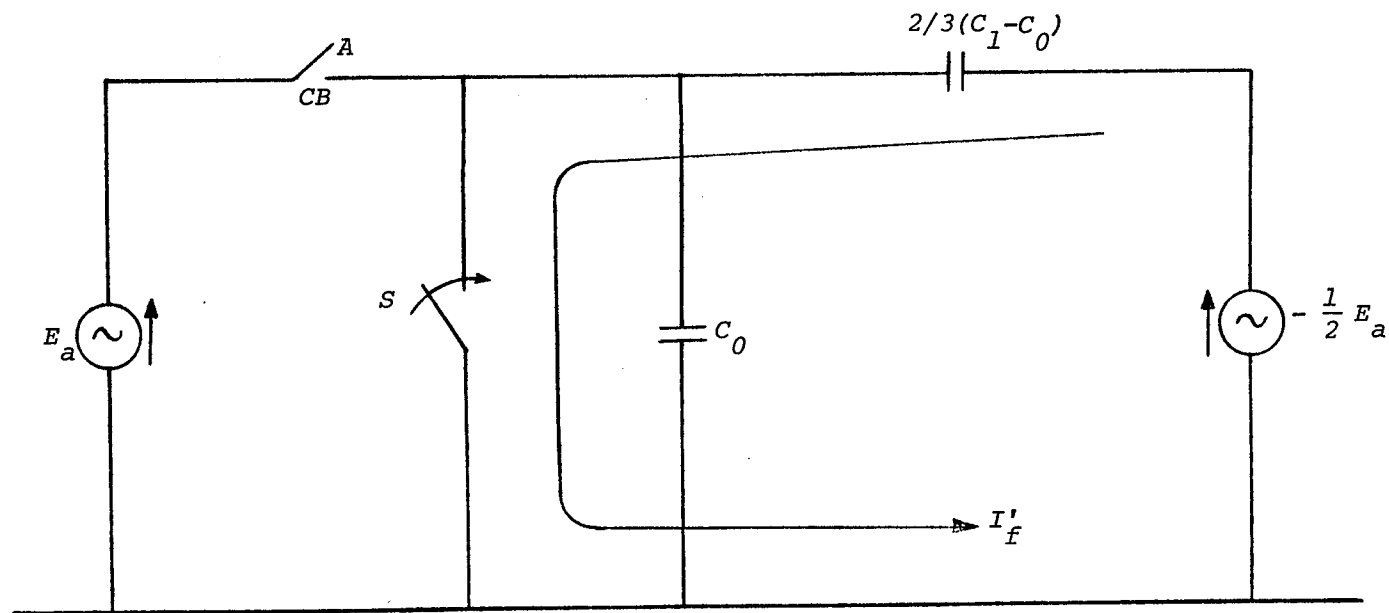


FIG. 2.3 - EQUIVALENT CIRCUIT FOR BASIC SYSTEM

With switch 'S' closed, the fault current  $I'_f$  is established in spite of the open breaker in phase A. This current is given as,

$$I'_f = -\frac{1}{3} E_a \omega (C_1 - C_0) , \quad (2.1)$$

where  $\omega$  is the system frequency in rad/sec. This current is also known as the 'secondary arc' current or 'residual arc' current. If the switch 'S' is open (no fault or cleared fault) then the line to ground fundamental frequency component voltage ( $V_{ff}$ ) on phase A is given by

$$V_{ff} = -E_a \frac{C_1 - C_0}{2C_1 + C_0} . \quad (2.2)$$

The Thevenin admittance seen from the fault terminals is given by,

$$Y_{tf} = \frac{\omega}{3} (2C_1 + C_0) . \quad (2.3)$$

From the above, it is evident, that,

$$I'_f = V_{ff} \cdot Y_{tf} . \quad (2.4)$$

## 2.2 INDUCTANCE METHOD OF REDUCING CAPACITIVE COUPLING EFFECT

Shunt reactors (inductors) which are ordinarily used for compensation of line charging KVAR can also be used to reduce the capacitive coupling effect. Fig. 2.4 indicates the possible configurations of shunt reactors that can be connected to power systems for fault suppression and compensation of line charging current. However, the arrangement 2.4(c) (known as the simple four-legged reactor scheme) is the most simple and therefore, preferable from technical and economical point of view. It is understood that the reactors are connected on the line side of circuit breakers.\* The zero sequence reactance is given by:

$$X'_0 = X'_1 + 3X_{SNT} \quad (2.5)$$

$X'_1$  denoting the positive sequence inductive reactance which is the same as the inductive reactance of the main reactors ( $X_{ST}$ ) while  $X_{SNT}$  is the inductive reactance of the auxiliary (neutral) reactor through which the star point of the main reactor group is earthed.

Using the configuration of Fig. 2.4(c) in connection with the system in Fig. 2.2, and using Thevenin's Theorem, an equivalent system representation is obtained as shown in Fig. 2.5. All the inductances and capacitances are replaced

---

\* Shunt reactors may also be connected to the tertiary of the source of terminal transformer in which case they play no role in the reduction of capacitive coupling effect.

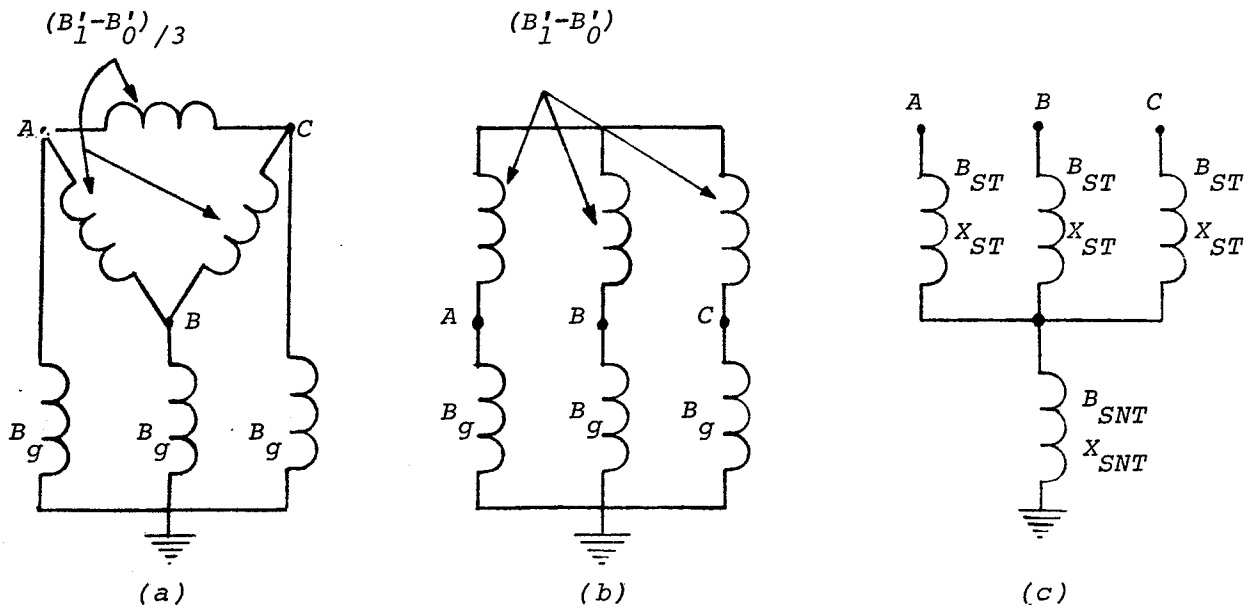


FIG. 2.4 - POSSIBLE CONNECTIONS OF SHUNT REACTORS

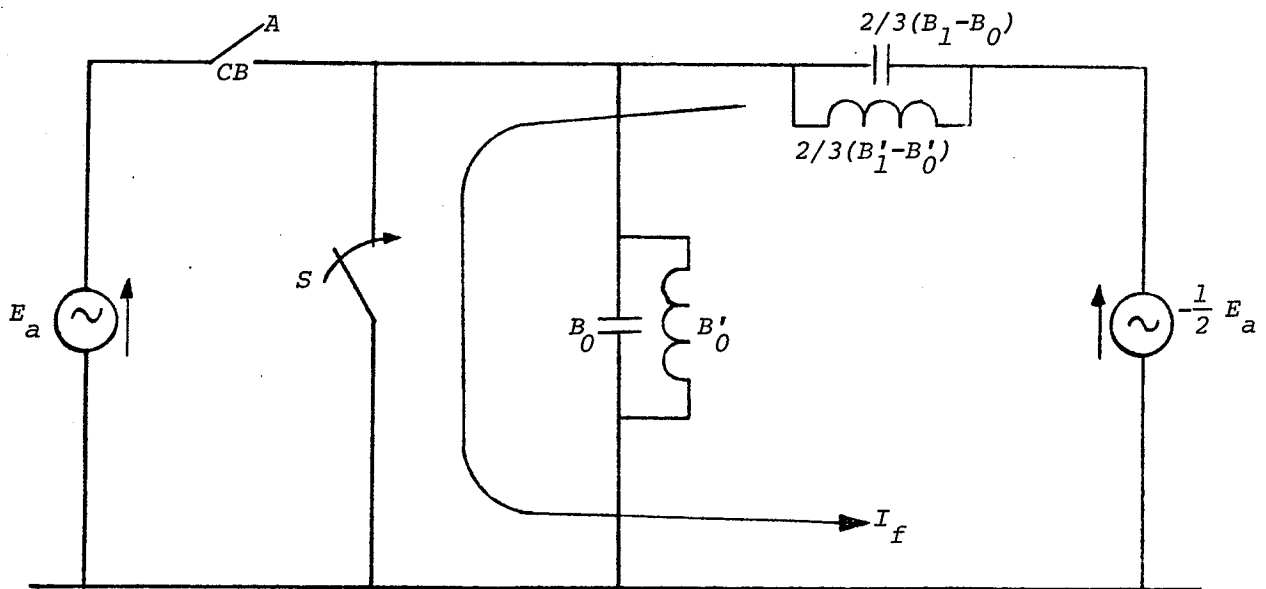


FIG. 2.5 - EQUIVALENT CIRCUIT FOR SHUNT REACTOR METHOD

by their respective susceptances. If  $2/3 (B'_1 - B'_0)$  resonates with  $2/3 (B_1 - B_0)$  at the system frequency then there will be infinite impedance in the path of the fault current and the fault will be cleared. If  $C_0$  and  $L'_0$  form a resonant circuit at the system frequency then  $V_{ff}$  could be very high which would tend to cause arc restriking. Even if this resonance is at another frequency it could cause  $V_{ff}$  to oscillate widely<sup>15</sup> thereby risking a restrike.

The degree of charging KVAR compensation is given by

$$F = \frac{1}{X'_1 B_1} \quad (2.6)$$

For maximum reduction of capacitive coupling effect:

$$B'_1 - B'_0 = B_1 - B_0 \quad (2.7)$$

As  $B'_1 = 1/X'_1$ ,  $B'_0 = 1/X'_0$  and  $B_{SNT} = \frac{1}{X_{SNT}}$ , rewriting the equation 2.5:

$$B_{SNT} = \frac{3B'_0 B'_1}{B'_1 - B'_0} \quad (2.8)$$

Using equations 2.5, 2.6, 2.7 and 2.8, it is possible to calculate the value of  $B_{SNT}$  (or  $X_{SNT}$ ) for a given value of  $F$  and for maximum reduction of capacitive coupling effect:

$$X_{SNT} = \frac{B_1 - B_0}{3FB_1(B_0 - (1-F)B_1)} \text{ ohms} \quad (2.9)$$

where  $B = \omega C$  for the entire line (in mhos) and  $F$  is given by the equation 2.6.

### 2.2.1 Recovery Voltage

The source frequency recovery voltage ( $V_{ff}$ ) across the arc path, after the secondary arc is extinguished, is the voltage across the switch symbol 'S' in Fig. 2.5 when the switch is open. The voltage  $V_{ff}$  is given by

$$\begin{aligned} V_{ff} &= -\frac{E_a}{3} \cdot \frac{2/3[(B_1 - B_0) - (B'_1 - B'_0)]}{(2B_{1/3} + B_{0/3}) - (2B'_{1/3} + B'_{0/3})} \\ &= -\frac{E_a [(B_1 - B_0) - (B'_1 - B'_0)]}{(2B_1 + B_0) - (2B'_1 + B'_0)} \quad . \quad (2.10) \end{aligned}$$

### 2.2.2 Secondary Arc Current

This is the current through the closed switch 'S' of Fig. 2.5. It is given by

$$I_f = -\frac{E_a}{3} \left\{ (B_1 - B_0) - (B'_1 - B'_0) \right\} \quad . \quad (2.11)$$

For a successful extinction of the arc, the current  $I_f$  should be as small as possible so that the energy generated by the arc will be less than the energy dissipated by the arc (through convection, etc.) and the arc will be extinguished.

From another point of view, it can be said that for a successful reclosing operation, the value of  $V_{ff}$  should be zero or very small so that the arc will not tend to restrike. If a fault Thevenin admittance had a constant value for any location of the fault for a given line, the problem of minimizing  $I_f$  and  $V_{ff}$  would be one and the same.

### 2.3 CAPACITANCE METHOD OF REDUCING CAPACITIVE COUPLING EFFECT

This method is explained with the help of Fig. 2.6 which is derived from Fig. 2.3, after connecting a capacitor  $B (= \omega C)$  across the contacts of the open breaker in phase A. Another fault current,  $I_f''$ , will be established, given by

$$I_f'' = E_a B . \quad (2.11)$$

This current is supplied from the source voltage  $E_a$  which is phase A of the source. Therefore, the total fault current is given by

$$I_f = I_f' + I_f'' = - E_a \frac{B_1 - B_0}{3} + E_a B . \quad (2.12)$$

If the capacitor  $B$  were chosen to be equal to  $(B_1 - B_0)/3$  then it is apparent that the total fault current  $I_f$  will be zero and the fault will be cleared.

If the switch 'S' were open, then  $V_{ff}$  (voltage across the switch) will also be zero for the value of  $B$  as selected above.  $Y_{tf}$ , the fault Thevenin admittance, will now be  $B_1$ .



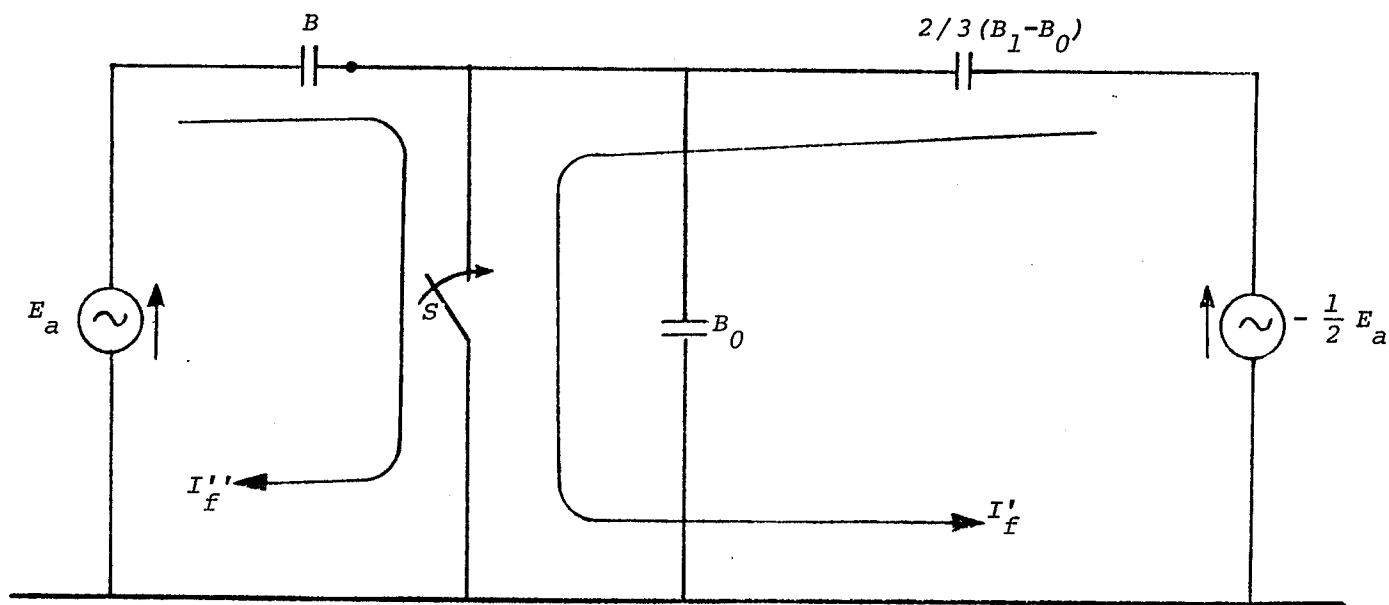


FIG. 2.6 - EQUIVALENT CIRCUIT FOR THE CAPACITANCE METHOD

Since a great majority of faults are single line to ground type, it seems most beneficial to choose  $B$  equal to  $(B_1 - B_0)/3$  for the line to ground faults and zero for all other types of faults. It is best to have this capacitor connected through a switch so that it may be disconnected through a switch for other than single line to ground faults.<sup>10</sup>

A possible relaying scheme, that incorporates the above, should have the following features:

1) Recognize the faulted phase following a single line to ground fault and initiate opening of the appropriate line breakers. The capacitor  $B$  will remain connected across the breaker poles.

2) For any other type of fault, open all the breakers as well as the switches in series with the capacitors.

It is understood that in both the above cases reclosing operations will follow after the dead time.

Obviously, the above relaying scheme will be more complicated than the one where 3-pole reclosing is used. However, it is possible in certain cases that the additional gain in transient stability achievable by single-phase reclosing would warrant the attendant increase in the complexity of relaying.

#### 2.4 THE METHOD OF USING DISCHARGE RESISTORS

This method consists of connecting the faulted phase conductor, through a resistance in series with a switch, to

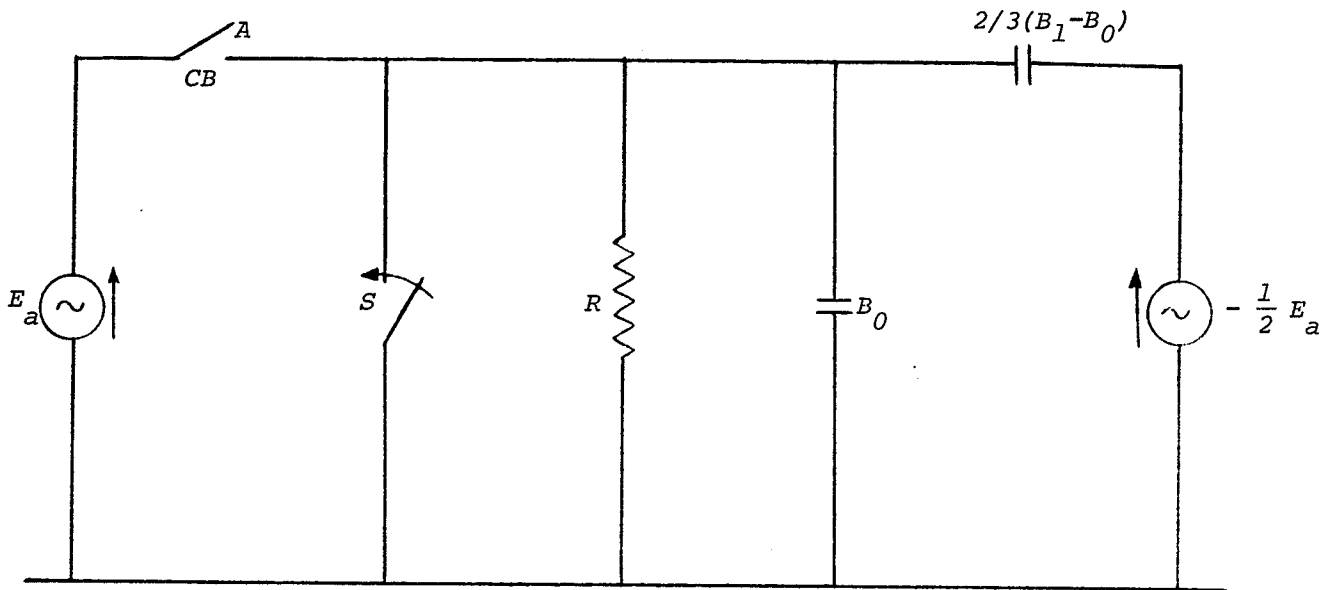


FIG. 2.7 - EQUIVALENT CIRCUIT FOR DISCHARGE RESISTANCE METHOD

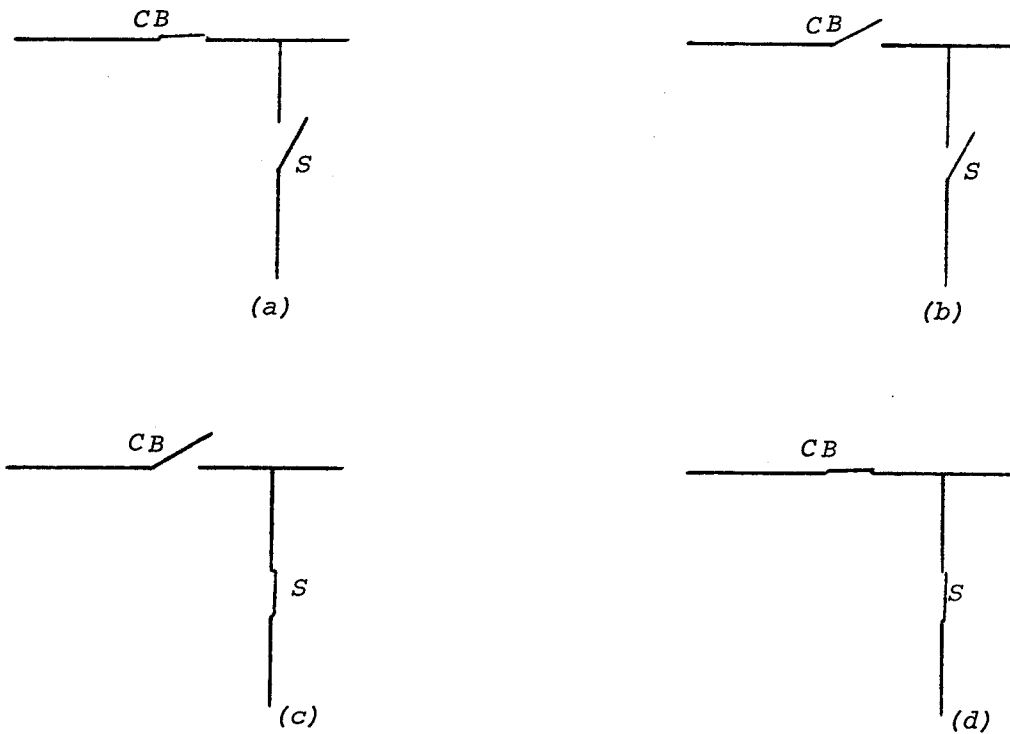


FIG. 2.8 - SEQUENCE OF LINE BREAKER AND DISCHARGE RESISTANCE SWITCHING

ground after that phase is disconnected from the source. An equivalent circuit, using Thevenin's Theorem, can be drawn as in Fig. 2.7. This is quite similar to Fig. 2.3 except that a resistor  $R$  has been connected across the fault. If  $R$  is zero then it provides a path by-passing the secondary arc (the arc path has a finite resistance). Thus the arc is extinguished and finally the current through the resistor can be switched off. It is apparent that for the best performance  $R$  should be zero. Then  $V_{ff}$  will also be zero. In any case,  $R$  should be much less than the arc resistance (a variable quantity) for this method to be effective.

It has been suggested that the value of  $R$  of the order of two times the line surge impedance could be useful in reducing the switched surge over-voltage during reclosing. Fig. 2.8 shows the four stages of operation. 'CB' and 'S' denote the line breaker and the switch (in series with the resistor), respectively. The four parts of Fig. 2.8 are explained as follows:

Normal operating condition is shown by (a). Opening of the breaker following a fault is shown in (b). The resistance is now connected to the line to by-pass the arc current as shown in (c). Part (d) shows that the breaker is reclosed after the necessary delay. Switching surge over-voltage is reduced because the resistor is in parallel to the line. Finally the resistor is disconnected, reverting back to the state of normal operation as shown in (a).

## CHAPTER III

-SINGLE-POLE SWITCHING-  
REPRESENTATION OF TRANSMISSION LINES

The analysis in the previous chapter was based on some simplifying assumptions. However, for a proper investigation, the system should be studied in a state as close to the actual system as possible. In this chapter different ways of representation will be discussed. A discussion of various methods of solution will also be included.

### 3.1 SYSTEM REPRESENTATION

Fig. 3.1 shows a one-line diagram representation of the system selected for the study. The system consists of a transmission line connecting two machines through WYE-DELTA transformers.  $V_S$  and  $V_R$  are the L-N voltages at the sending and receiving ends, respectively, of the transmission line under balanced conditions of operation and  $\delta$  is the angle between them (power angle).  $^*X_{\alpha S}$  and  $X_{0S}$  are the  $\alpha$  component and 0 component source reactances, respectively, for the sending end while  $X_{\alpha R}$  and  $X_{0R}$  are the corresponding quantities for the receiving end.  $E_{\alpha S}$  and  $E_{\alpha R}$  are the machine internal

---

\* In this study source negative sequence reactance is assumed to be the same as the source positive sequence reactance. Therefore the terms positive sequence reactance and  $\alpha$  component reactance will be interchangeably used.

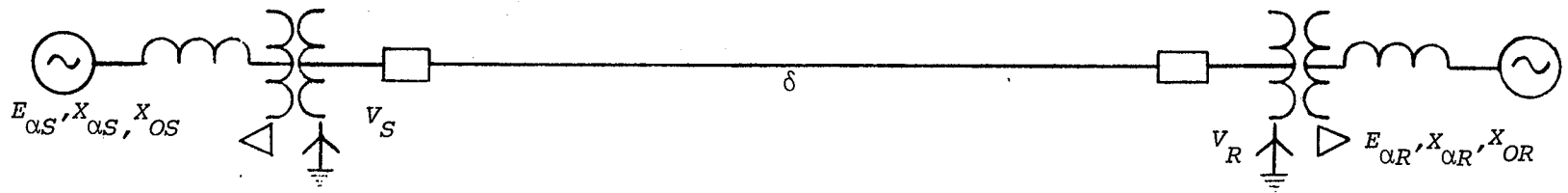


FIG. 3.1 - SINGLE LINE REPRESENTATION OF THE SYSTEM

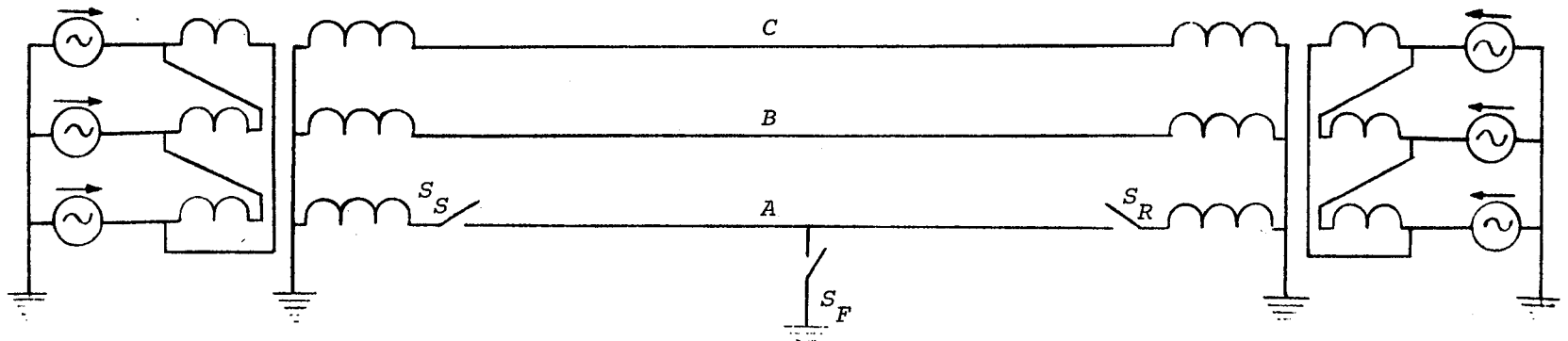


FIG. 3.2 - 3-PHASE REPRESENTATION OF THE SYSTEM

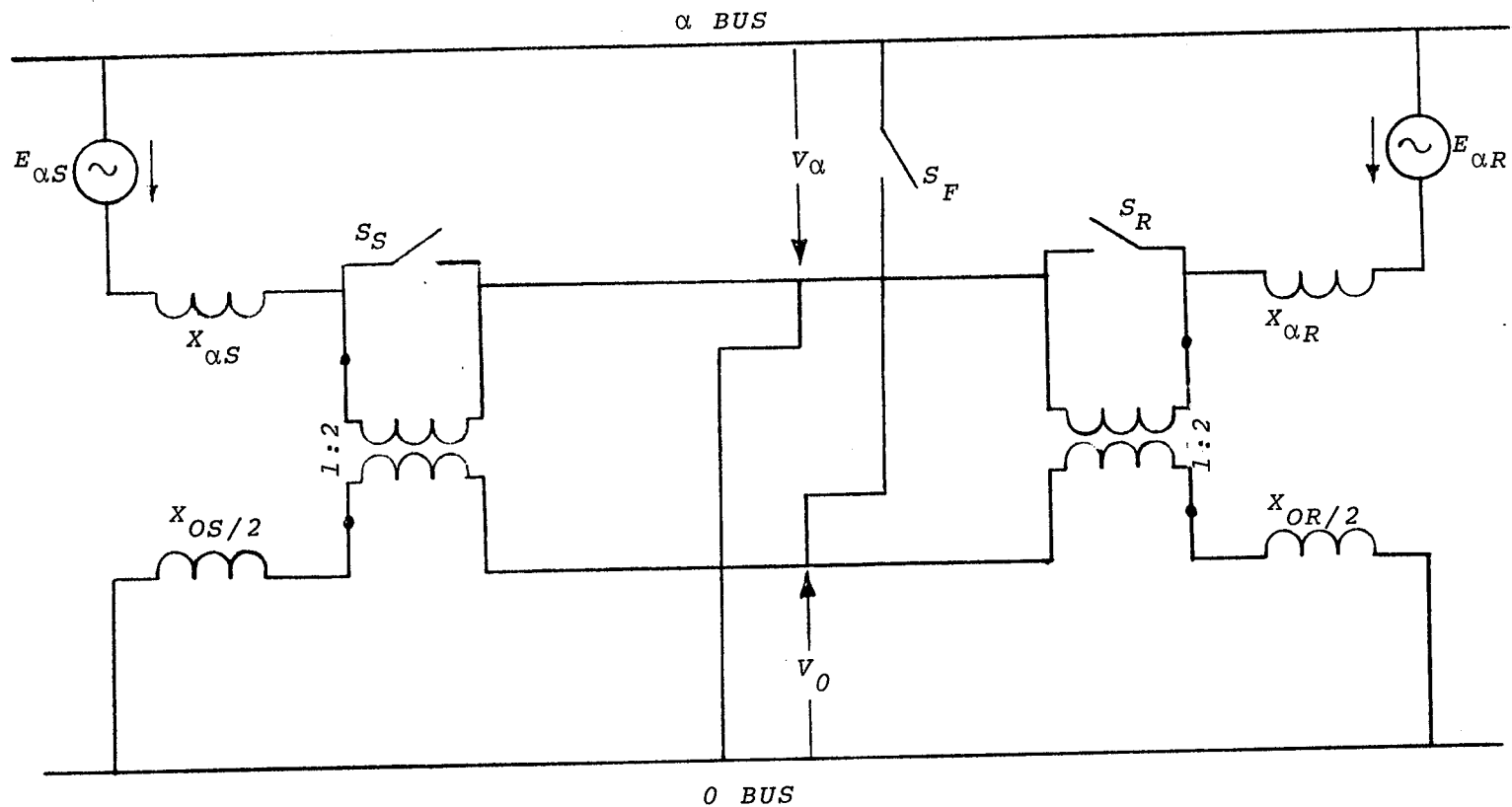


FIG. 3.3 -  $\alpha, \beta, 0$  COMPONENT REPRESENTATION OF SINGLE PHASE SWITCHING

NOTE:  $\beta$  Component does not contribute to the quantities associated with Phase A.

voltages at the sending and receiving ends, respectively, under balanced operating conditions (voltage behind the source reactance).  $\delta_g$  (not shown in the Fig. 3.1) is the angle between  $E_{\alpha S}$  and  $E_{\alpha R}$ . Since the actual system is unbalanced (open breaker and line to ground fault), a carefully detailed representation is necessary. Different types of representations are described below.

### 3.2 REPRESENTATION OF TRANSPOSED LINES

#### a) 3-Phase Representation

Fig. 3.2 shows the system in the 3-phase form without using any compensation scheme. A single line to ground fault (SL-G) occurs on phase A (through the switch  $S_f$ ). Breakers  $S_S$  and  $S_R$  are opened to clear the fault. When the switches  $S_S$ ,  $S_R$ , and  $S_f$  are open, the SL-G voltage on phase A is  $V_{ff}$ . This representation may be used for a study on an actual system or on a model thereof.

#### b) Representation by Components

An unbalanced 3-phase network can be represented in terms of component networks which are suitably interconnected. For the system under consideration,  $\alpha$ ,  $\beta$ , 0 components provide the most effective representation. This is so because of the fact that only one phase (phase A) is involved in the unbalances and therefore, only  $\alpha$  and 0 component networks are of interest (assuming that it is not required to determine voltages or currents associated with phases B and C). Fig. 3.3



shows how the  $\alpha$  and  $0$  component networks are interconnected. All resistances and reactances in the  $0$  network are half of their actual values. This is necessary in order to satisfy the conditions of interconnections. This way of representation assumes that the transmission line is fully transposed. This representation can be used for a digital computer program (or on a network calculator).

c) Conditions for Component Network Interconnections

There are two types of unbalances that are associated with the system. Conditions for the interconnection of component networks will be derived<sup>16</sup> for each type.

3.2.1 Open Breaker

Consider the system shown in the Fig. 3.4.1 where the breaker in phase A is open. Let  $V_a$ ,  $V_b$ , and  $V_c$  be the voltages across the breaker contacts and let  $i_a$ ,  $i_b$ , and  $i_c$  be the currents through them in phases A, B, and C. Then it implies

$$\begin{aligned} i_a &= 0 \\ v_b &= v_c = 0 . \end{aligned} \quad (3.1)$$

Expressing the equations 3.1 in terms of  $\alpha$ ,  $\beta$ ,  $0$  components, it follows that

$$\begin{aligned} i_\alpha + i_0 &= 0 \\ -\frac{1}{2} v_\alpha + \frac{\sqrt{3}}{2} v_\beta + v_0 &= 0 \\ -\frac{1}{2} v_\alpha - \frac{\sqrt{3}}{2} v_\beta + v_0 &= 0 . \end{aligned} \quad (3.2)$$

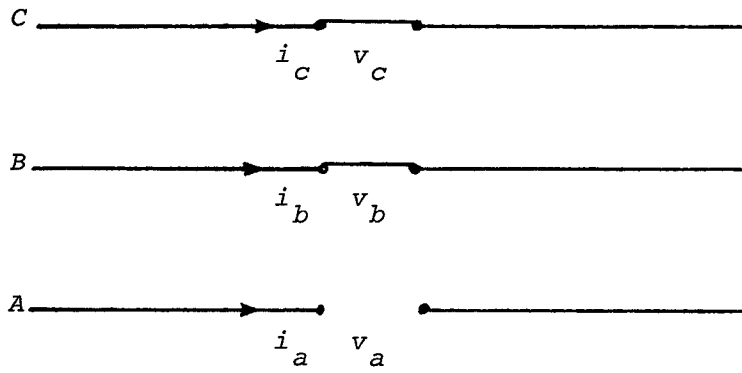


FIG. 3.4.1 - OPEN BREAKER

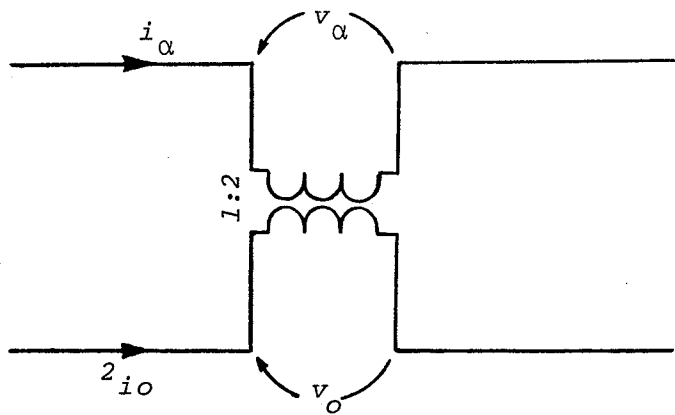


FIG. 3.4.2 - INTERCONNECTION OF COMPONENT NETWORKS

From the equations 3.2 we obtain the conditions of interconnection as,

$$\begin{aligned} i_{\alpha} &= i_o \\ v_{\alpha} &= 2v_o \\ v_{\beta} &= 0 . \end{aligned} \tag{3.3}$$

Fig. 3.4.2 shows the actual interconnection.

### 3.2.2 SL-G Fault Through a Resistance R

Consider the system shown in Fig. 3.5.1 where a line to ground fault exists in phase A through a resistance R. Let  $V_a$ ,  $V_b$  and  $V_c$  be the voltages across the fault simulating switches and let  $I_a$ ,  $I_b$ , and  $I_c$  be the fault currents in the phases A, B, and C. Then

$$\begin{aligned} V_a &= 0 \\ I_b &= I_c = 0 . \end{aligned} \tag{3.4}$$

Expressing the equations 3.4 in terms of  $\alpha$ ,  $\beta$ , and 0 components it implies

$$\begin{aligned} V_{\alpha} + V_o &= 0 \\ -\frac{1}{2} I_{\alpha} + \frac{\sqrt{3}}{2} I_{\beta} + I_o &= 0 \\ -\frac{1}{2} I_{\alpha} - \frac{\sqrt{3}}{2} I_{\beta} + I_o &= 0 . \end{aligned} \tag{3.5}$$

From the equations 3.5, we obtain the conditions of interconnection as,

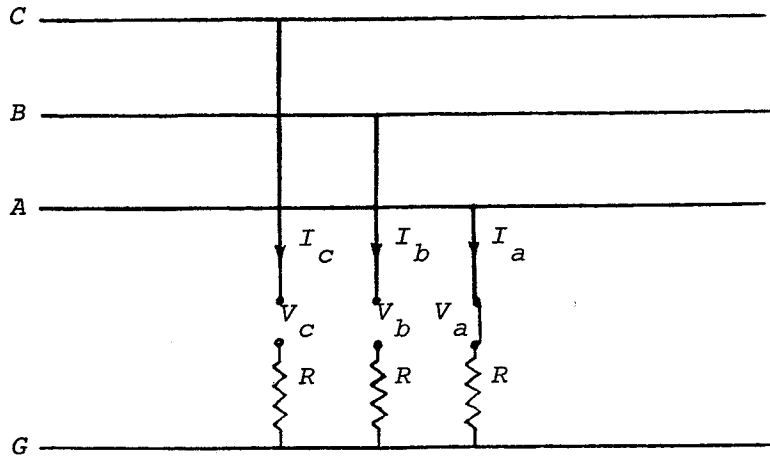


FIG. 3.5.1 - LINE TO GROUND FAULT THROUGH RESISTANCE R

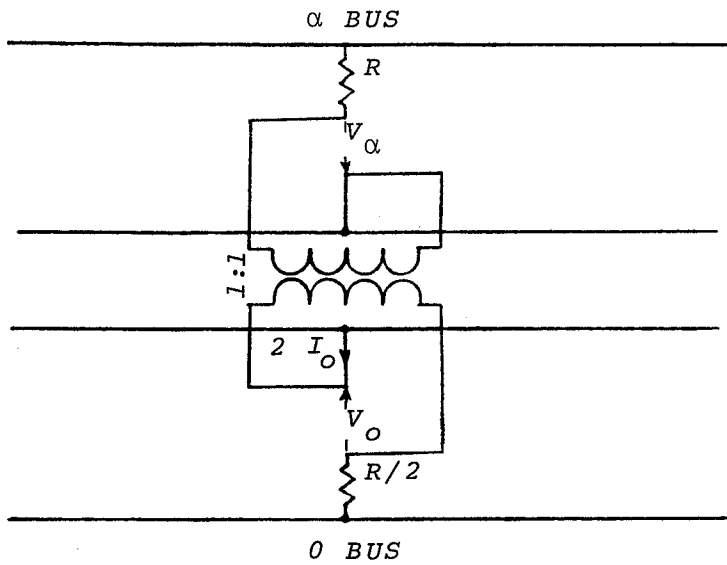


FIG. 3.5.2 - INTERCONNECTION OF COMPONENT NETWORKS

$$\begin{aligned}
 V_{\alpha} &= -V_o \\
 I_{\alpha} &= 2 I_o \\
 I_{\beta} &= 0 .
 \end{aligned}
 \tag{3.6}$$

Fig. 3.5.2 shows the actual interconnection. In the method of using discharge resistors, a resistance  $R$  is connected between phase A and ground. This is the same as an SL-G fault through a resistance  $R$ .

### 3.3 USE OF SIMPLE FOUR-LEGGED REACTORS

As mentioned earlier, shunt reactors which are usually used for the compensation of line charging KVAR can also be used to reduce the capacitive coupling effect. Simple four-legged reactors that can be used at line ends or at the midpoint, depending upon the line length, are more effective on fully transposed lines. Fig. 3.6 shows the system in the 3 phase set up. Four-legged reactors  $X_{ST}$  and  $X_{SNT}$  are shown to be connected at both ends of the line.

The reactor bank can be expressed in terms of  $\alpha$  and  $0$  components. These components are connected in the component diagram (Fig. 3.3) at proper locations. The conditions for component network interconnections are the same as derived in 3.2.1. The admittance matrix is given in Fig. 3.6.2.

### 3.4 USE OF CAPACITORS

For single pole reclosing, the capacitors of specified value can be connected across circuit breaker contacts. When

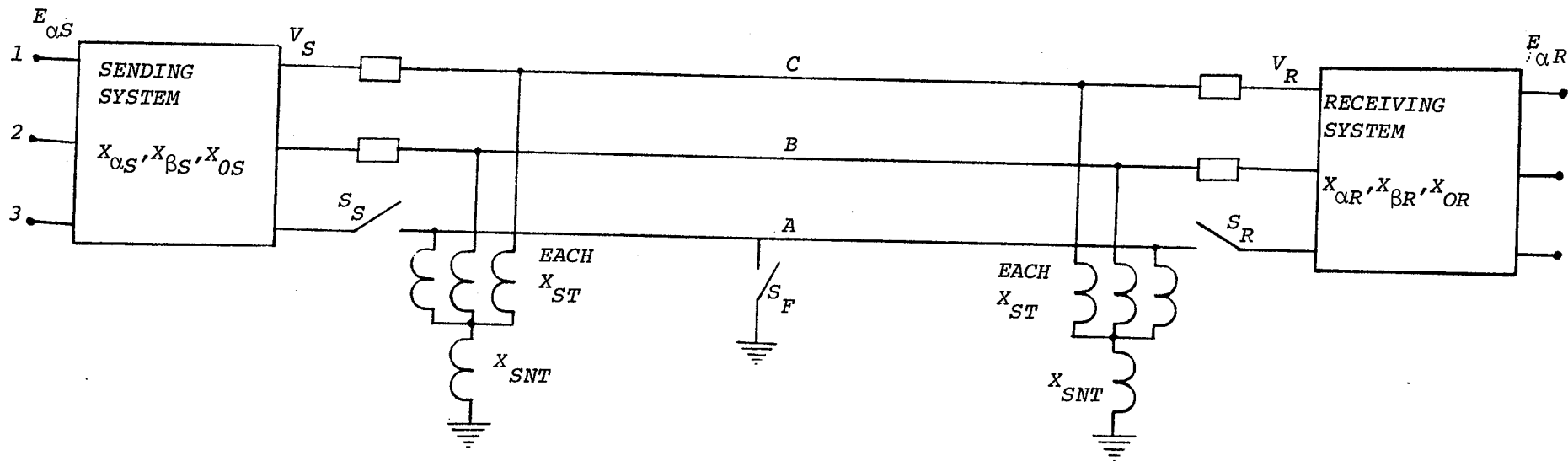
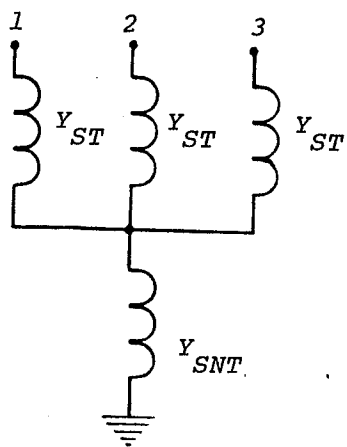


FIG. 3.6.1 - 3-PHASE REPRESENTATION OF THE SYSTEM USING SIMPLE FOUR-LEGGED REACTORS



For fault on any phase, admittance matrix is given by

$$[Y_S] = \begin{bmatrix} Y_1 & -Y_2 & -Y_2 \\ -Y_2 & Y_1 & -Y_2 \\ -Y_2 & -Y_2 & Y_1 \end{bmatrix}$$

where

$$Y_1 = \frac{Y_{ST}(2Y_{ST} + Y_{SNT})}{3Y_{ST} + Y_{SNT}}$$

$$Y_2 = \frac{Y_{ST}^2}{3Y_{ST} + Y_{SNT}}$$

FIG. 3.6.2 - SIMPLE FOUR-LEGGED REACTOR BANK

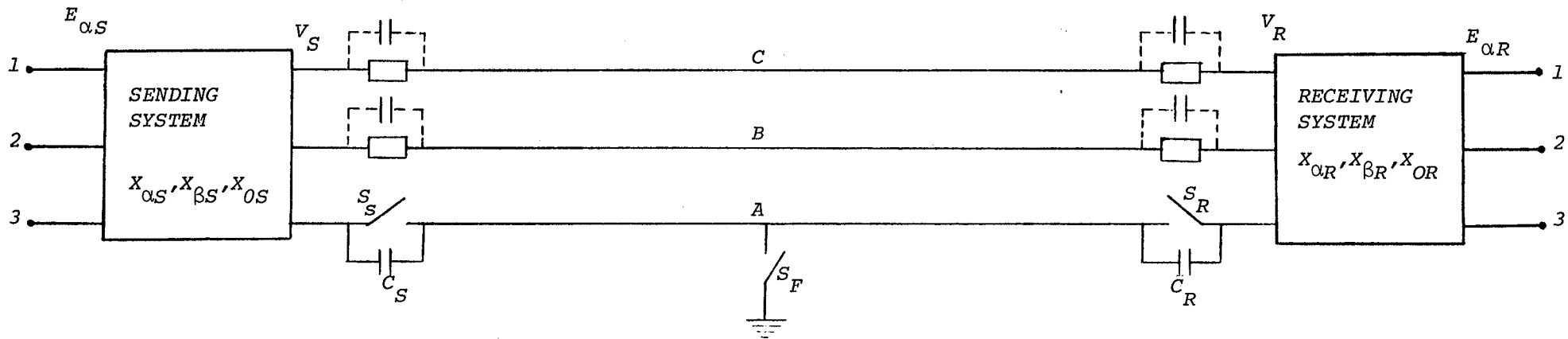


FIG. 3.7.1 - 3-PHASE REPRESENTATION OF THE SYSTEM USING CAPACITORS

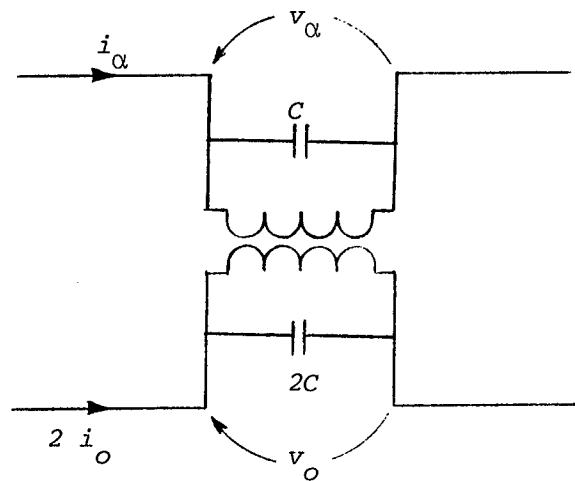


FIG. 3.7.2 - OPEN BREAKER - ACTUAL INTERCONNECTION

the breaker is open following a non-permanent single line to ground fault, the faulted phase conductor is connected to the source through the capacitor. Values of these capacitors can be selected to minimize the potential of the faulted conductor with respect to the ground, thereby extinguishing the residual arc.

The system has been shown in the Fig. 3.7.1 in the 3-phase arrangement. The actual interconnection of capacitors in the component network is shown in Fig. 3.7.2. The conditions for the interconnections are the same as in 3.2.1.

### 3.5 METHODS OF SOLUTION

This section is mainly concerned with solving the problem with the aid of a digital computer or any kind of numerical computational device. The problem presents itself as one of circuit analysis and, therefore, it is in order to discuss various methods of solving a circuit pertaining to this problem. Two such methods are discussed below. It may be pointed out that the suitability of the various methods was judged from the standpoint of computer programming, viz., availability of pertinent sub-routines, formulation of simple and compact sub-routines as part of the program, etc. In this context, methods such as mesh analysis, loop analysis, node analysis are not considered different from each other.



### 3.5.1 Mesh Analysis

This is a well known technique and needs little description. The transmission line part of Fig. 3.3 (for both  $\alpha$  and 0) is represented in terms of a series of  $\pi$  sections of 20 miles each (or any suitable length depending upon length of transmission line). Fig. 3.8 shows the resulting network. Solution of this network, using mesh analysis technique, will result in the  $\alpha$  and 0 voltage at various locations on the line and their sum will give  $V_{ff}$ . The number of mesh equations to be solved is equal to twice the number of  $\pi$  sections (on  $\alpha$  or 0) plus four. Thus the minimum number of equations to be solved is eight, considering only one location on the line, e.g., the mid point, apart from the two ends. Cramer's rule can be used to solve for the necessary currents. To solve for another location, the procedure must be repeated after making the necessary changes. If it is desired to compute voltages at various points on the line, simultaneously, then the number of meshes will increase and Cramer's rule will not be very convenient, especially if there are something like 24 mesh equations. Computer programs for matrix inversion (if available for complex numbers) could be used to solve such networks. Normally such programs are equipped to handle matrices of orders large enough to suit a practical problem, e.g., a 300 mile long line with 20 mile  $\pi$  sections generating a matrix in the order of 34 which is not a very big matrix. However, as the  $\pi$  section length becomes smaller, the magnitudes of the

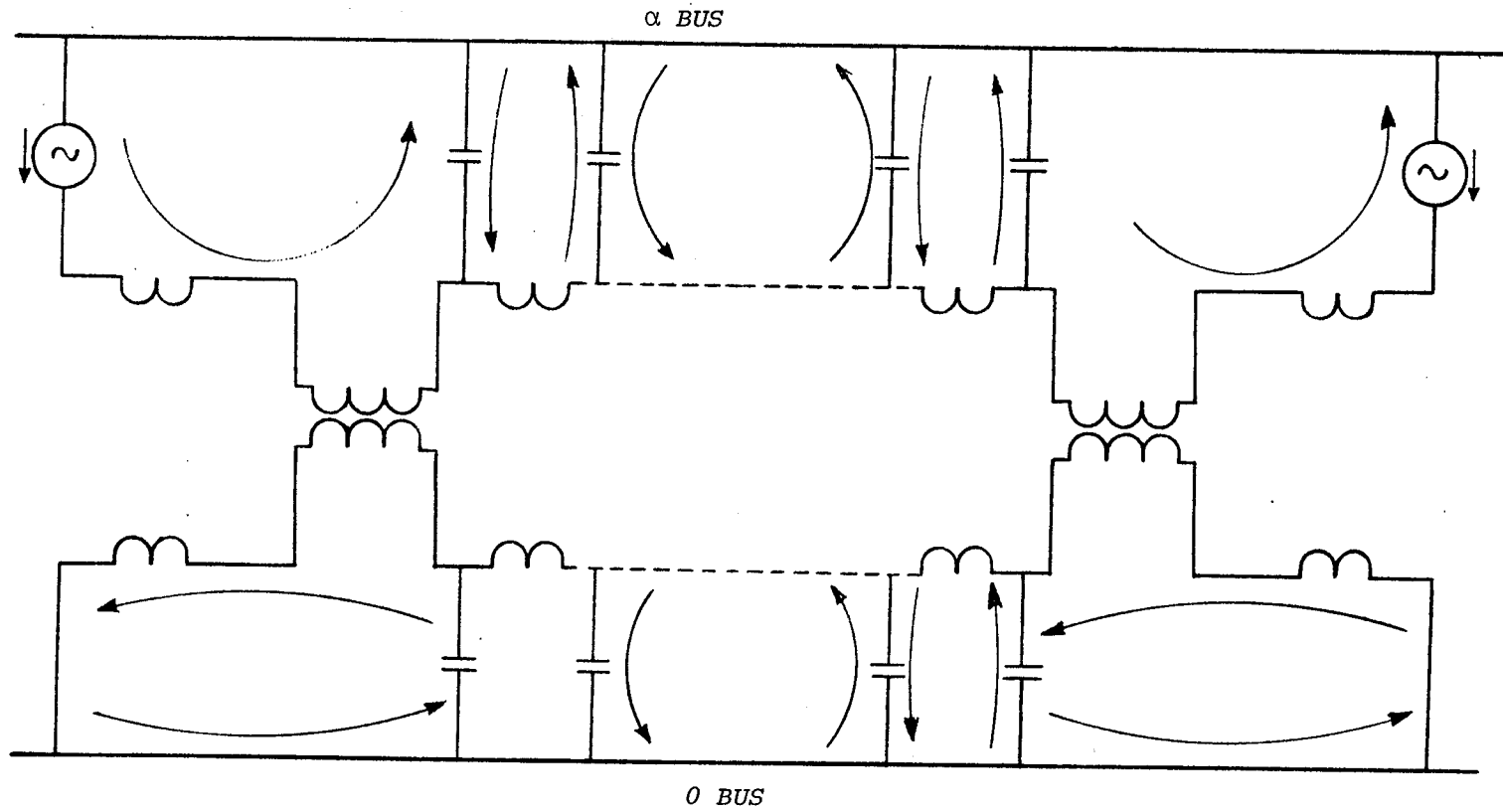


FIG. 3.8 - MESH ANALYSIS

impedances making up the elements of the matrix (mostly shunt capacitances) become larger. This can have two effects. In the first place, the real part of the matrix element (only the main diagonal elements have these) becomes very small relative to the imaginary part. Secondly, the size of the matrix elements themselves become larger. These two can have important implications on the accuracy of the results from the standpoint of rounding off errors and the floating point number limit for the particular computer. This technique is not being used for analysis in this thesis.

### 3.5.2 Two-Port Network Analysis

Two-port network is a well-known technique and is used in power system calculations in the form of ABCD constants. Fig. 3.9 shows a general two-port network and its input/output quantities. The input quantities can be expressed in terms of output quantities or vice versa. These expressions are given by equations 3.7.1 and 3.7.2, while equation 3.7.3 is a relationship that must be satisfied if the network consists of linear, bilateral elements only.

$$\begin{aligned} V_1 &= AV_2 + BI_2 \\ I_1 &= CV_2 + DI_2 \end{aligned} \quad (3.7.1)$$

$$\begin{aligned} V_2 &= DV_1 - BI_1 \\ I_2 &= -CV_1 + AI_1 \end{aligned} \quad (3.7.2)$$

$$AD - BC = 1 \quad (3.7.3)$$

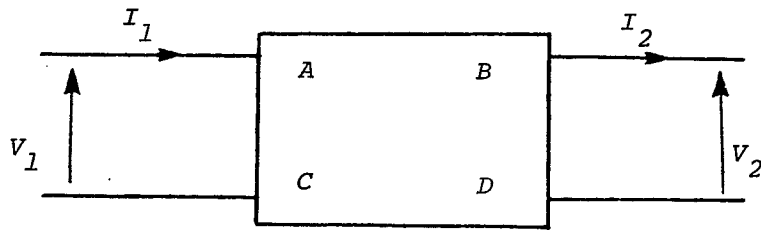


FIG. 3.9 - TWO-PORT NETWORK

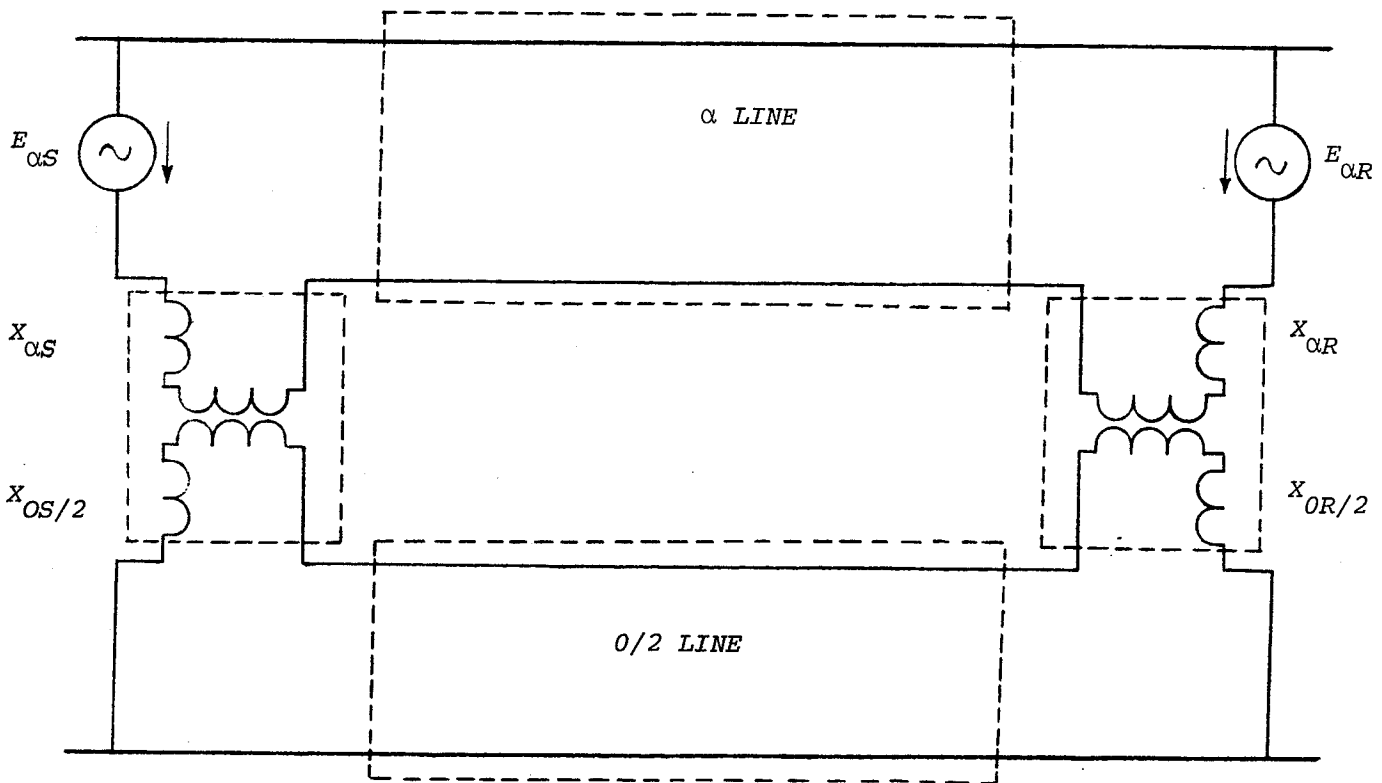


FIG. 3.10 - ACTUAL INTERCONNECTION OF COMPONENT NETWORKS

Relationships to combine two-port networks in cascade or in parallel may be found in many textbooks and are well known. These are used for network reduction as will be shown later.

Fig. 3.10 shows the circuit of Fig. 3.3, partitioned in terms of two-port network blocks. Only the voltages at the ends of the  $\alpha$  and  $0$  lines are of interest because once they are known, voltages anywhere else on the line can be computed. It is possible to solve the circuit of Fig. 3.10 directly and obtain the voltages mentioned above. A program written to do just that would be rather long and could not be used if the circuit configuration were changed to accommodate other balances.

It is more convenient, therefore, to further simplify the circuit of Fig. 3.10 and use the principle of superposition. Fig. 3.11 shows the circuit of Fig. 3.10, redrawn with only the source voltage. The ABCD constants of Fig. 3.11 are derived from the corresponding networks of Fig. 3.10. A further simplification is shown in the Fig. 3.12 where the two-port networks  $(ABCD)_1$  and  $(ABCD)_2$  are obtained by series combinations of  $(ABCD)_\alpha$  with  $(ABCD)_R$  and  $(ABCD)_S$  with  $(ABCD)_0$ , respectively. This circuit can now be solved.\* It may be noted that  $V_{11}$ ,  $I_{11}$  and  $V_{22}$ ,  $I_{22}$  are quantities at one of the ends of the  $\alpha$  and  $0$  components of transmission line. From

---

\* A further simplification, by combining the two-port networks into one, is possible. But after the final network is solved, it will then be necessary to separate it into two parts to compute the required voltages.

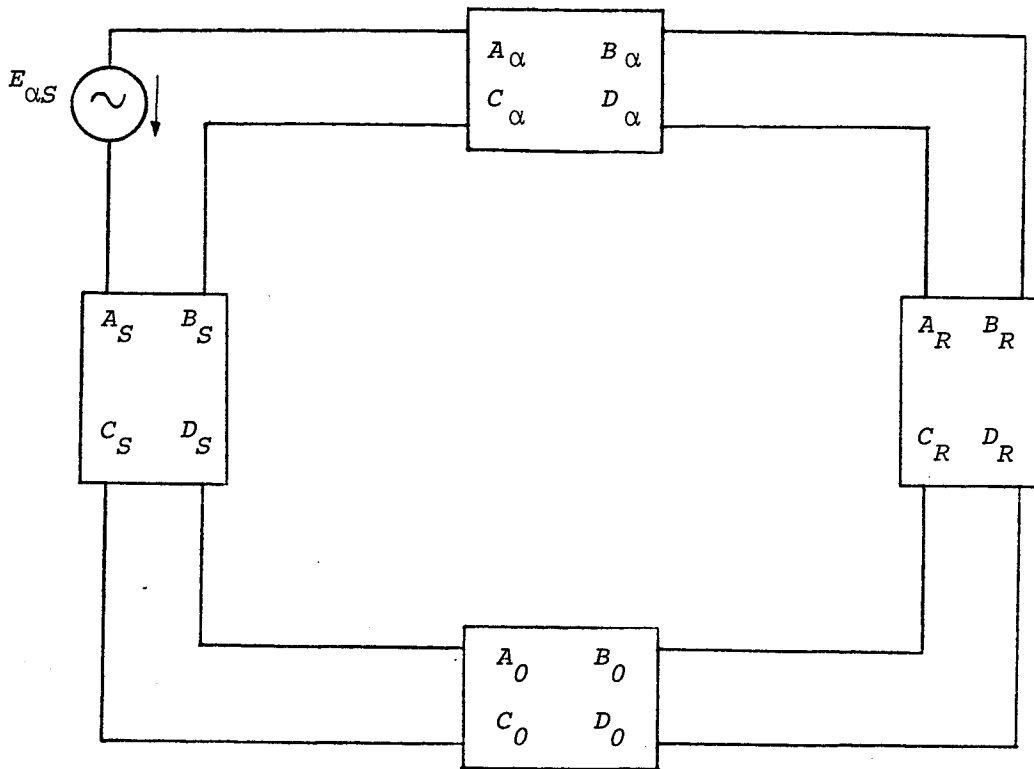


FIG. 3.11 - SIMPLIFIED CIRCUIT OF FIG. 3.10 - USING PRINCIPLE OF SUPERPOSITION

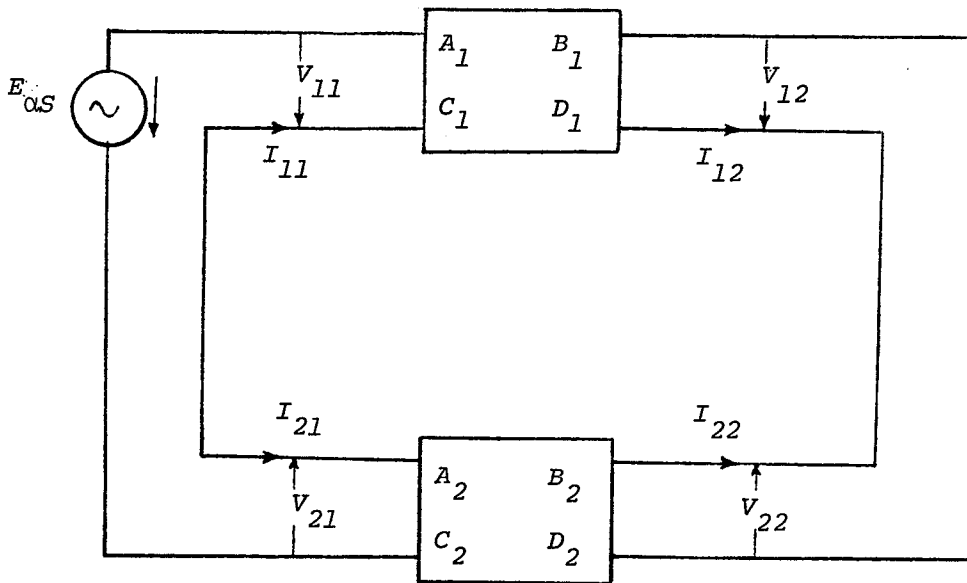


FIG. 3.12 - SIMPLIFIED CIRCUIT OF FIG. 3.11

these and from equations 3.7.1 and 3.7.2, the corresponding quantities at the other ends can be computed. Once the voltages at both ends of the line components are known, voltages at any other location on the line can be determined from transmission line theory. The same procedure is then repeated for the other source and the effects of the two are superimposed to obtain the total voltage at any location.

Any changes in the values of source  $X_{\alpha}$  and  $X_o$  and the values of compensation schemes (i.e.  $Y_{ST}$  and  $Y_{SNT}$  or  $C_S$  and  $C_R$ ) will require only the modifications of  $(ABCD)_S$  and  $(ABCD)_R$ . Changes in line length and the line constants will require modification of  $(ABCD)_{\alpha}$  and  $(ABCD)_o$ . Voltages  $E_{\alpha S}$  and  $E_{\alpha R}$  are dependent upon the line terminal conditions under balanced operation (pre-fault) and are determined as such.

It can be easily seen that from a computer programming point of view, the two-port method is better than the mesh equations method, because in the latter the whole circuit has to be solved every time a single parameter is changed.

### 3.6 MODIFICATION OF THE BASIC CIRCUIT

All the above-mentioned changes in parameter value did not modify the basic circuit of Fig. 3.10. However, for the required studies (using compensation schemes, etc.), the basic circuit needs modification, and such cases are described below.

### 3.6.1 Shunt Reactor Connection at Line Ends

The reactor bank is expressed in terms of  $\alpha$  and  $0$  components. These components are connected in the component diagram at proper locations. Fig. 3.13 shows the reactors in the  $\alpha$  circuit expressed in terms of ABCD constants, connected on either side of  $\alpha$  line component. The same procedure is followed for the  $0$  line component. The three two-port networks in Fig. 3.13 are then combined to arrive at the configuration of Fig. 3.10. The rest of the procedure is unchanged.

### 3.6.2 Shunt Reactor Connection at the Mid-Point

This would require splitting the line network in two parts as shown in Fig. 3.14 for the  $\alpha$ -component network. The same procedure is followed for the  $0$ -component network using the appropriate constants. Once again the three two-port network in series must be combined into one two-port network to obtain the configuration of Fig. 3.10. Slight program changes will be necessary in computing the voltage distribution on the line because of the discontinuity introduced by the shunt reactors.

### 3.6.3 Connection of Discharge Resistors Between the Faulted Phase and Ground

It has already been mentioned in section 3.2.2 that the connection of the discharge resistors is the same as an SL-G fault through a resistance  $R$ . Fig. 3.5.2 shows the interconnecting network that must be used to connect the  $\alpha$  and  $0$  networks at the location of these resistors. The resistances



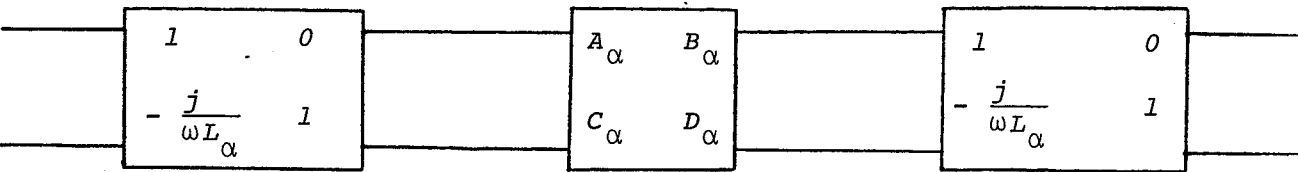


FIG. 3.13 - SHUNT REACTORS AT THE ENDS OF THE LINE

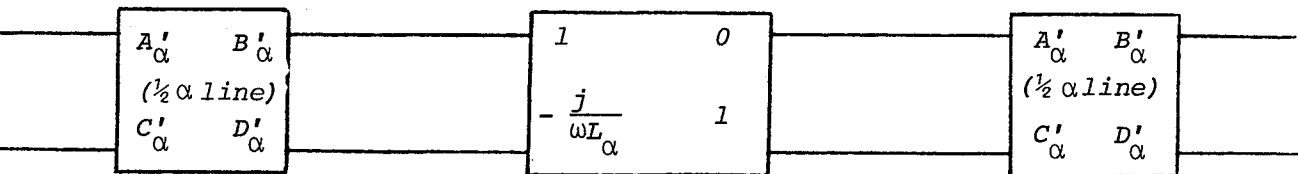


FIG. 3.14 - SHUNT REACTORS AT THE LINE MID-POINT

shown in the Fig. 3.5.2 should be included in forming the two-port network for this interconnection. Solution of the circuit will follow the same procedure as in the above section.

#### 3.6.4 Connection of Capacitors Across Circuit Breakers in the Faulted Phase

The actual interconnection of capacitors in the  $\alpha$  and 0 networks has been shown in the Fig. 3.7.2. The capacitors shown in the Fig. 3.7.2 should be included in forming the two-port network at the sending and receiving ends. The rest of the procedure will be the same as described above.

### 3.7 REPRESENTATION OF UNTRANSPOSED LINES

It has already been mentioned that simple four-legged reactor scheme will not sufficiently reduce the secondary arc current on long untransposed lines because of unequal inter-phase capacitances. For these lines, if modified four-legged reactors<sup>10</sup> are used in conjunction with simple four-legged reactors, the scheme will effectively reduce the secondary arc current and recovery voltage.

#### 3.7.1 Modified Four-Legged Reactor Bank

The Modified Four-Legged Reactor<sup>10</sup> scheme was developed for high speed, single-pole reclosing on untransposed lines. The modified four-legged reactor bank includes four switches whose operations are co-ordinated with the line breakers. This scheme with associated neutral switch positions for various

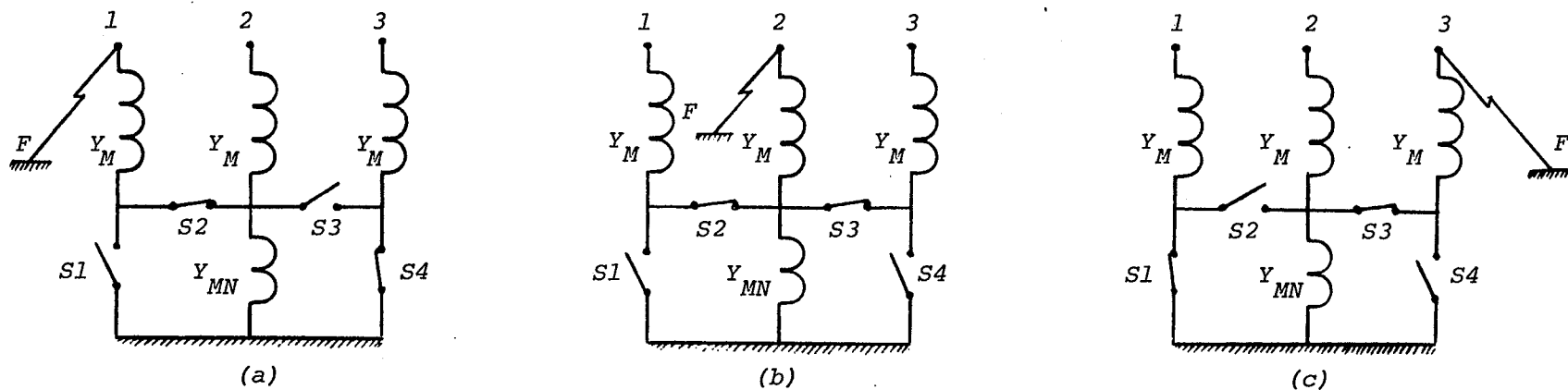
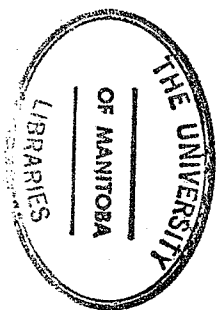


FIG. 3.15 - MODIFIED FOUR-LEGGED REACTOR BANK SWITCH POSITIONS FOR VARIOUS PHASE-TO-GROUND FAULTS:

- a) and c) OUTER PHASE FAULTS and
- b) MIDDLE PHASE FAULTS

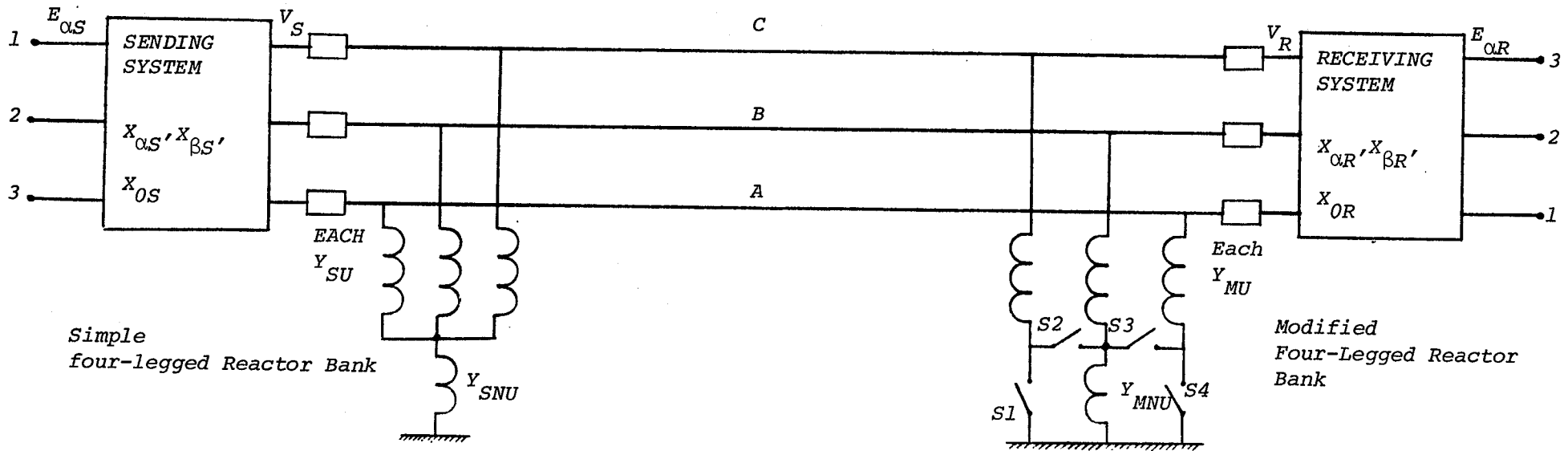


phase to ground faults is shown in the Fig. 3.15.

The equivalent capacitive admittance matrix for a transposed line is a symmetrical matrix with identical diagonal elements and identical off-diagonal elements. The equivalent admittance matrix of a simple four-legged reactor bank also has the same structure. Thus a simple four-legged reactor bank, in addition to its duty during system normal conditions, is used to compensate phase-to-phase and phase to ground capacitances of transposed transmission lines during single-pole switching to aid and ensure the secondary arc current extinction.

The equivalent capacitive admittance matrix of an untransposed line also is a symmetrical matrix, but neither the diagonal elements nor the off-diagonal elements are identical. For example, mid-to-outer phase capacitances for a 500 KV line is 3.5 to 3.7 times<sup>17</sup> larger than the outer-to-outer phase capacitances. Again for single-pole switching purposes, the reactive admittance matrix for the compensation banks must match the capacitive admittance matrix. The above scheme satisfies this condition. The simple four-legged reactor banks ensure sufficient compensation between outer phases; the modified four-legged reactor bank provides additional compensation required for the mid-to-outer phase capacitances.

The admittance matrices  $Y_M$  for Fig. 3.15(a), 3.15(b), and 3.15(c) are given by equations 3.8.1, 3.8.2 and 3.8.3, respectively.



FAULTED PHASE	SWITCH OPERATIONS			
	S1	S2	S3	S4
1	0	C	0	C
2	0	C	C	0
3	C	0	C	0

"0" = SWITCH CLOSED

"C" = SWITCH OPEN

FIG. 3.16 - SYSTEM REPRESENTATION WITH A SIMPLE AND A MODIFIED FOUR-LEGGED SHUNT REACTOR BANK

Fault on phase 1,

$$[Y_M] = \begin{bmatrix} Y'_{1M} & -Y'_{2M} & 0 \\ -Y'_{2M} & Y'_{1M} & 0 \\ 0 & 0 & Y_{1M} \end{bmatrix} \quad (3.8.1)$$

Fault on phase 2,

$$[Y_M] = \begin{bmatrix} Y_{1M} & -Y_{2M} & -Y_{2M} \\ -Y_{2M} & Y_{1M} & -Y_{2M} \\ -Y_{2M} & -Y_{2M} & Y_{1M} \end{bmatrix} \quad (3.8.2)$$

Fault on phase 3,

$$[Y_M] = \begin{bmatrix} Y_{1M} & 0 & 0 \\ 0 & Y'_{1M} & -Y'_{2M} \\ 0 & -Y'_{2M} & Y'_{1M} \end{bmatrix} \quad (3.8.3)$$

where  $Y'_{1M} = \frac{Y_M (Y_M + Y_{MN})}{(2Y_M + Y_{MN})}$ ,  $Y'_{2M} = \frac{Y_M^2}{2Y_M + Y_{MN}}$

and  $Y_{1M} = \frac{Y_M (2Y_M + Y_{MN})}{3Y_M + Y_{MN}}$ ,  $Y_{2M} = \frac{Y_M^2}{3Y_M + Y_{MN}}$

As mentioned earlier the admittance matrix for a simple four-legged reactor is similar to equation 3.8.2.

### 3.7.2 System Equivalent

A system diagram with a simple and modified four-legged shunt reactor bank has been shown in the Fig. 3.16. Its equivalent circuit is shown in the Fig. 3.17. The system is reduced to two buses ( $V_S$  and  $V_R$ ) connected by a pi-section which takes

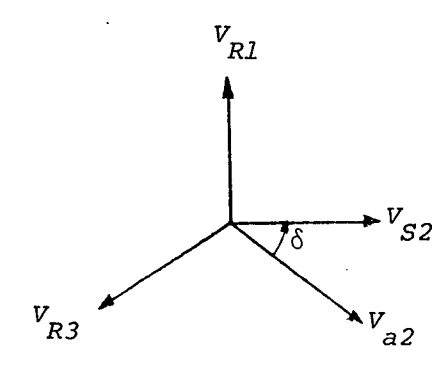
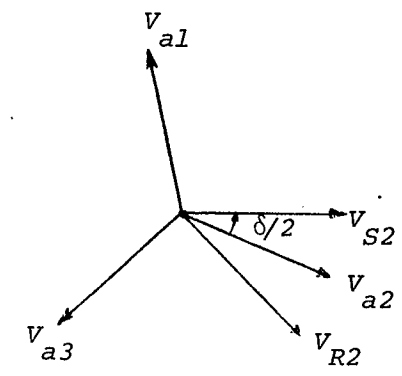
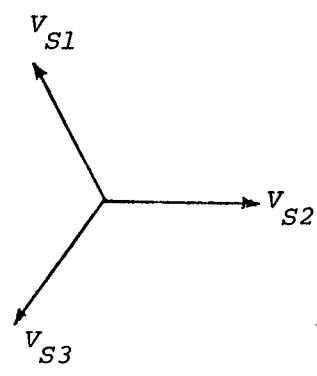
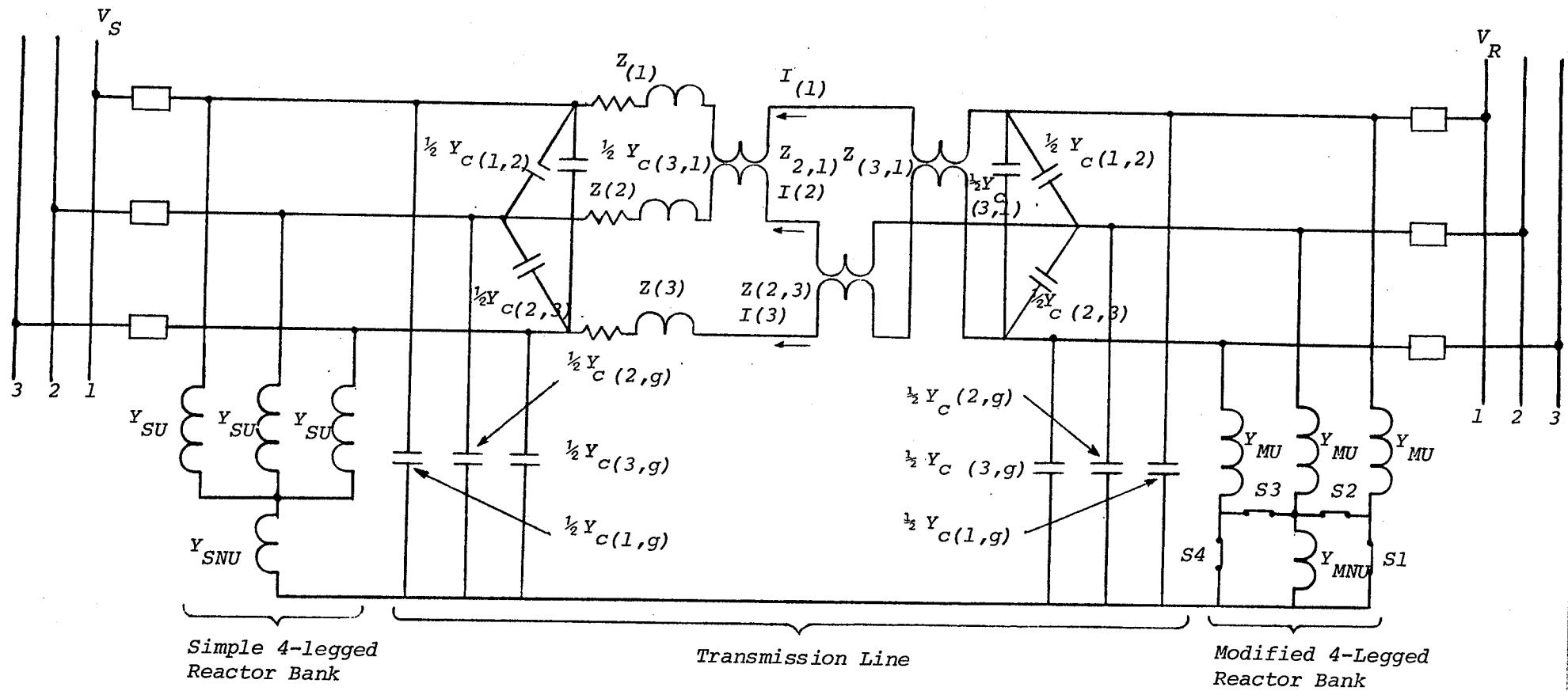


FIG. 3.17 - SYSTEM EQUIVALENT AND VECTOR DIAGRAMS FOR AN UNTRANSPPOSED LINE

into account the static and magnetic coupling between the phases.

Assuming that the breakers in faulted phase (i) are opened, the secondary current can be represented as:

$$I_{f(i)} = I_{c(i)} + I_{\ell(i)} \quad (3.9)$$

where  $I_{c(i)}$  is the electrostatic capacitive component and  $I_{\ell(i)}$  is the electromagnetic component.

The capacitive component  $I_{c(i)}$  mainly depends on the line voltage and the interphase admittances, namely

$$I_{c(i)} = Y_{eq(i,h)} V_a(h) + Y_{eq(i,k)} V_a(k) \quad (3.10)$$

where  $Y_{eq(i,h)}$  and  $Y_{eq(i,k)}$  are equivalent interphase admittances between the faulted phase (i) and healthy phases (h and k).

The inductive coupling  $I_{\ell}$  depends, mainly, on the load current in the healthy phases ( $I_{(h)}$  and  $I_{(k)}$ , their inductive coupling to the opened phase ( $X_{i,h}$  and  $X_{i,k}$ ) and the equivalent phase to ground admittance  $Y_{eq(i,g)}$  of the opened phase 'i'. That is:

$$I_{\ell(i)} = - Y_{eq(i,g)} \left\{ I_{(h)} X_{(i,h)} + I_{(k)} X_{(i,k)} \right\} \quad (3.11)$$

The general equation for the total secondary arc current ( $I_f$ ) can be expressed by substituting equations (3.10) and (3.11) in equation (3.9):

$$I_{f(i)} = Y_{eq(i,h)} V_a(h) + Y_{eq(i,k)} V_a(k) - Y_{eq(i,g)} \left\{ I_{(h)} X_{(i,h)} + I_{(k)} X_{(i,k)} \right\} \quad (3.12)$$



Appendix B shows the detailed circuit analysis which leads to the expressions for  $V_{ff}$  and  $I_f$  for various cases.

### 3.7.3 Useful Shunt Reactor Arrangements

The main goal for single-phase switching (SPS) schemes is to reduce the magnitude of secondary arc current ( $I_f$ ) to a given value ( $I_{min}$ ) which will ensure the arc extinction during SPS dead time. The most frequent arrangements are given in Fig. 3.18, arrangement A, B and C, respectively.

Arrangement A is the most typical and therefore, the most important reactor arrangement. This can be mainly used for long transmission lines. This scheme is being considered for analysis in this thesis.

A modified four-legged reactor bank can be used to reduce the secondary arc current ( $I_f$ ) on relatively short transmission lines which require only one shunt reactor for normal system conditions. This is the arrangement B, shown in Fig. 3.18.

Extra long EHV transmission lines may be compensated by three shunt reactor banks as shown in the arrangement C of Fig. 3.18. A modified four-legged reactor bank at one line terminal and the second modified bank with a simple four-legged reactor at the other terminal, can be used in this scheme. In this case the optimum neutral reactances can be obtained assuming that the relative impedances  $\frac{X_{mn}}{X_m}$  for both modified reactor banks are equal. Equivalent admittances  $Y_{(i,h)}$ ,  $Y_{(i,k)}$  and  $Y_{(i,g)}$  for the arrangement A are defined in Appendix B.

NOTE:

- \* RM = MODIFIED FOUR-LEGGED REACTOR BANK
- RS = SIMPLE FOUR-LEGGED REACTOR BANK

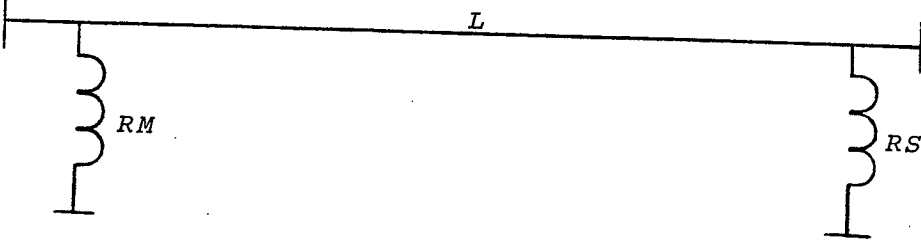
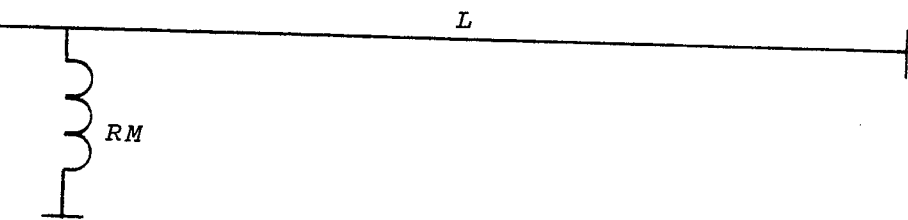
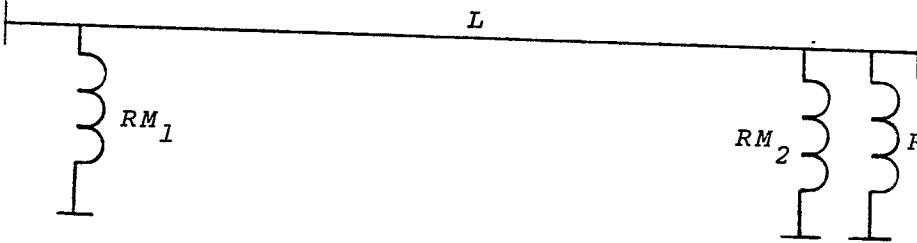
ARRANGEMENT	REACTOR LOCATIONS*
A	
B	
C	

FIG. 3.18 - SHUNT REACTOR ARRANGEMENTS ON UNTRANSPOSED TRANSMISSION LINES

### 3.8 STUDY ON A DIGITAL COMPUTER

For the study of this problem on a digital computer, the circuits of Figs. 3.3 and 3.17 were used. The study was made on an IBM 370/168 computer. The digital program is written in FORTRAN and implemented by the IBM WATFIV compiler.

Various computer programs were written to compute the value of  $V_{ff}$ , which in some cases, required a very involved programming. As may have been observed in sections 3.5.2 and 3.7.2, the process of solution consists of many repetitive steps. Therefore, the programs written for the computation of  $V_{ff}$  are based on a number of sub-routines.

It is not necessary to enumerate the various advantages associated with digital computing with reference to accuracy, and ease of formulating the input data, etc. These are all quite well known. However, as a check, some of the results obtained were compared with those obtained from field tests,<sup>19</sup> and other digital and transient Network Analyses studies.<sup>17, 20</sup>

CHAPTER IV

NUMERICAL ANALYSIS AND RESULTS

A simplified analysis of the basic problem has been made and the methods of system representation and solution have been studied. In this chapter numerical details of the system and a summary of the various cases studied (in the form of tables and graphs) are given.

4.1 SYSTEM STUDIED

A single line diagram of the system studied has already been shown in Fig. 3.1. The transmission line used<sup>18</sup> for the study has constants as shown in Table 4.1.

TABLE 4.1

---

Base Quantities

Base Power	=	1000 MVA
Base Voltage	=	500 KV (L-L)
Base Current	=	1150 A
Base Impedance	=	250 $\Omega$

Line Construction

320 Km, Flat Tower Configuration, 3 conductor bundle

Line Spacing

Phase-to-phase = 12.20 meters

Phase-to-ground = 22.25 meters

Conductor Size

954 MCM, ACSR 45/7

Line Parameters

Transposed

- Positive Sequence Resistance ,  $r_1 = 0.0232$  ohms/km
- Positive Sequence Inductance ,  $\ell_1 = 9.45 \times 10^{-4}$  henries/km
- Positive Sequence Capacitance ,  $c_1 = 1.23 \times 10^{-8}$  farads/km
- Zero Sequence Resistance ,  $r_0 = 0.386$  ohms/km
- Zero Sequence Inductance ,  $\ell_0 = 3.23 \times 10^{-3}$  henries/km
- Zero Sequence Capacitance ,  $c_0 = 8.40 \times 10^{-9}$  farads/km

from which,

Line impedance matrix:

$$[Z] = \begin{bmatrix} .144 + j.642 & .121 + j.286 & .121 + j.286 \\ .121 + j.286 & .144 + j.642 & .121 + j.286 \\ .121 + j.286 & .121 + j.286 & .144 + j.642 \end{bmatrix} \text{ ohms/km}$$

Line admittance matrix:

$$[Y] = \begin{bmatrix} j4.146 & -j.493 & -j.493 \\ -j.493 & j.4.146 & -j.493 \\ -j.493 & -j.493 & j.4.146 \end{bmatrix} \times 10^{-6} \text{ mhos/km}$$

Untransposed

Line impedance matrix:

$$[Z] = \begin{bmatrix} .111 + j.580 & .110 + j.236 & .108 + j.188 \\ .110 + j.236 & .132 + j.576 & .110 + j.236 \\ .108 + j.188 & .110 + j.236 & .111 + j.580 \end{bmatrix} \text{ ohm/km}$$

Line admittance matrix:

$$[Y] = \begin{bmatrix} j4.059 & -j.657 & -j.185 \\ -j.657 & j4.193 & -j.657 \\ -j.185 & -j.657 & j4.059 \end{bmatrix} \times 10^{-6} \text{ mhos/km}$$

4.2 SUMMARY OF CASES STUDIED AND BASE CASE

A base case with parameter values shown in the Table

4.2.1 was studied. A number of cases were studied by varying

TABLE 4.2.1

Transmission Line Length	320 Km
$V_S$ , $V_R$	1.0 p.u.
$\delta$	25° (1.06 p.u. power)
$X_{\alpha S}$ , $X_{\alpha R}$	0.25 p.u.
$X_{0S}/X_{\alpha S}$ , $X_{0R}/X_{\alpha R}$	0.5

the magnitudes of the parameters of the base case, one at a time. All of these cases are described in Table 4.2.2. Under the column "Remarks" only the parameter being varied is indicated, all other parameters being assumed to have the base case values. Unless otherwise mentioned,  $Q_{RST}$  and  $X_{SNT}$  for transposed lines are 120 MVAR and 155  $\Omega$  (for  $F = .65$ ), respectively, at each end. For untransposed lines the values of  $Q_{RSU}$  at the S.E. and  $Q_{RMU}$  at the R.E. are 135 MVAR (for  $F = 0.7$ ) each. The neutral reactor values for  $X_{SNU}$  and  $X_{MNU}$  are 90  $\Omega$  and 60  $\Omega$  respectively. These are the optimum values selected to minimize  $V_{ff}$  at the mid-point of the line. All the reactor values for untransposed lines have been obtained by using the optimization technique described in the literature.<sup>10</sup> Also it may be noted that for the sake of clarity, graphs are drawn only for the extreme values of the parameters being varied (see Fig. 4.1.2). However, the effect of entire range of such variation is indicated by another set of graphs (see Fig. 4.1.3). The maximum (or minimum) values of  $V_{ff}$

TABLE 4.2.2

CASE NUMBER	REF. FIGURE	REMARKS
1.1	4.1.1	Base case; as mentioned in Table 4.2.1
1.2	4.1.2 4.1.3	$X_{\alpha S}$ varied - 0 to 0.6 p.u.; $X_{\alpha S} = X_{\alpha R}$
1.3	4.1.4 4.1.5	$X_{OS}/X_{\alpha S}$ varied - 0.5 to 1.5; $X_{OS}/X_{\alpha S} = X_{OR}/X_{\alpha R}$
1.4	4.1.6 4.1.7	$V_S/V_R$ varied - 0.95 to 1.15; $V_R = 1$ p.u.
1.5	4.1.8 4.1.9	$\delta$ varied - 0 to 45°
1.6	4.1.10 4.1.11	Line length varied - 80 to 480 km (at 1.0 p.u. power)
1.7	4.1.12	Line length varied - 80 to 480 km ( $\delta = 25^\circ$ )

indicated by these graphs, have been plotted in this manner to indicate the range of variation of  $V_{ff}$  over the entire line length.

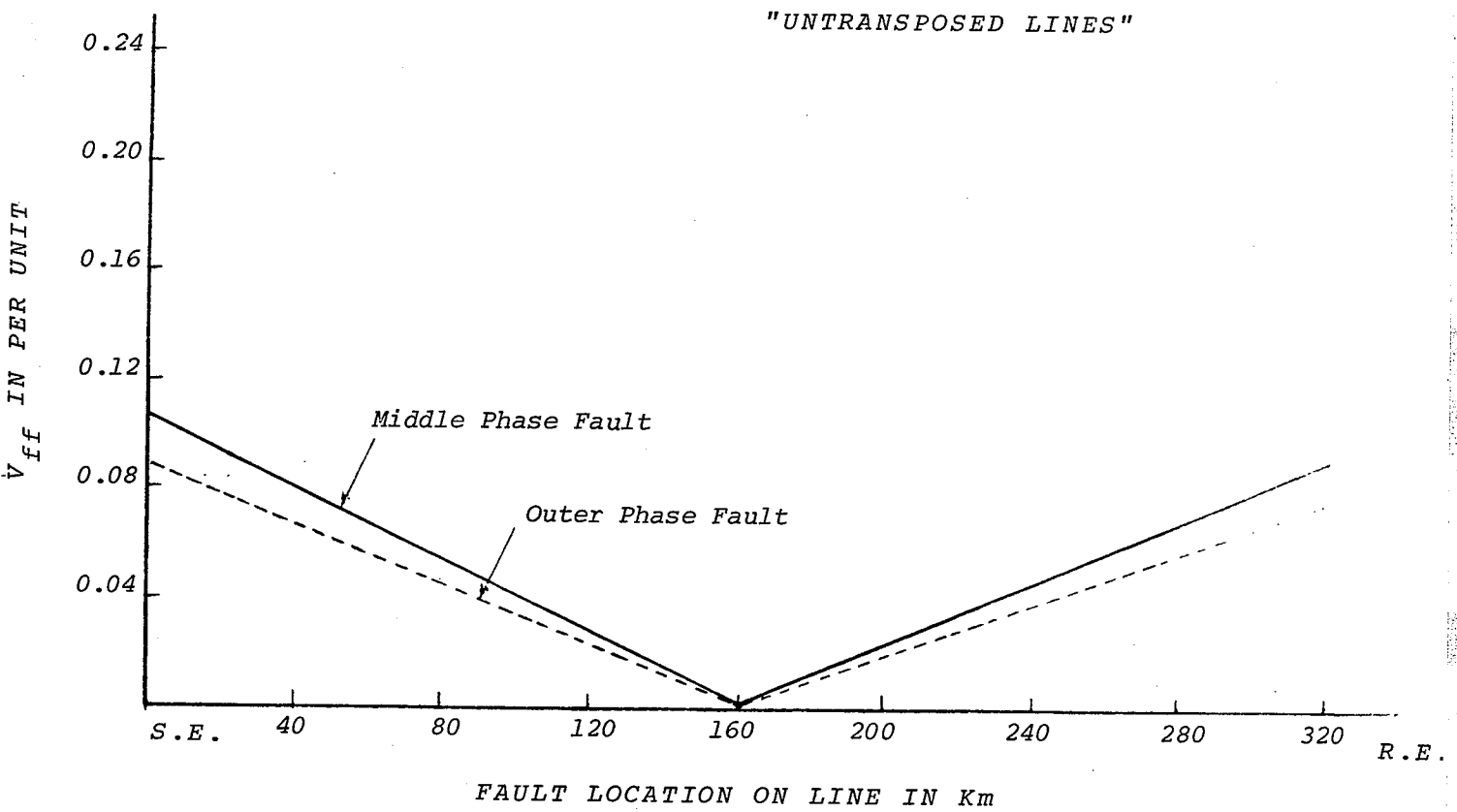
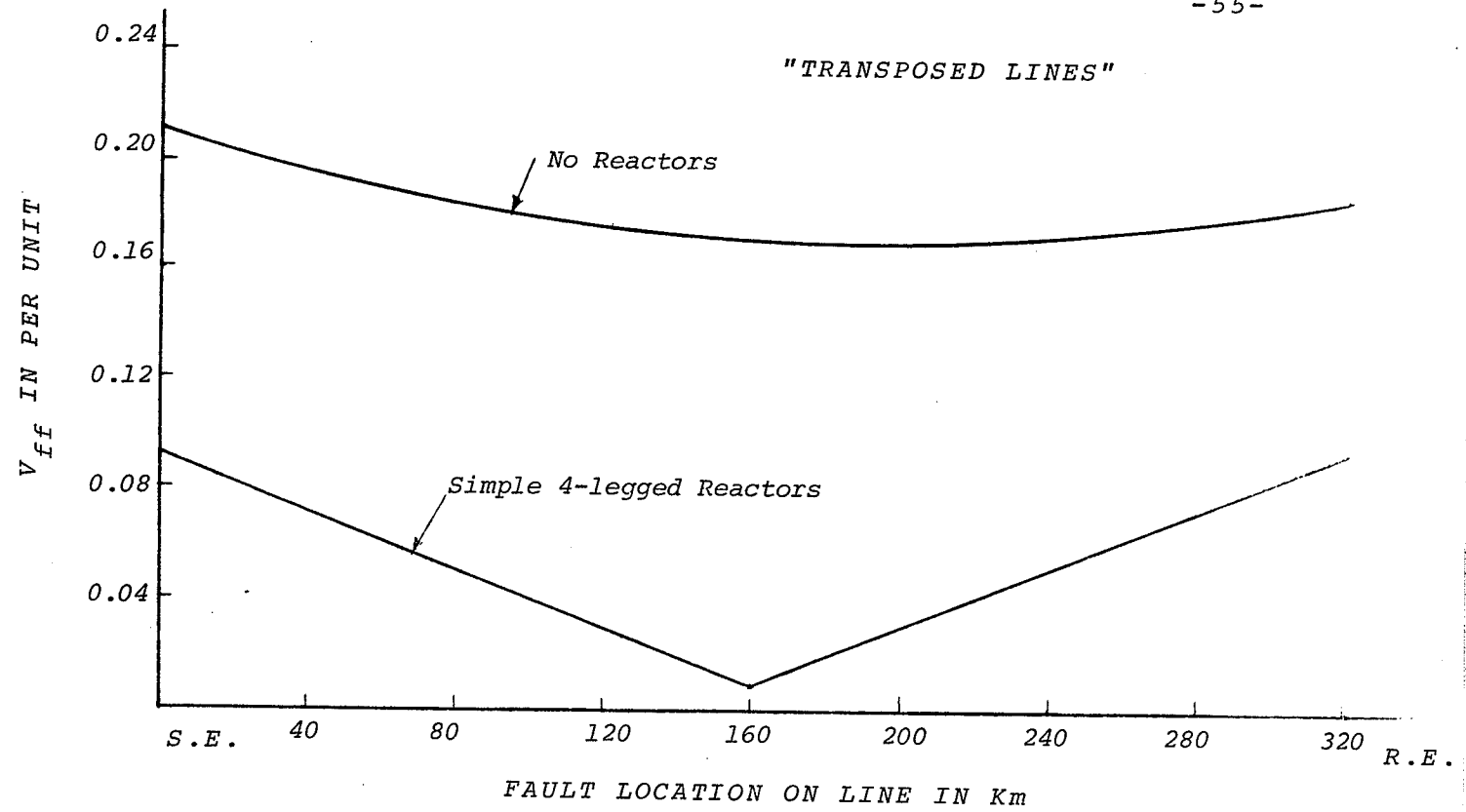


FIG. 4.1.1 - BASE CASE;  $V_{ff}$  AS A FUNCTION OF FAULT LOCATION



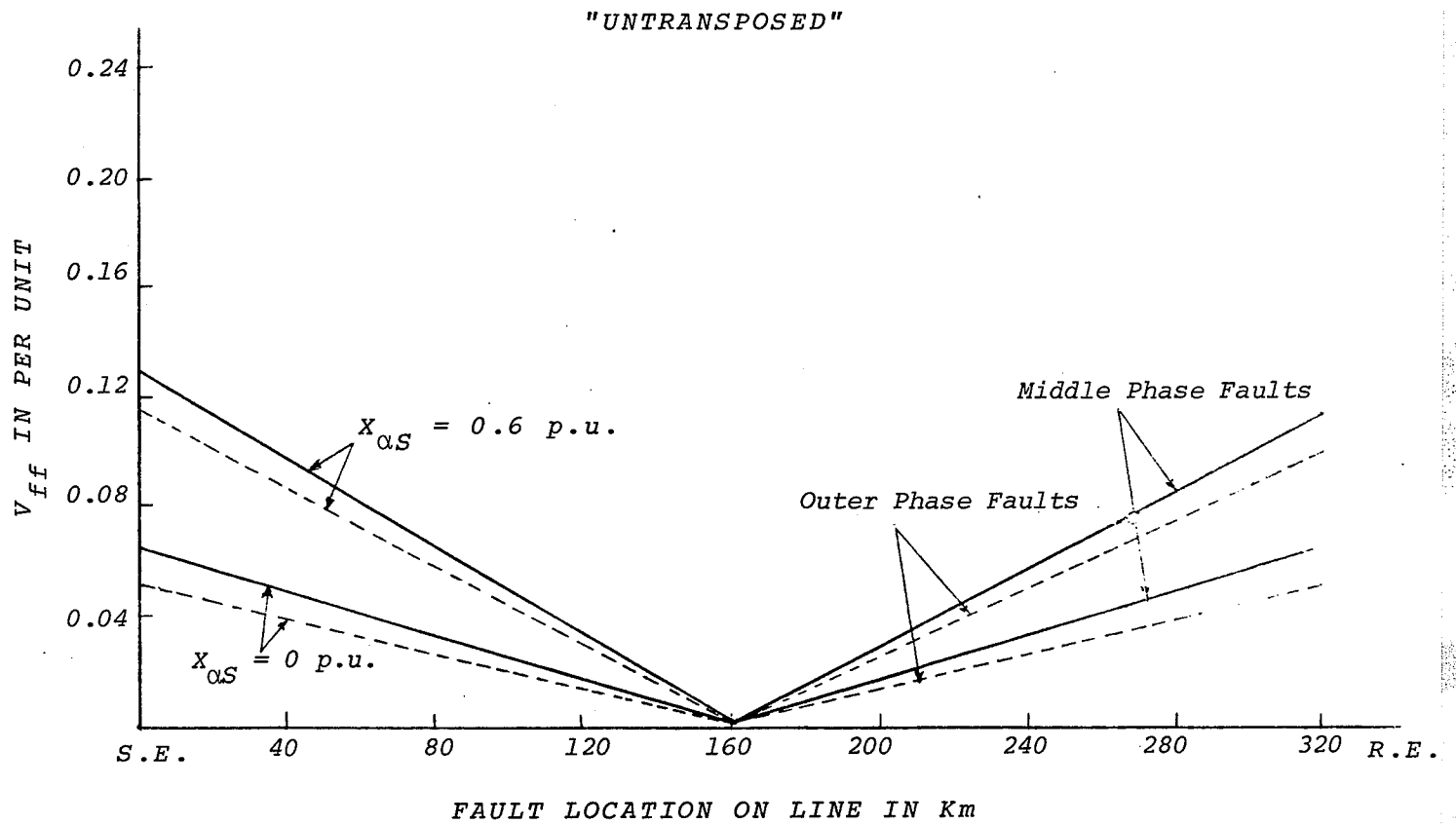
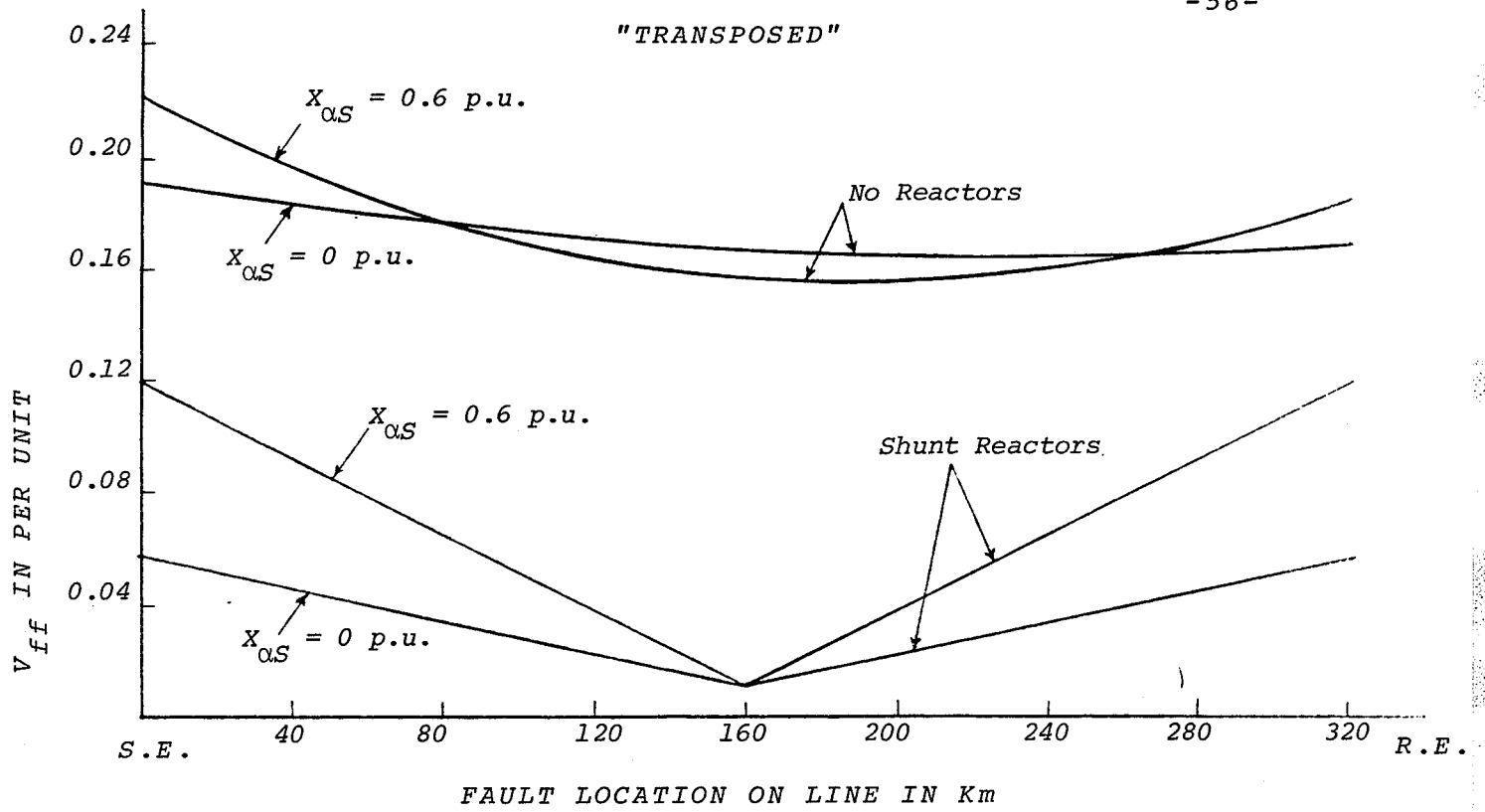
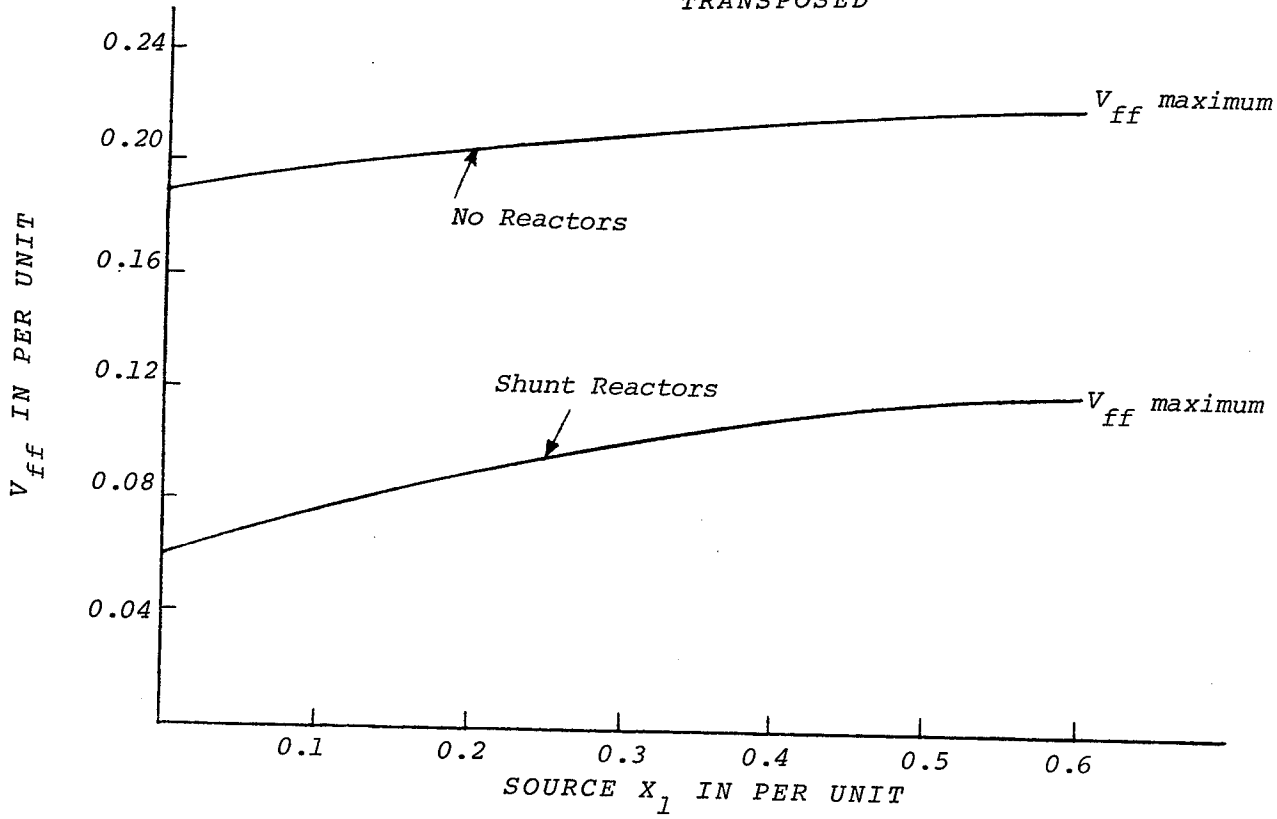


FIG. 4.1.2 - PROFILE OF  $V_{ff}$  FOR TWO VALUES OF SOURCE  $X_1$



"UNTRANSPOSED"

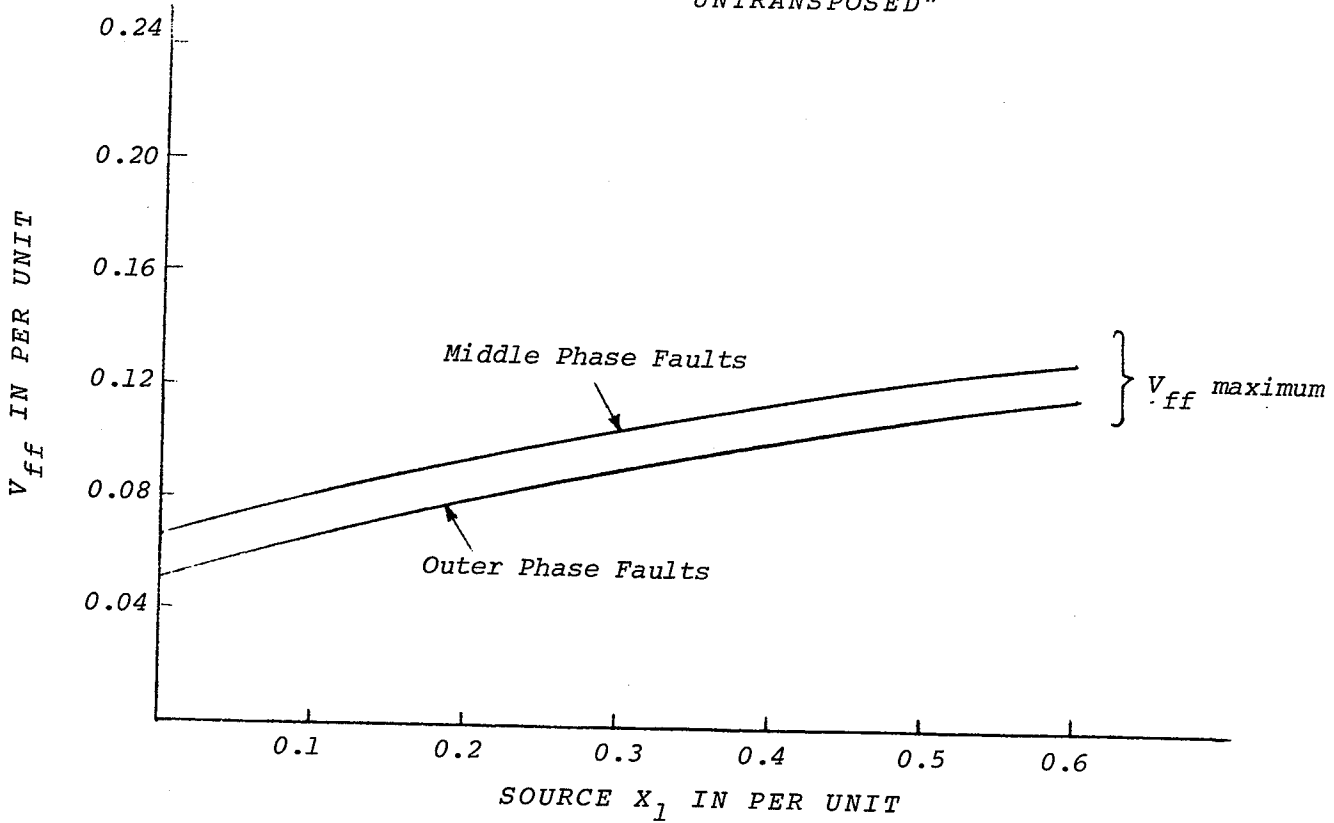


FIG. 4.1.3 - EFFECT OF SOURCE  $X_1$  VARIATION

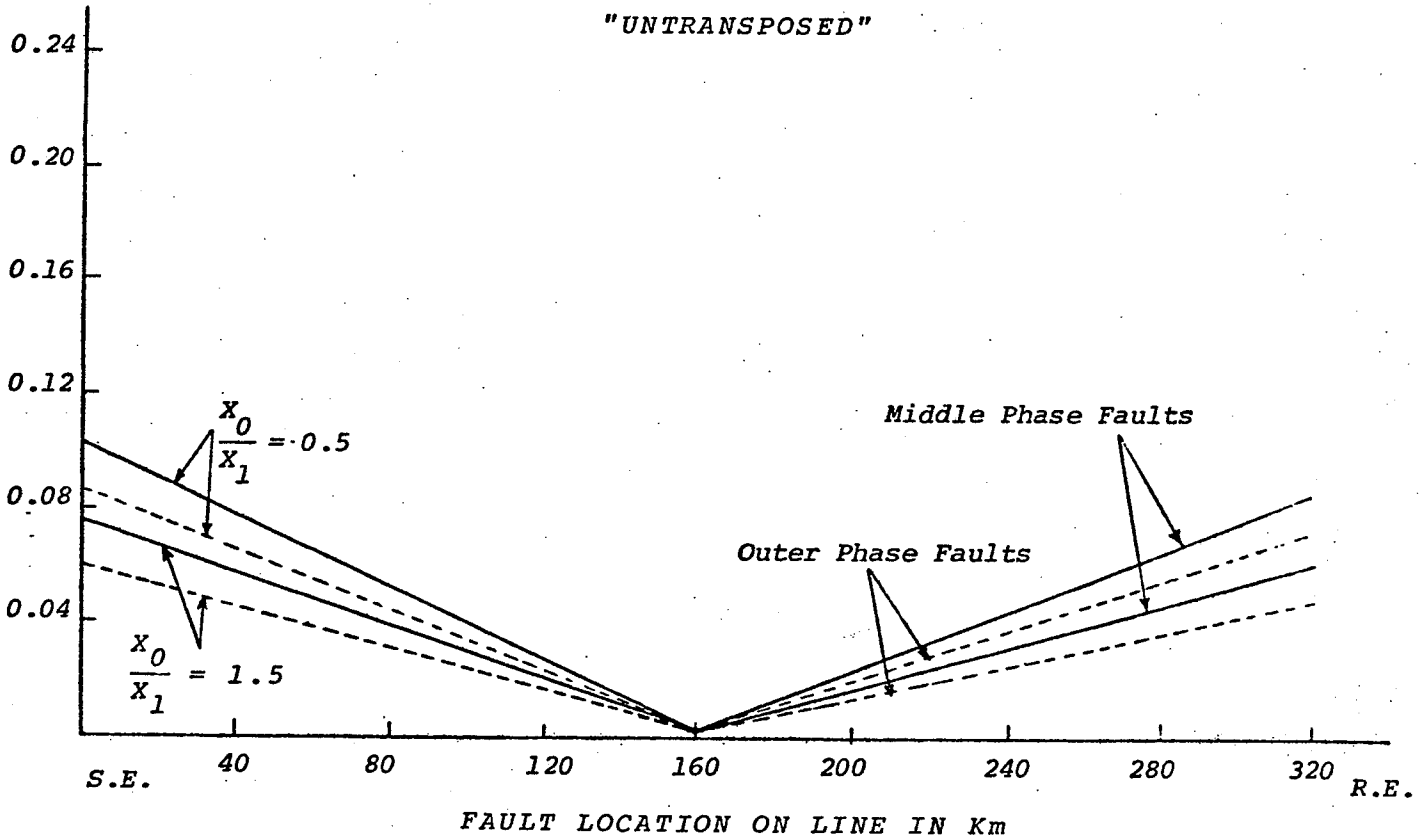
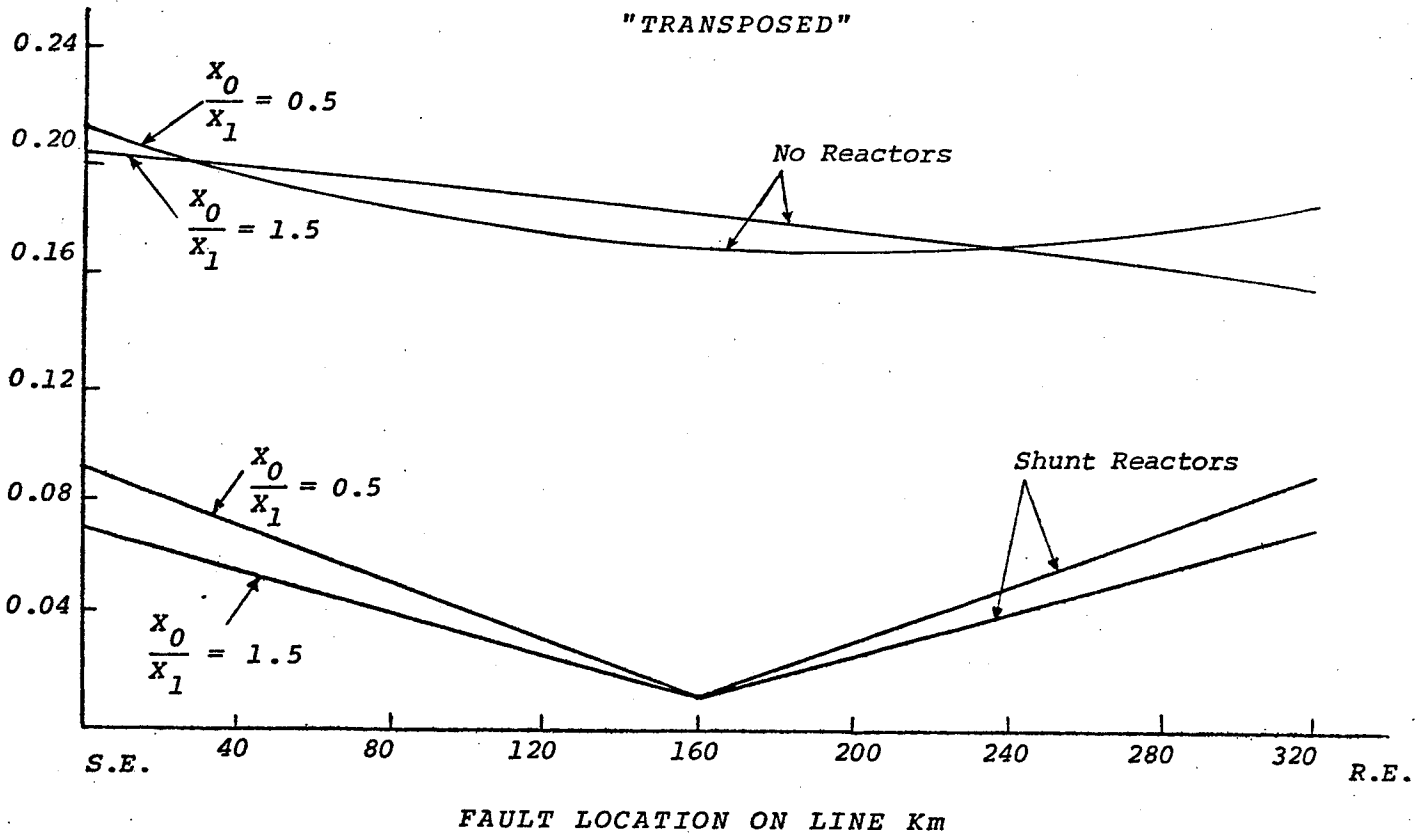


FIG. 4.1.4 - PROFILE OF  $V_{ff}$  FOR TWO VALUES OF SOURCE  $\frac{x_0}{x_1}$

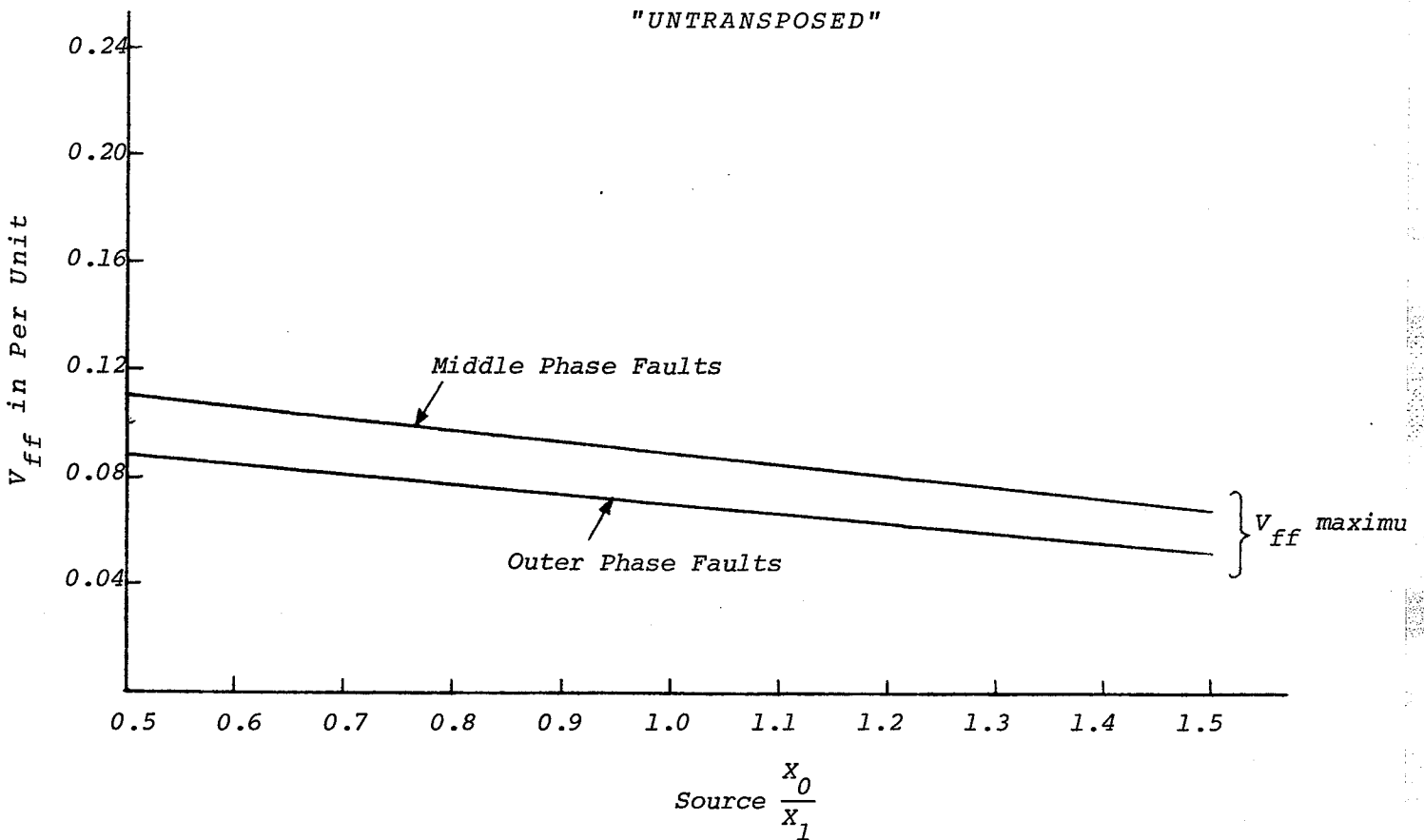
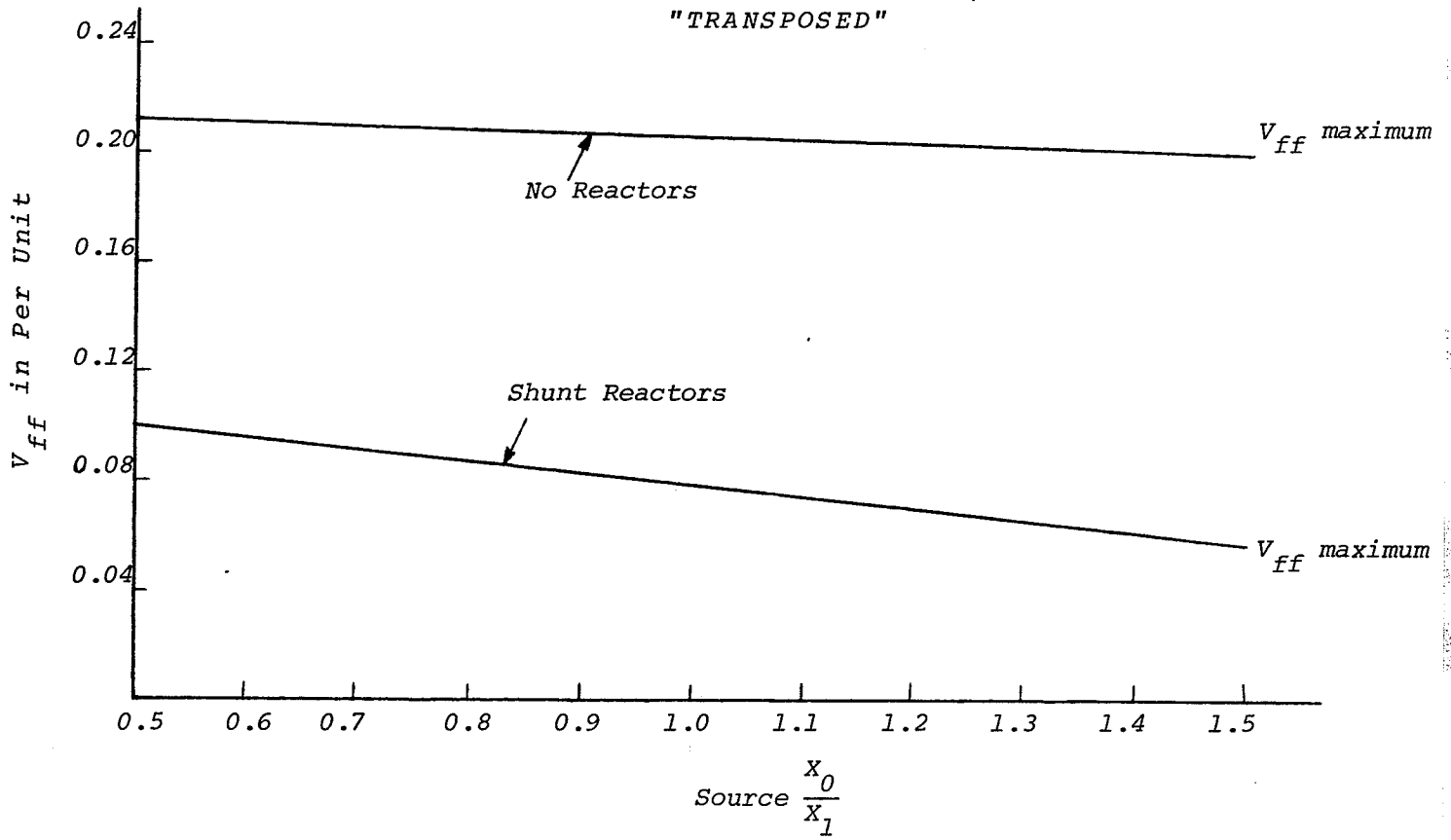


FIG. 4.1.5 - EFFECT OF SOURCE  $\frac{X_0}{X_1}$

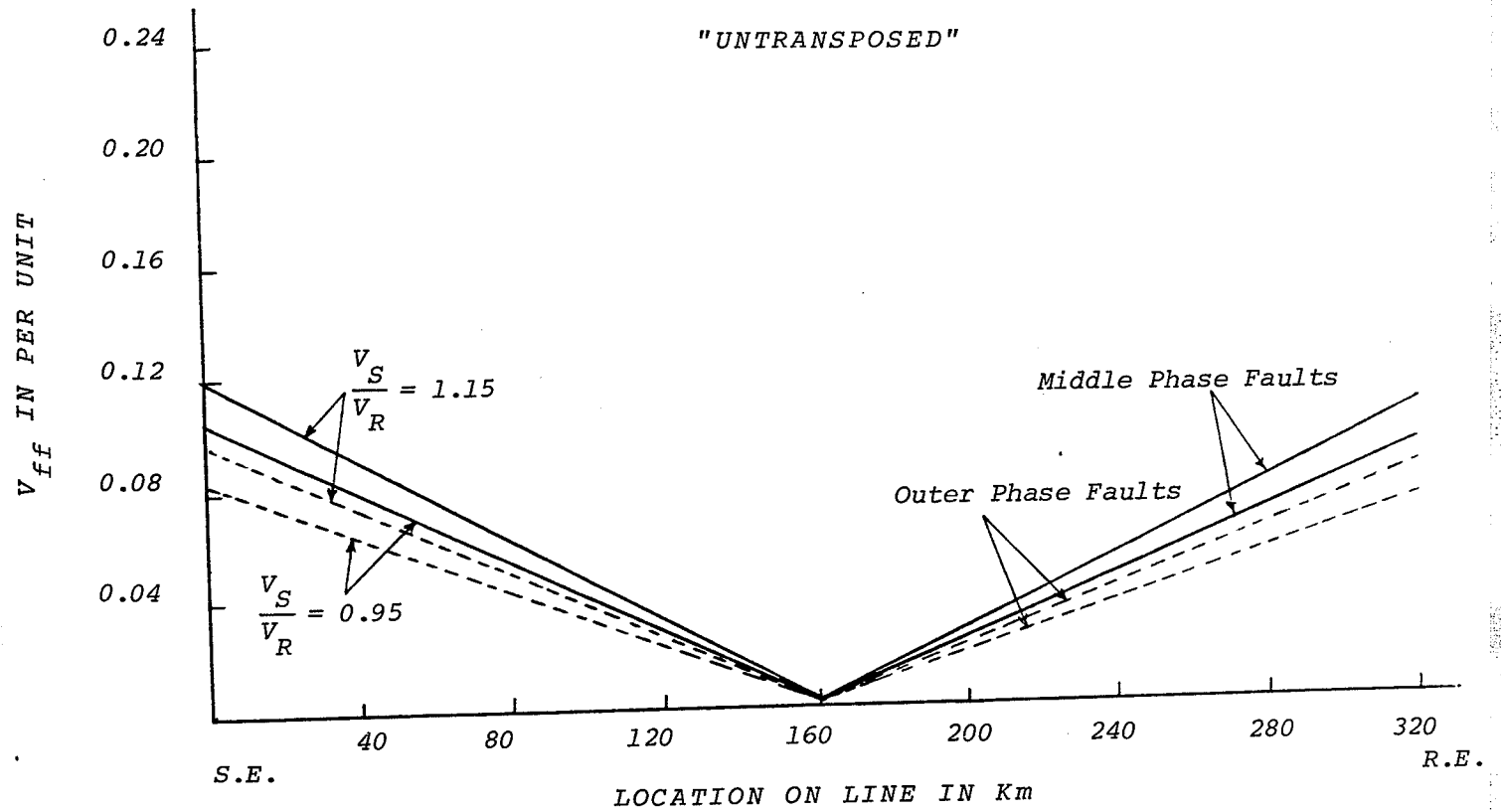
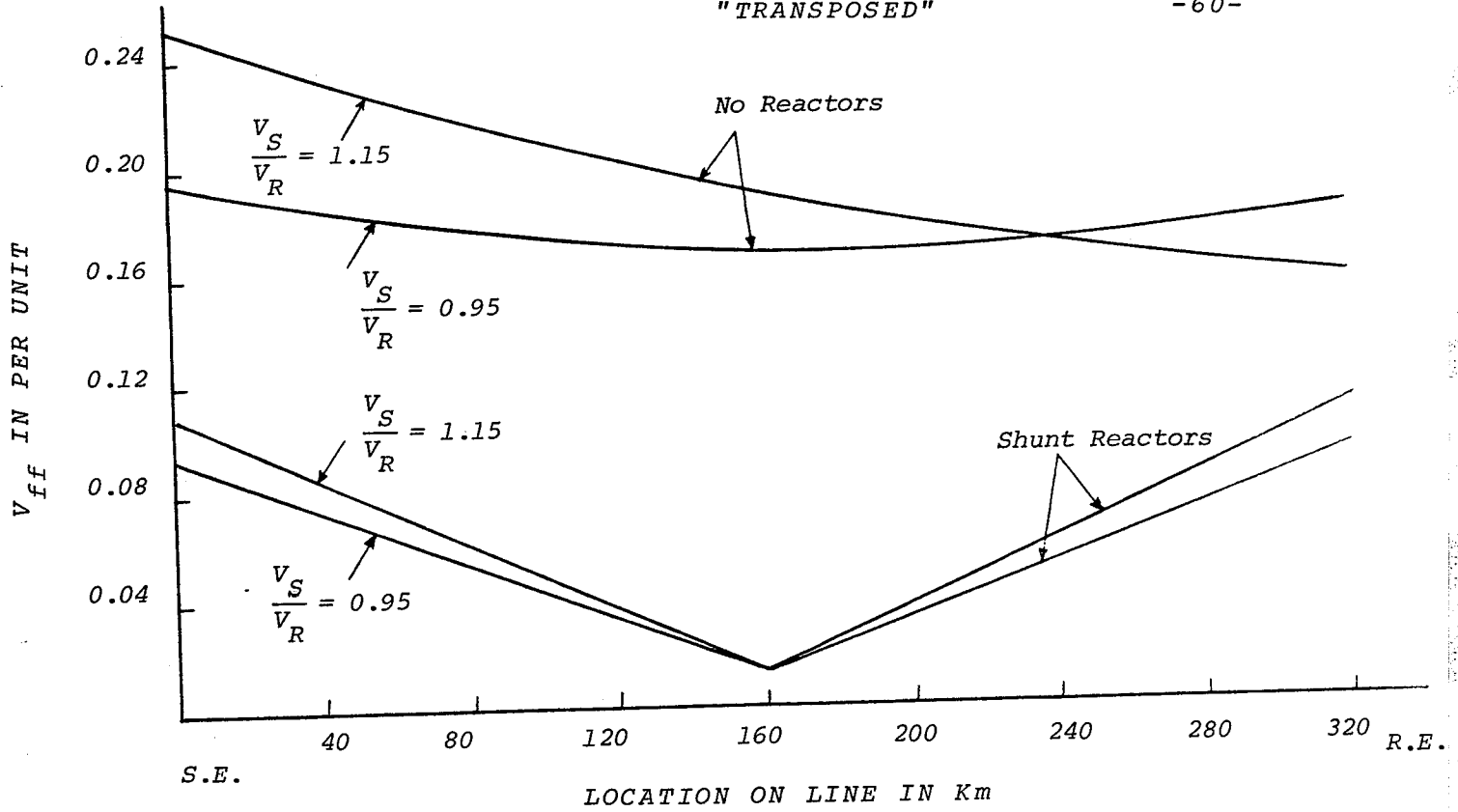
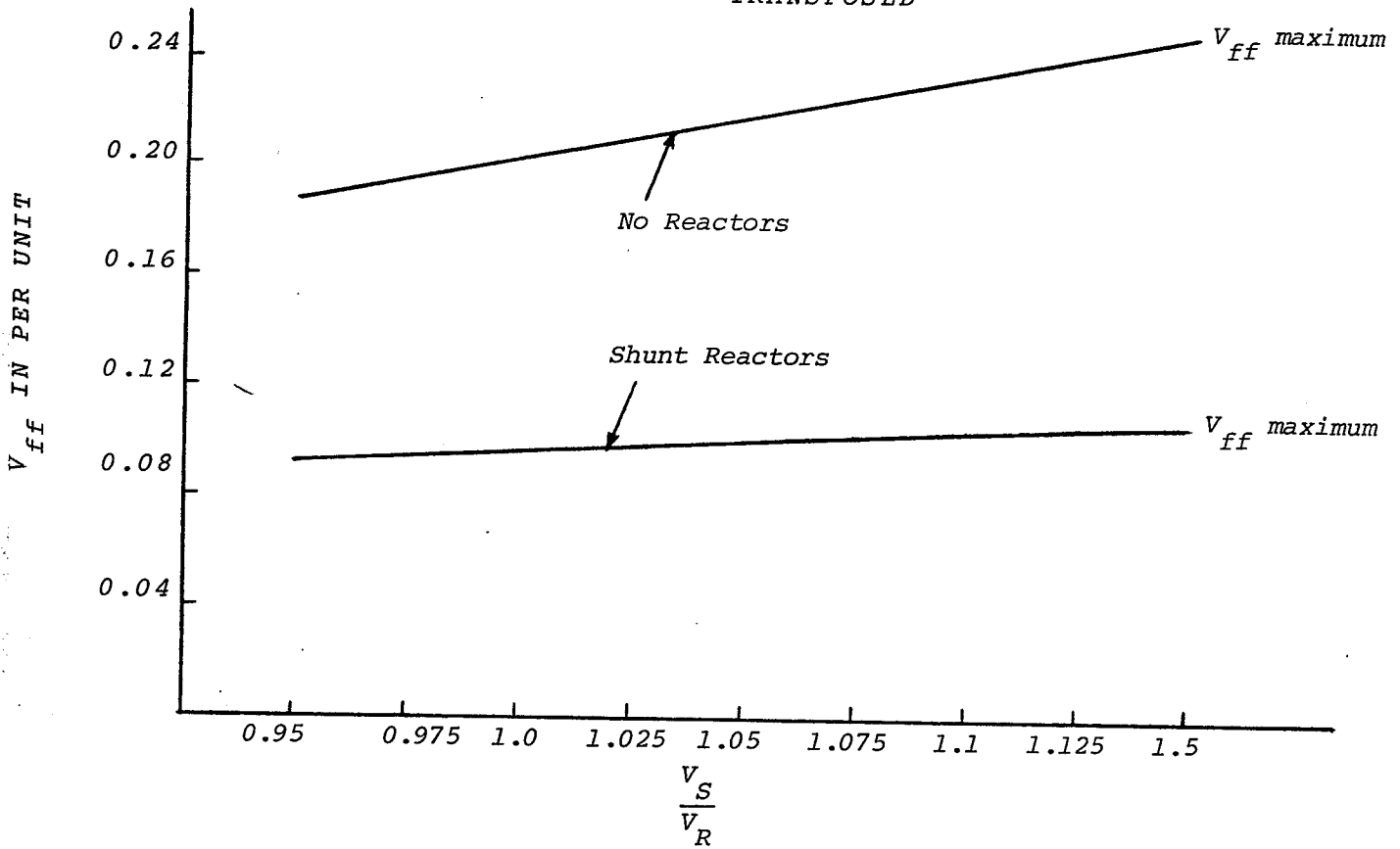


FIG. 4.1.6 - PROFILE OF  $V_{ff}$  FOR TWO VALUES OF  $\frac{V_S}{V_R}$

"TRANSPOSED"



"UNTRANSPOSED"

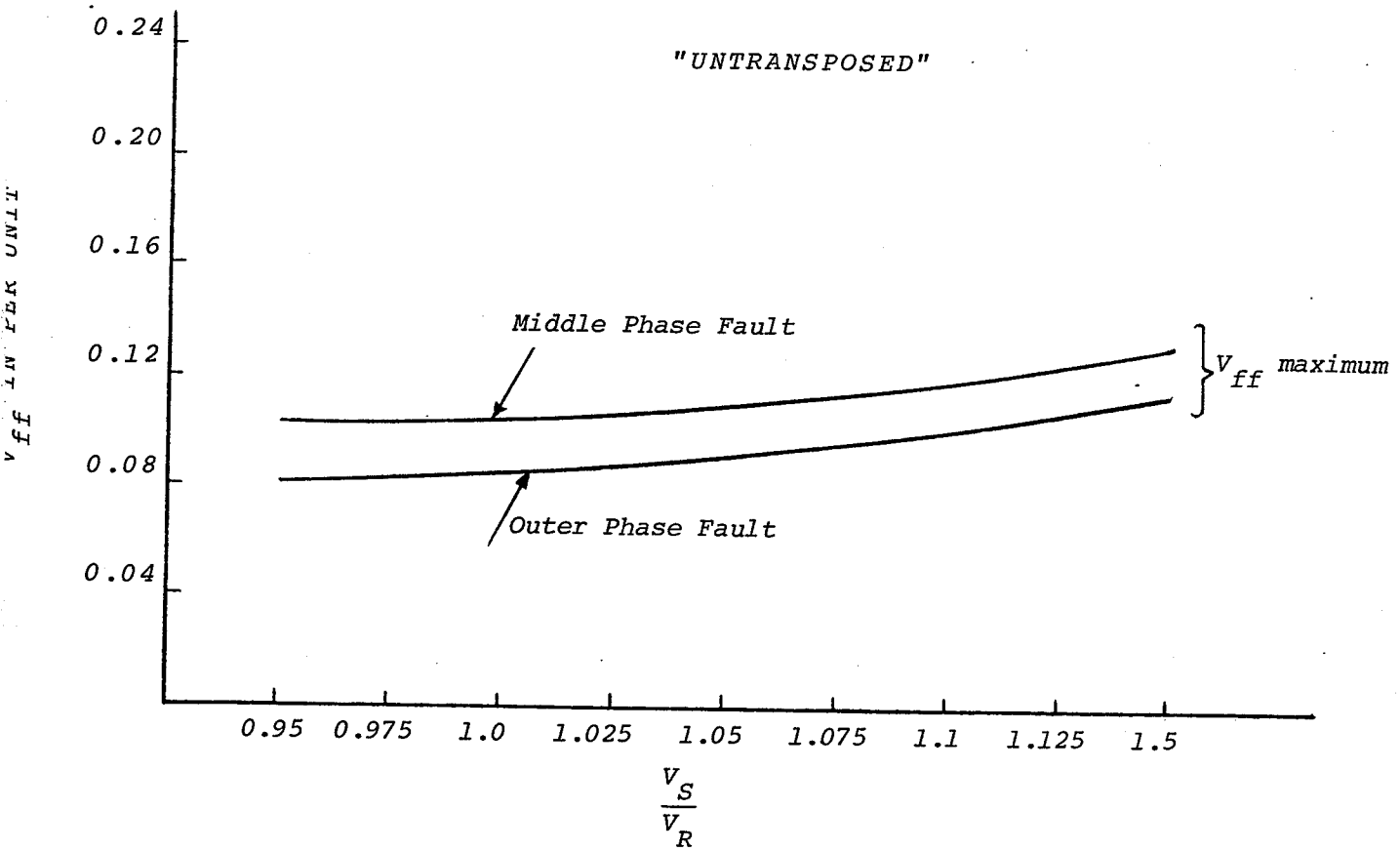


FIG. 4.1.7 - EFFECT OF VARIATION OF  $\frac{V_S}{V_R}$

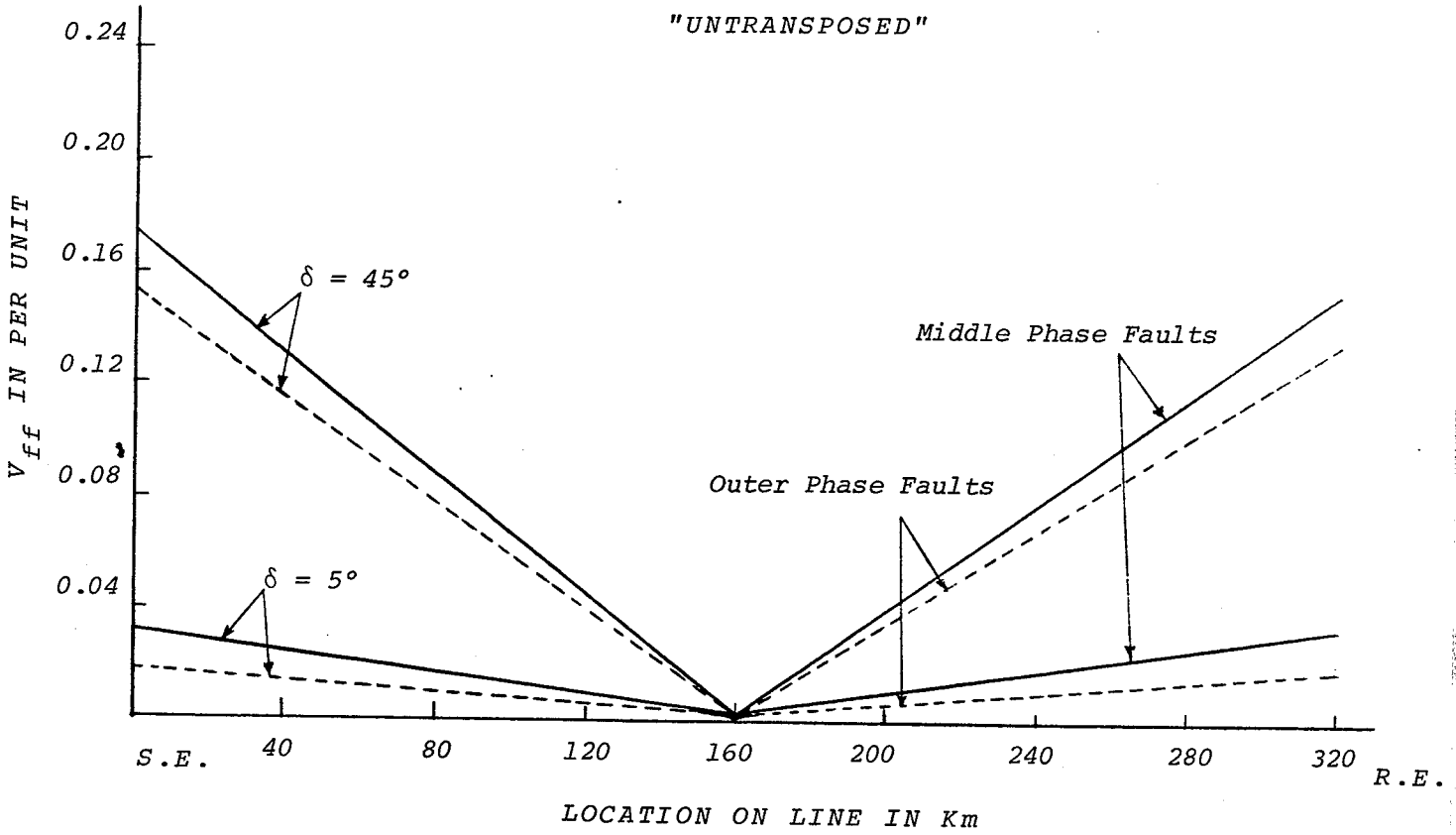
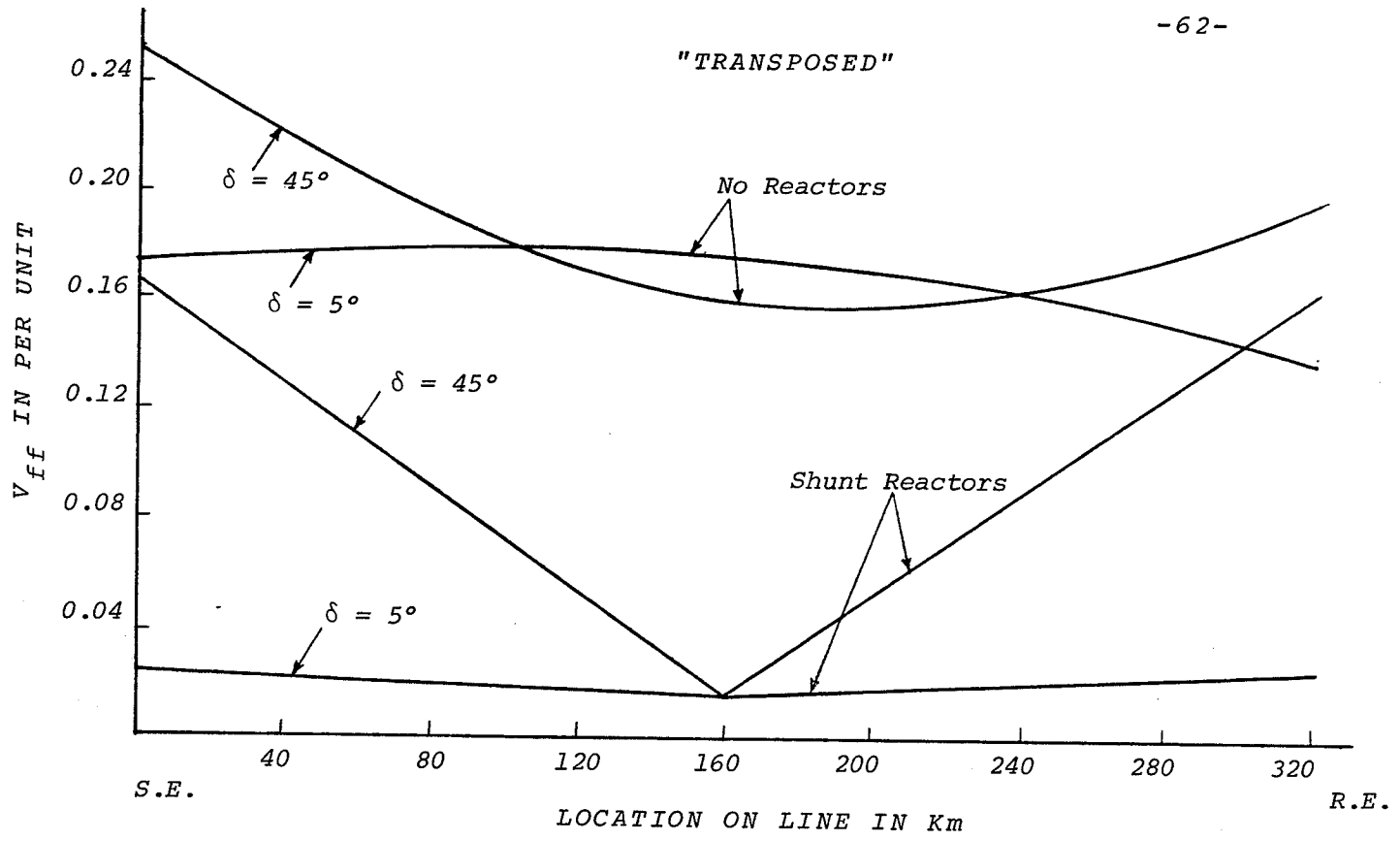
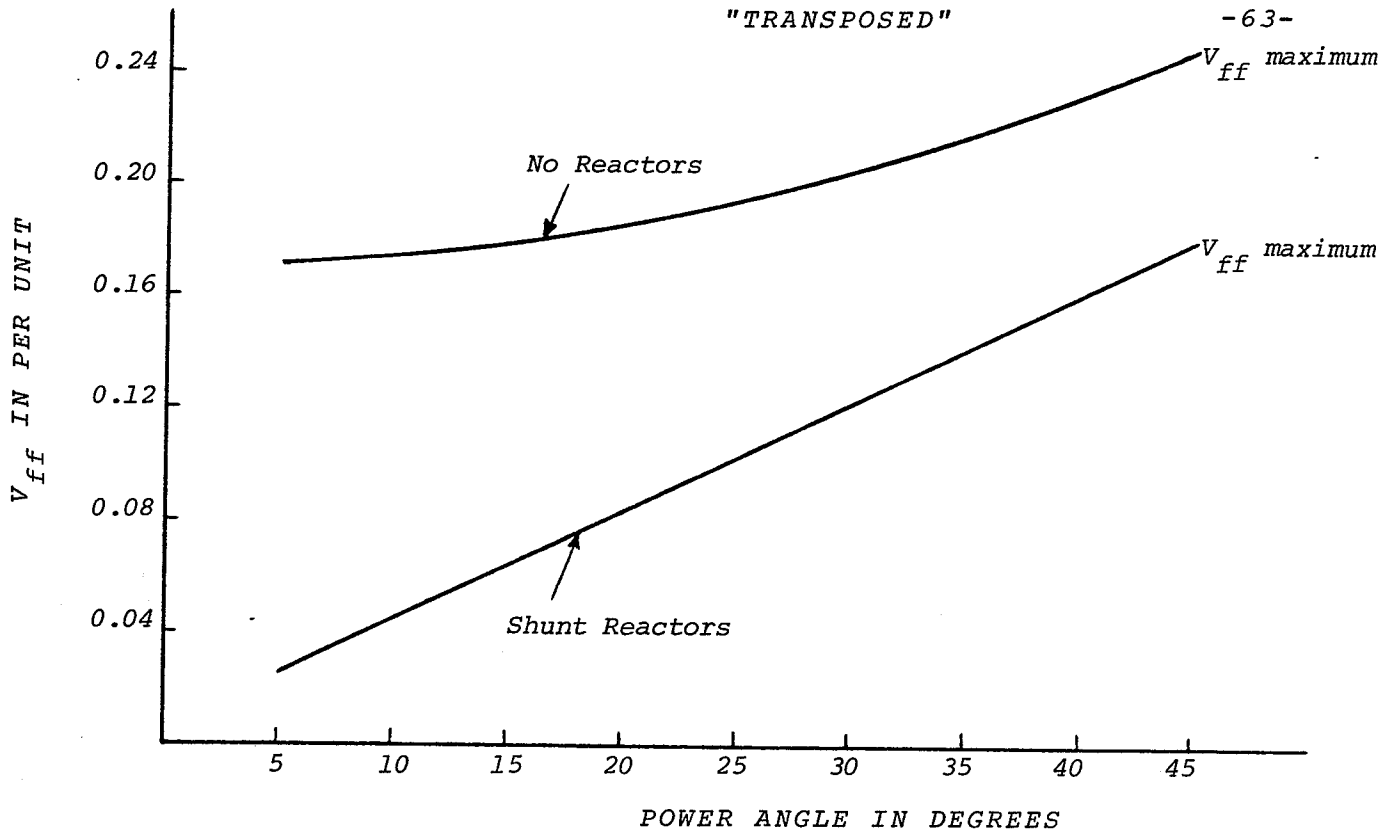


FIG. 4.1.8 - PROFILE OF  $V_{ff}$  FOR TWO VALUES OF  $\delta$

"TRANSPOSED"

-63-



"UNTRANSPOSED"

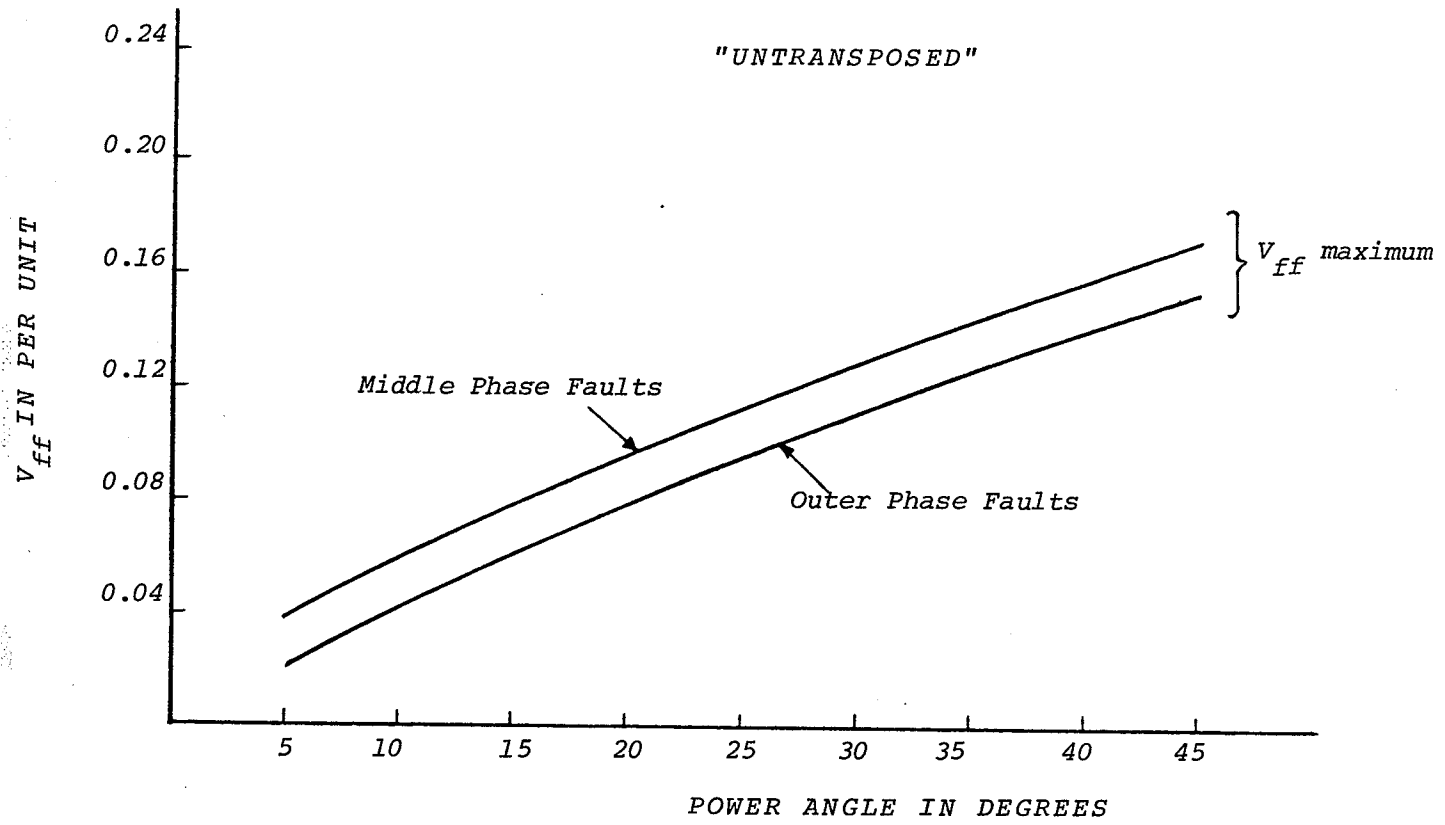


FIG. 4.1.9 - EFFECT OF VARIATION OF  $\delta$



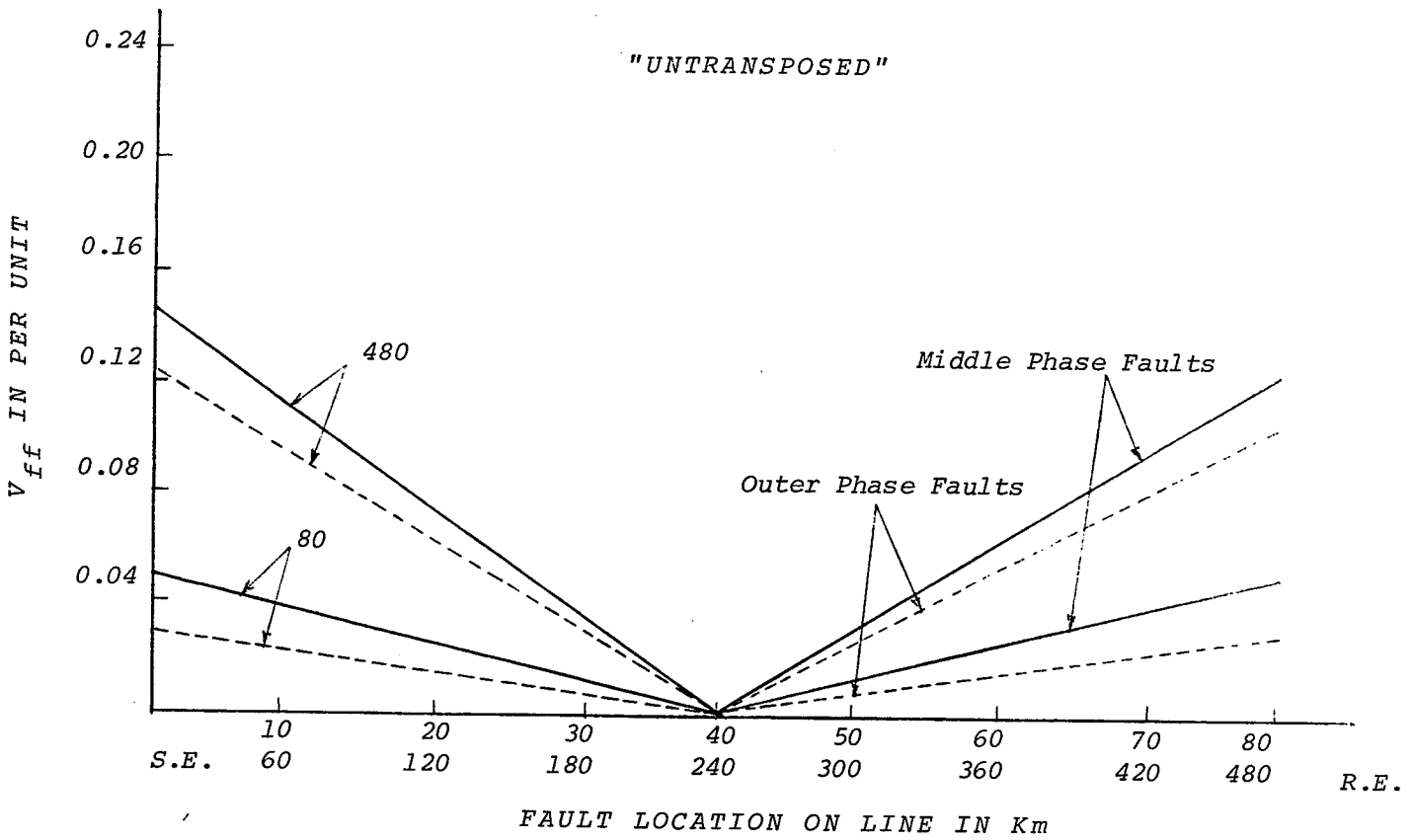
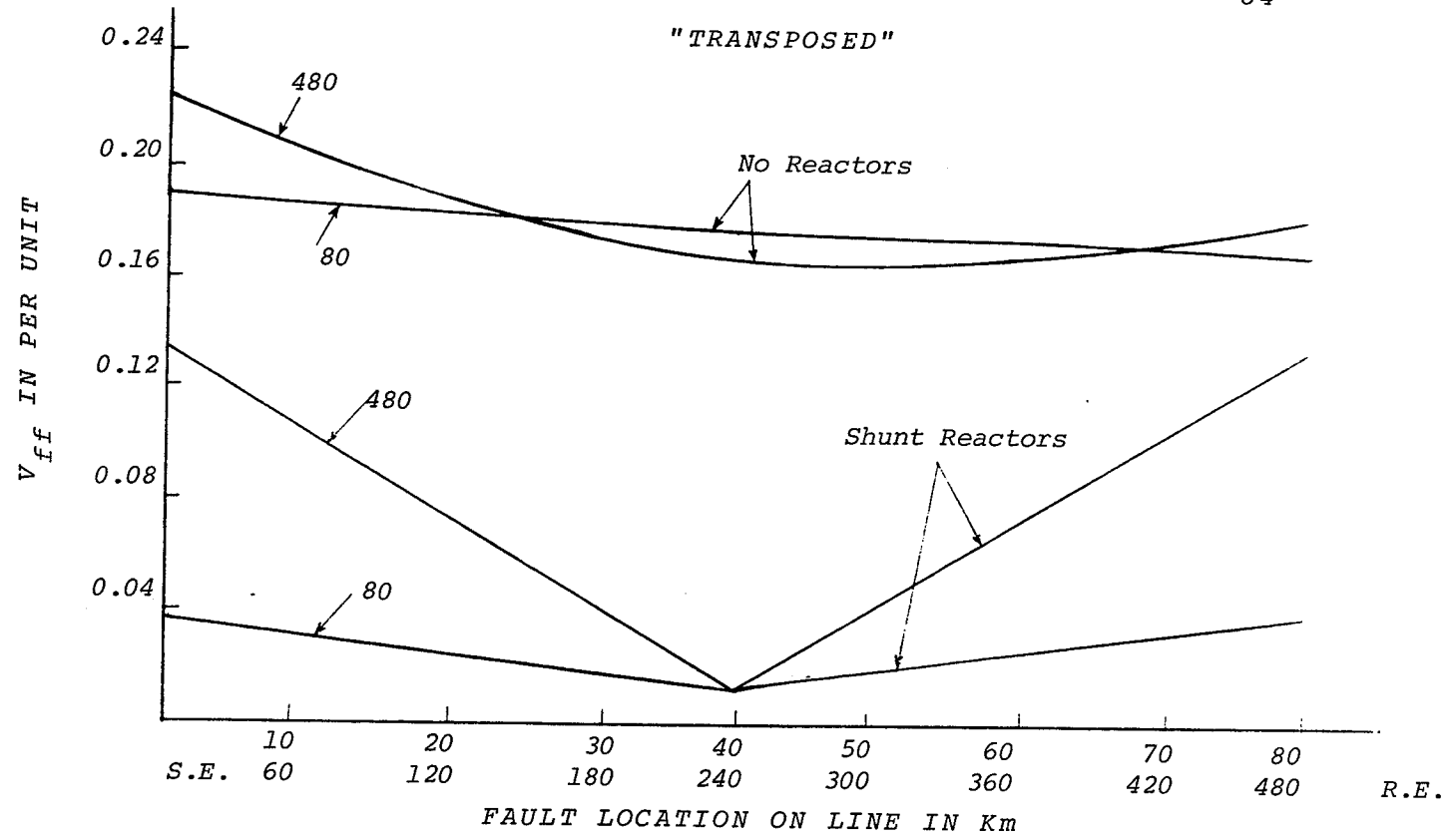


FIG. 4.1.10 - PROFILE OF  $V_{ff}$  FOR TWO VALUES OF LINE LENGTH

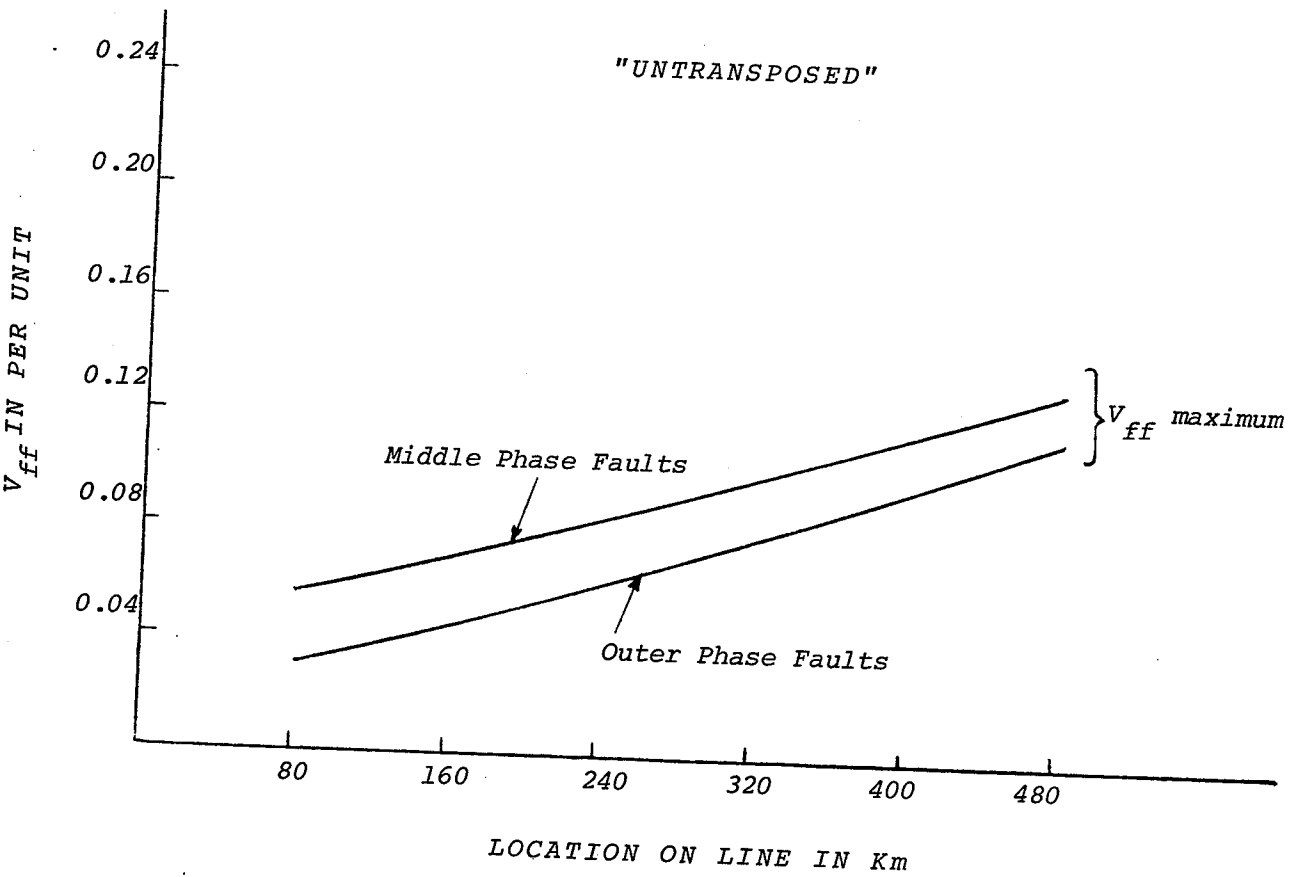
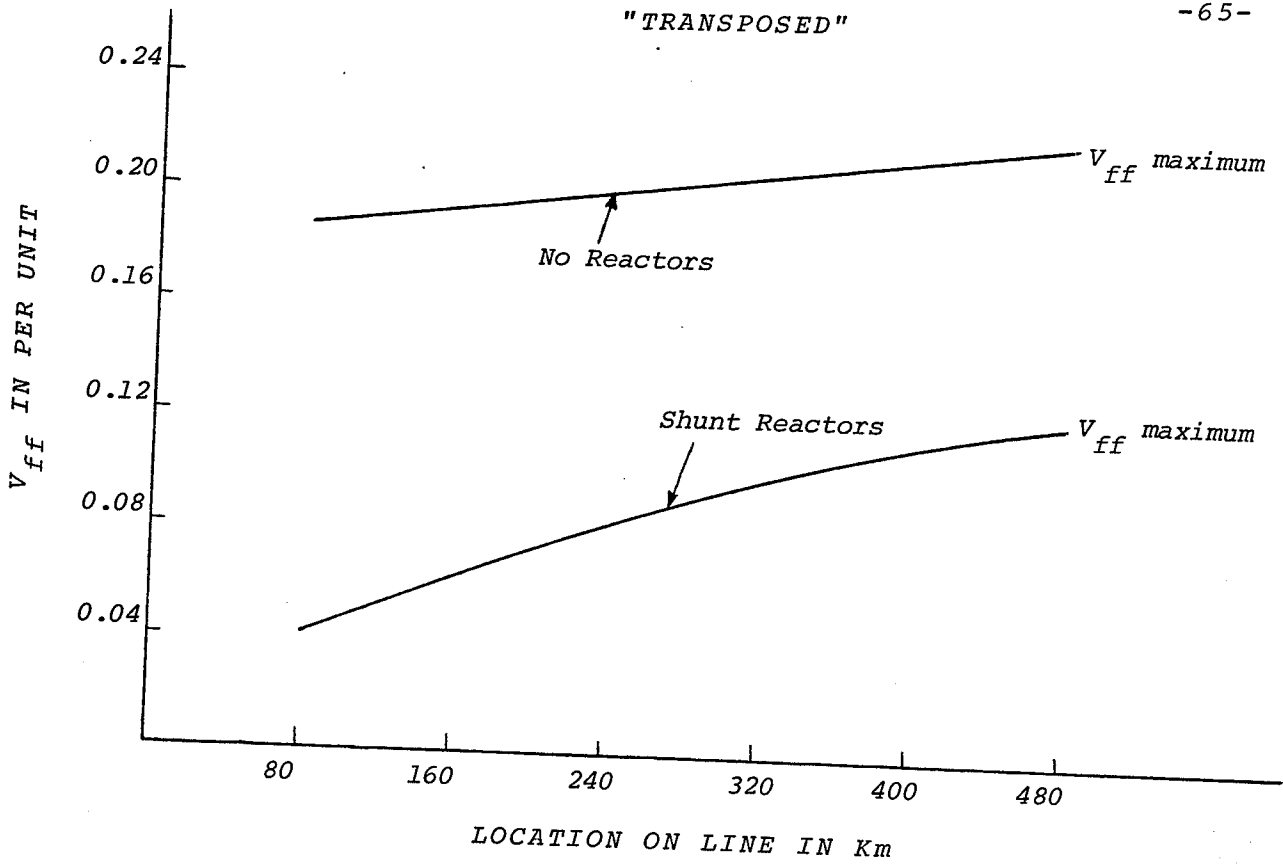
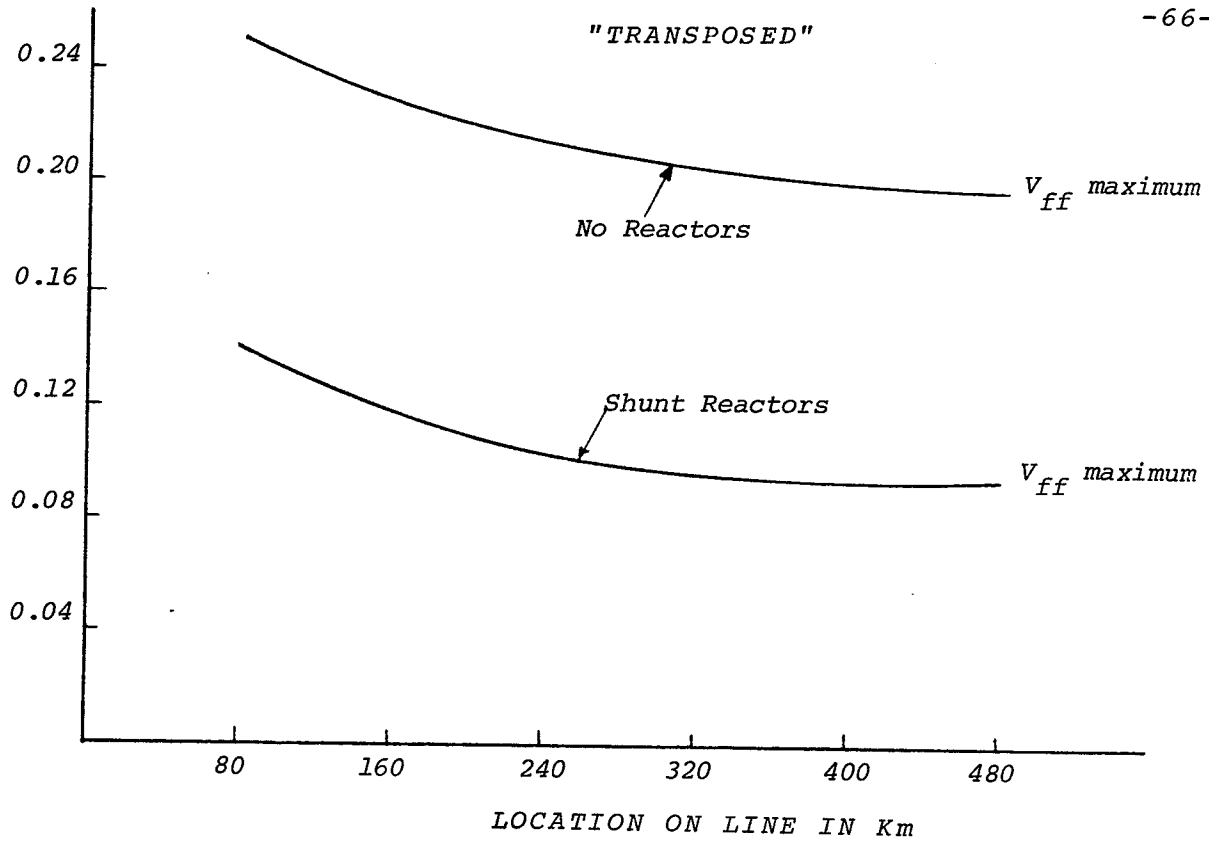


FIG. 4.1.11 - EFFECT OF VARIATION OF LINE LENGTH FOR SAME INITIAL LOADING

$V_{ff}$  IN PER UNIT



$V_{ff}$  IN PER UNIT

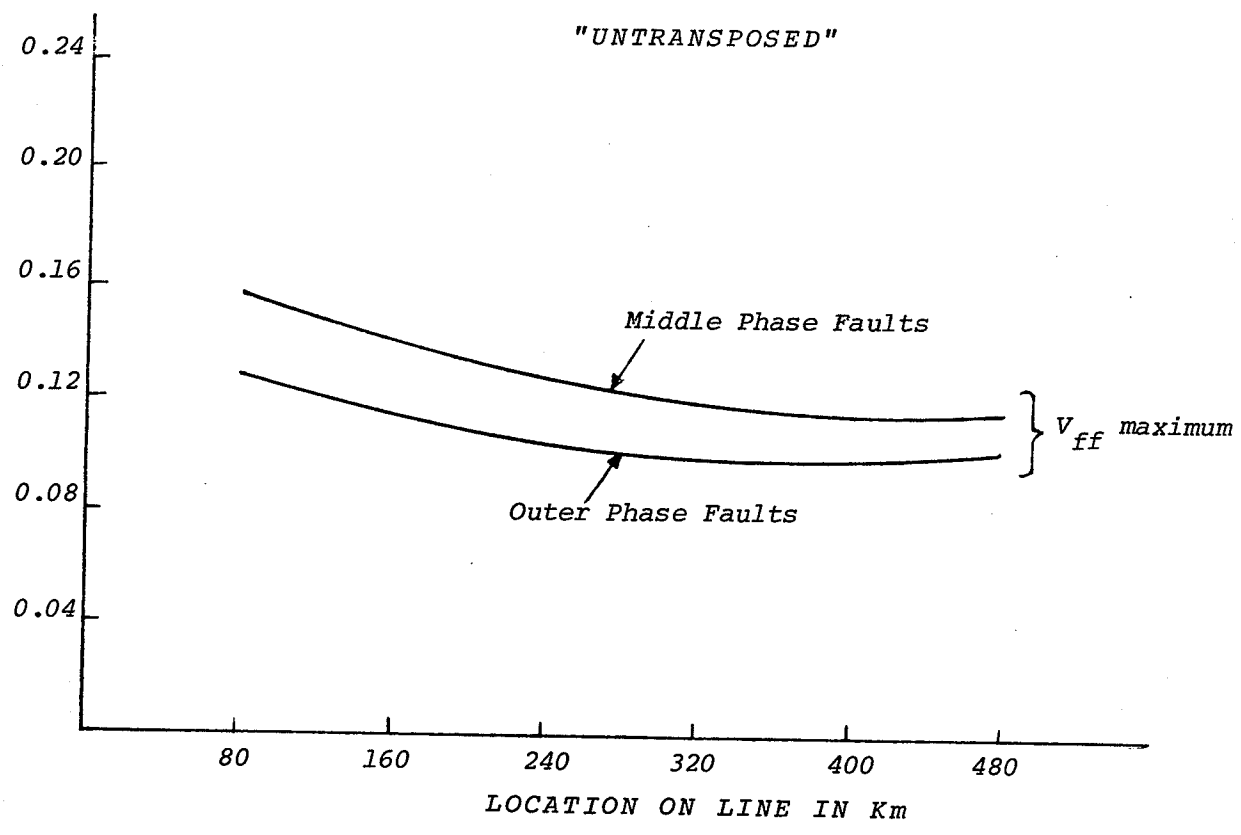


FIG. 4.1.12 - EFFECT OF VARIATION OF LINE LENGTH FOR SAME INITIAL LOADING

4.3.1 Variation of  $X_{\alpha S}$  for Constant  $X_{OS}$

A transmission line, designed to carry a certain amount of load, is terminated on WYE-DELTA transformers (see Fig. 3.1) which are of proportionate MVA capacity. Therefore,  $X_{OS}$  and  $X_{OR}$ , which are the reactances of the transformers, themselves, can be taken to be nearly constant for MVA rating concerned. However, the system beyond the DELTA can be expected to have various values of reactances depending upon the nature of the system. Table 4.3.1 lists cases where  $X_{OS}$  and  $X_{OR}$  were kept at 0.125 p.u. (base case value) while  $X_{\alpha S}$  and  $X_{\alpha R}$  were varied (thus varying  $X_0/X_\alpha$  ratio).

TABLE 4.3.1

CASE NUMBER	REF. FIGURE	REMARKS
2.1	4.2.1	$X_{\alpha S}$ varied 0 to 0.6 p.u. $X_{\alpha S} = X_{\alpha R}$ , $X_{OS} = X_{OR} = 0.125$ p.u.

4.3.2 Unequal Source Reactances at the Two Ends

This situation is quite likely to occur in practice when two sources of unequal capacity are connected by the line. Two cases were studied; (a)  $X_{\alpha R}$ ,  $X_{OS}/X_{\alpha S}$ , and  $X_{OR}/X_{\alpha R}$  were kept constant at the base case values and  $X_S$  was varied; (b)  $X_{\alpha R}$ ,  $X_{OR}$  and  $X_{OS}$  were kept constant at the base case values and  $X_{\alpha S}$  was varied. Table 4.3.2 lists these two cases.

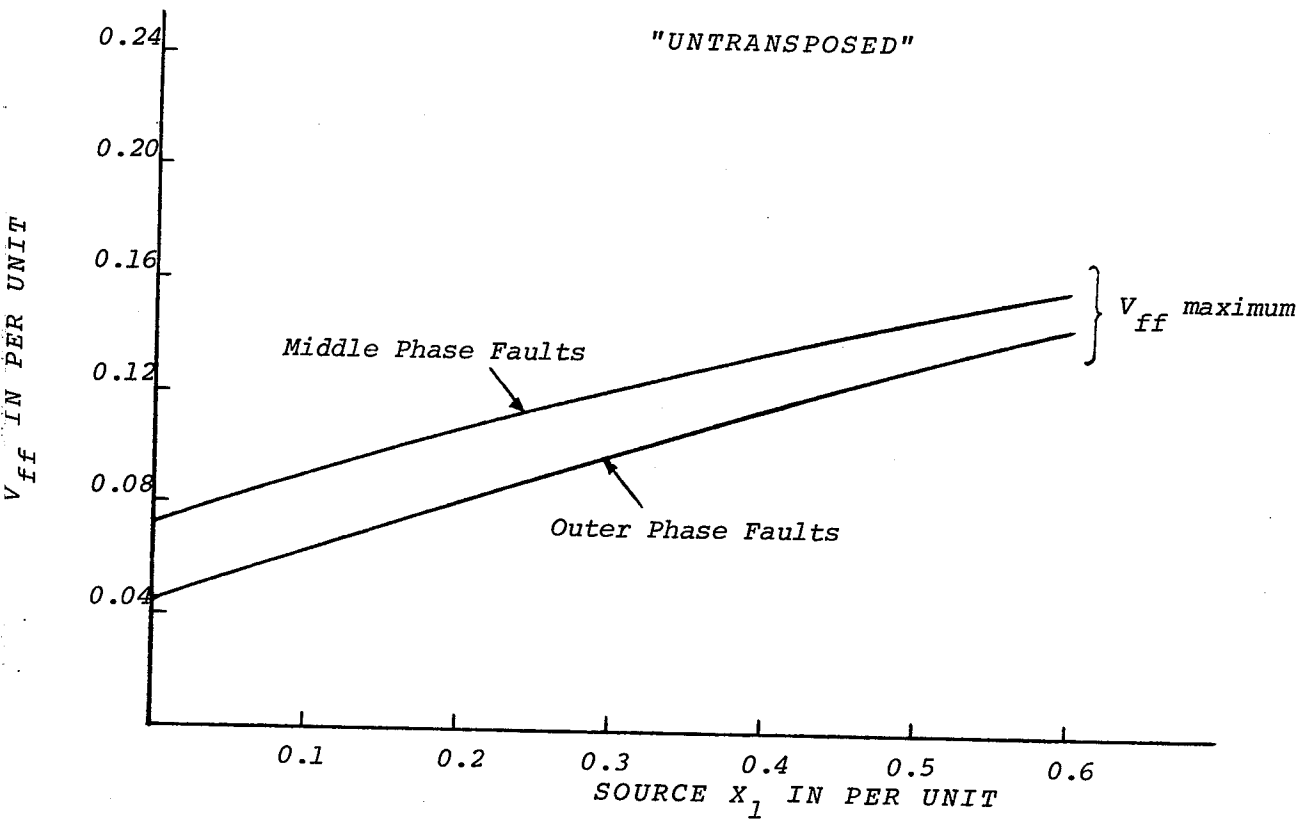
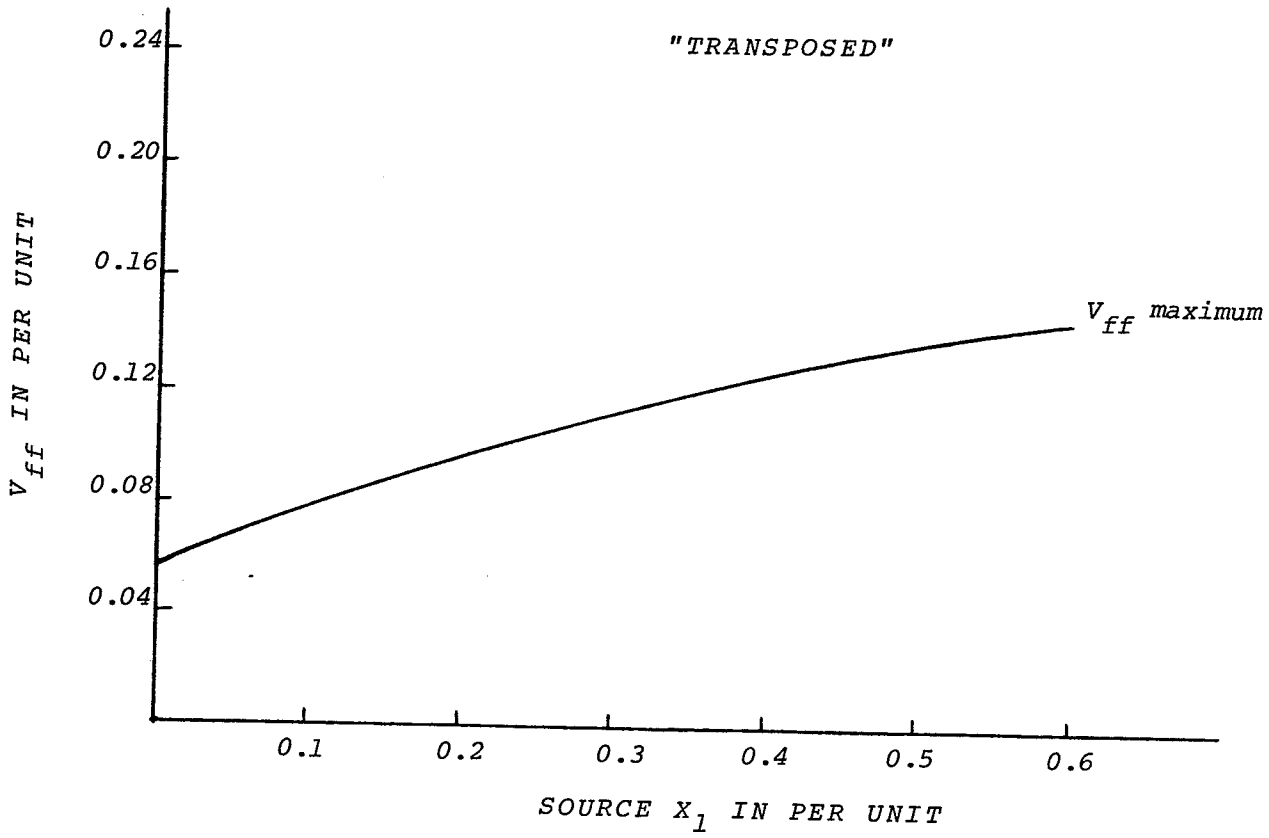


FIG. 4.2.1 - EFFECT OF SOURCE  $X_1$  VARIATION  
(CONSTANT SOURCE  $X_0$ )

TABLE 4.3.2

CASE NUMBER	REF. FIGURE	REMARKS
2.2	4.2.2	$X_{\alpha S}$ varied - 0.05 to 0.5 p.u., $X_{\alpha R} = 0.25$ p.u., $X_{OS}/X_{\alpha S} = X_{OR}/X_{\alpha R} = 0.5$
2.3	4.2.3	$X_{\alpha S}$ varied - 0.05 to 0.5 p.u., $X_{\alpha R} = 0.25$ , $X_{OS} = X_{O5} = 0.125$ p.u.

4.3.3 Variation of  $R_o$  and  $l_o/l_1$  of the Line  
-----

The zero sequence quantities of a transmission line are dependent upon the characteristics of the ground return circuits, namely the earth and overhead ground wires, if any. The effect of the variation of these quantities has been studied and the cases listed in Table 4.3.3. The base case results are plotted for comparison.

TABLE 4.3.3

CASE NUMBER	REF. FIGURE	REMARKS
2.4	4.2.4	$R_o$ reduced by 50 percent from base case value
2.5	4.2.5	$l_o/l_1$ for line with values 3.0, 2.2; $r_o/l_1$ same as for the base case.

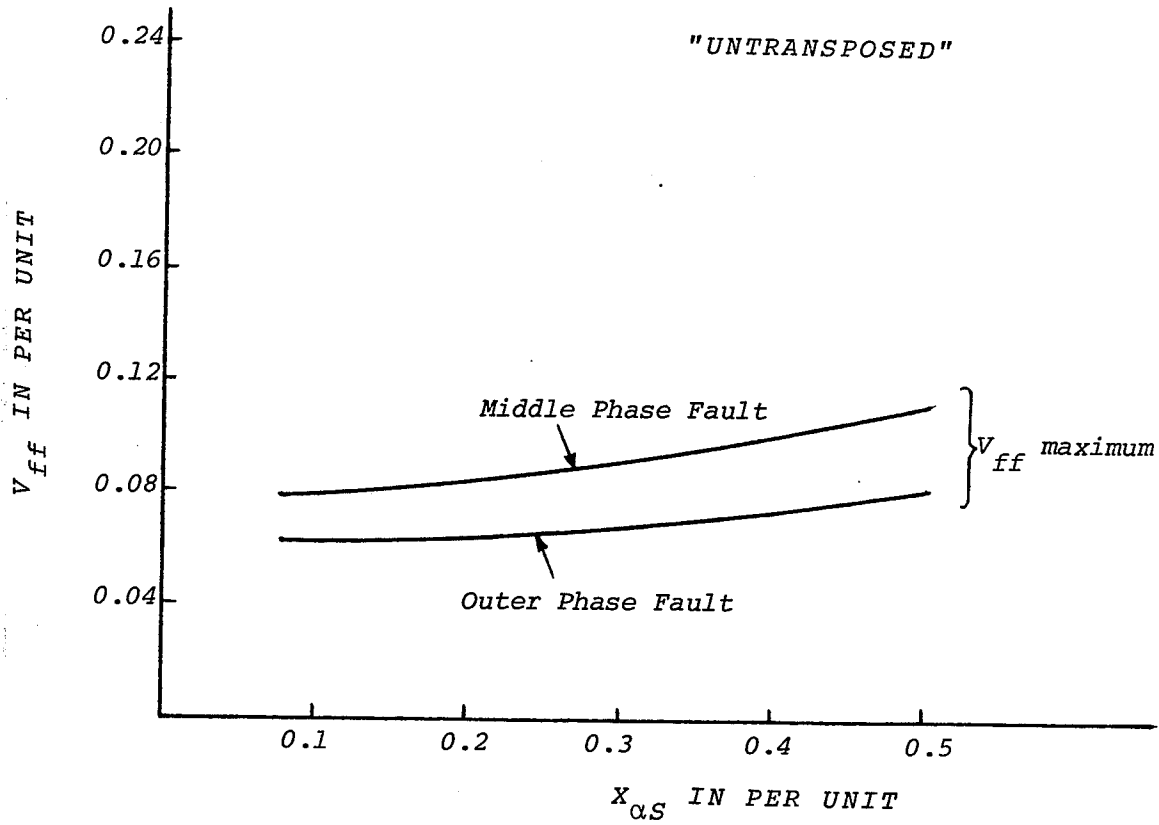
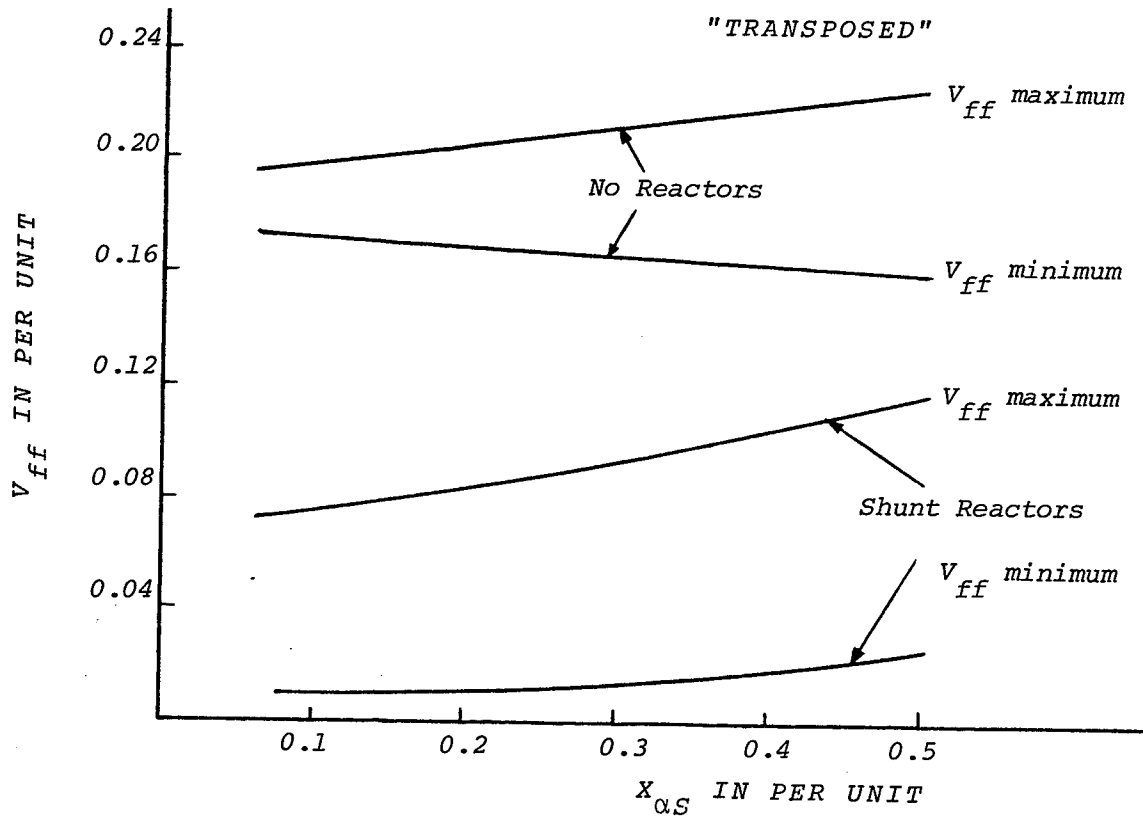


FIG. 4.2.2

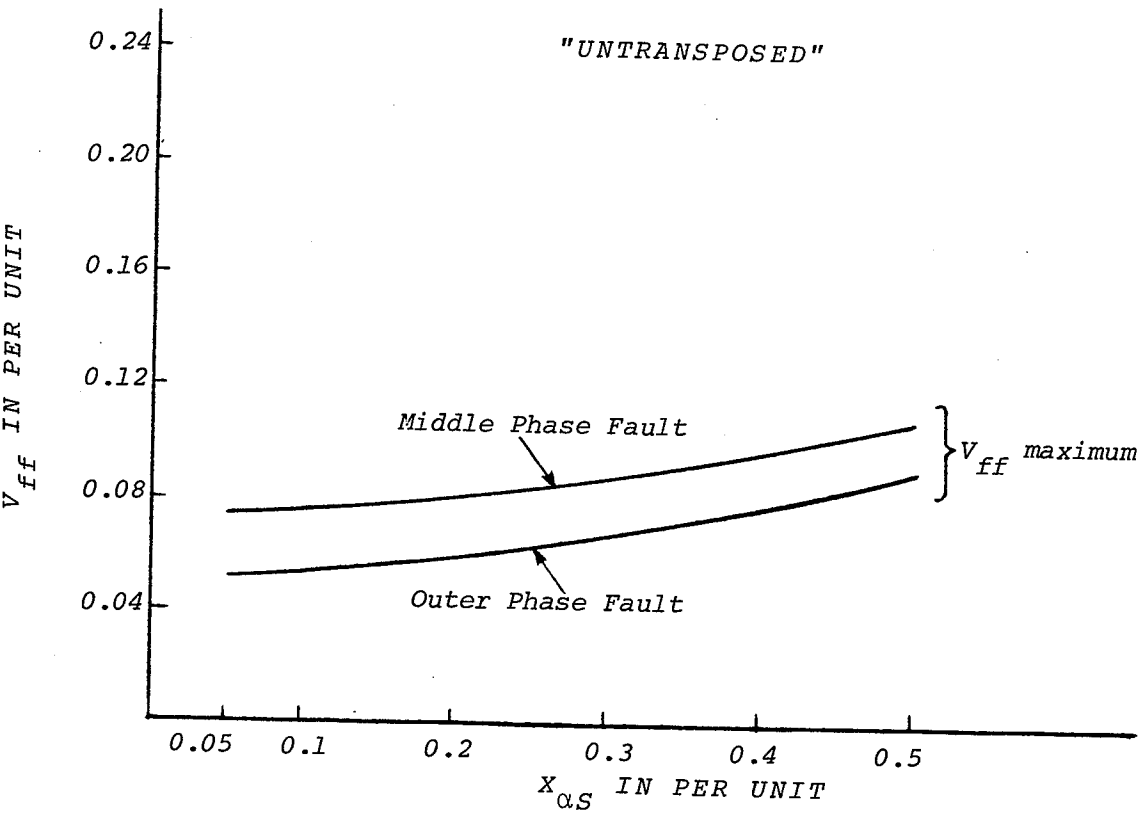
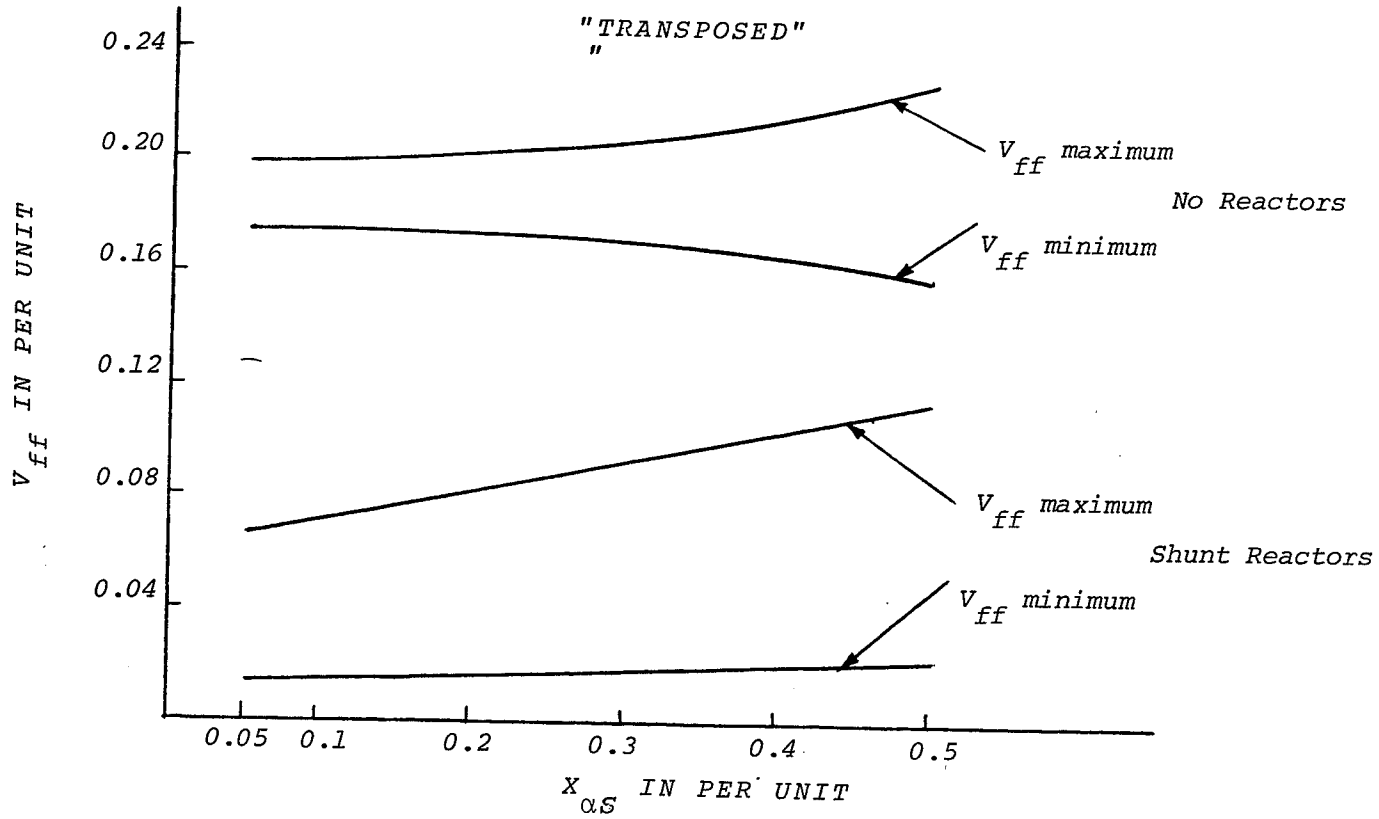


FIG. 4.2.3



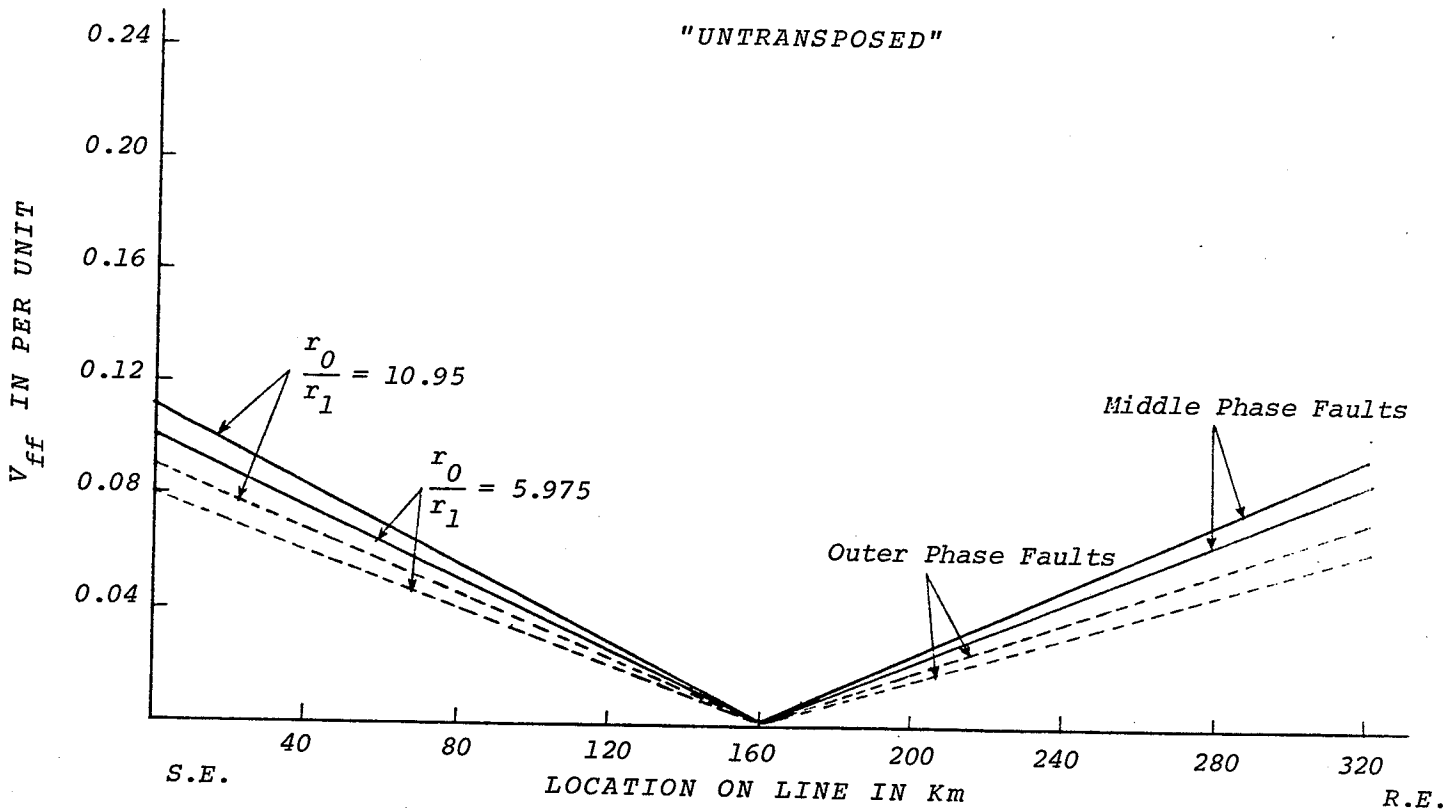
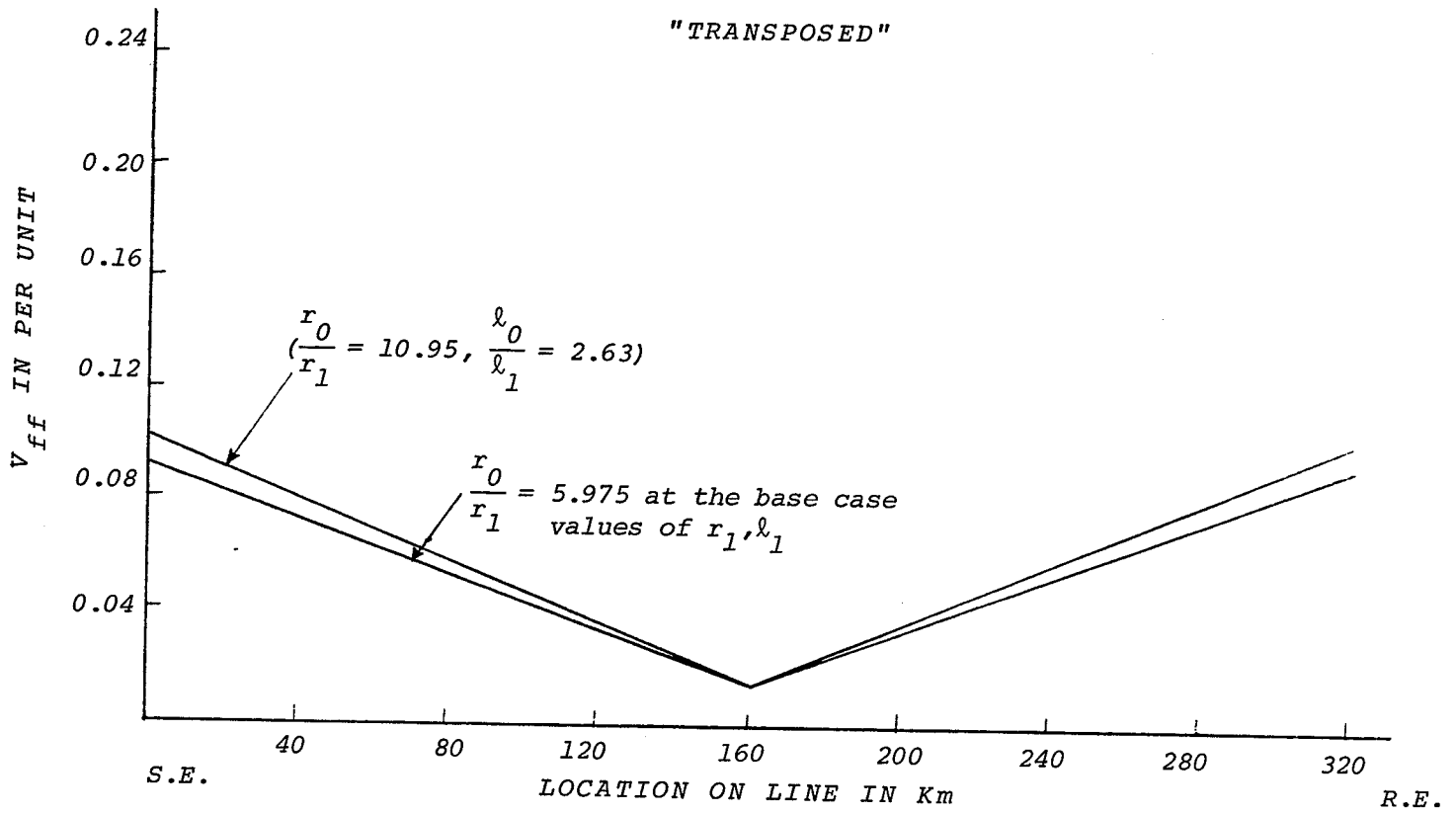


FIG. 4.2.4 - PROFILE OF  $V_{ff}$  - TWO VALUES OF  $\frac{\gamma_0}{\gamma_1}$  RATIO

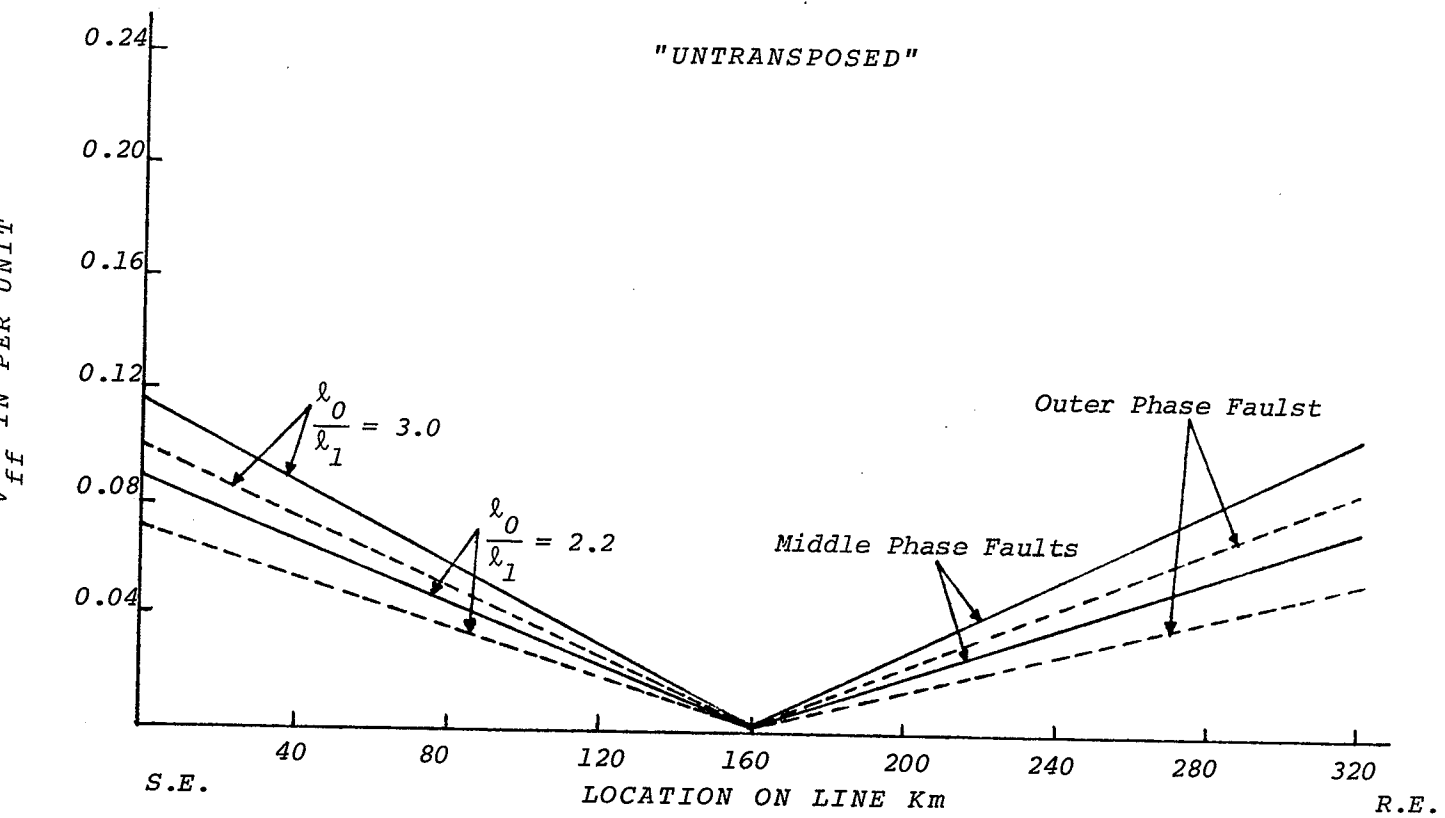
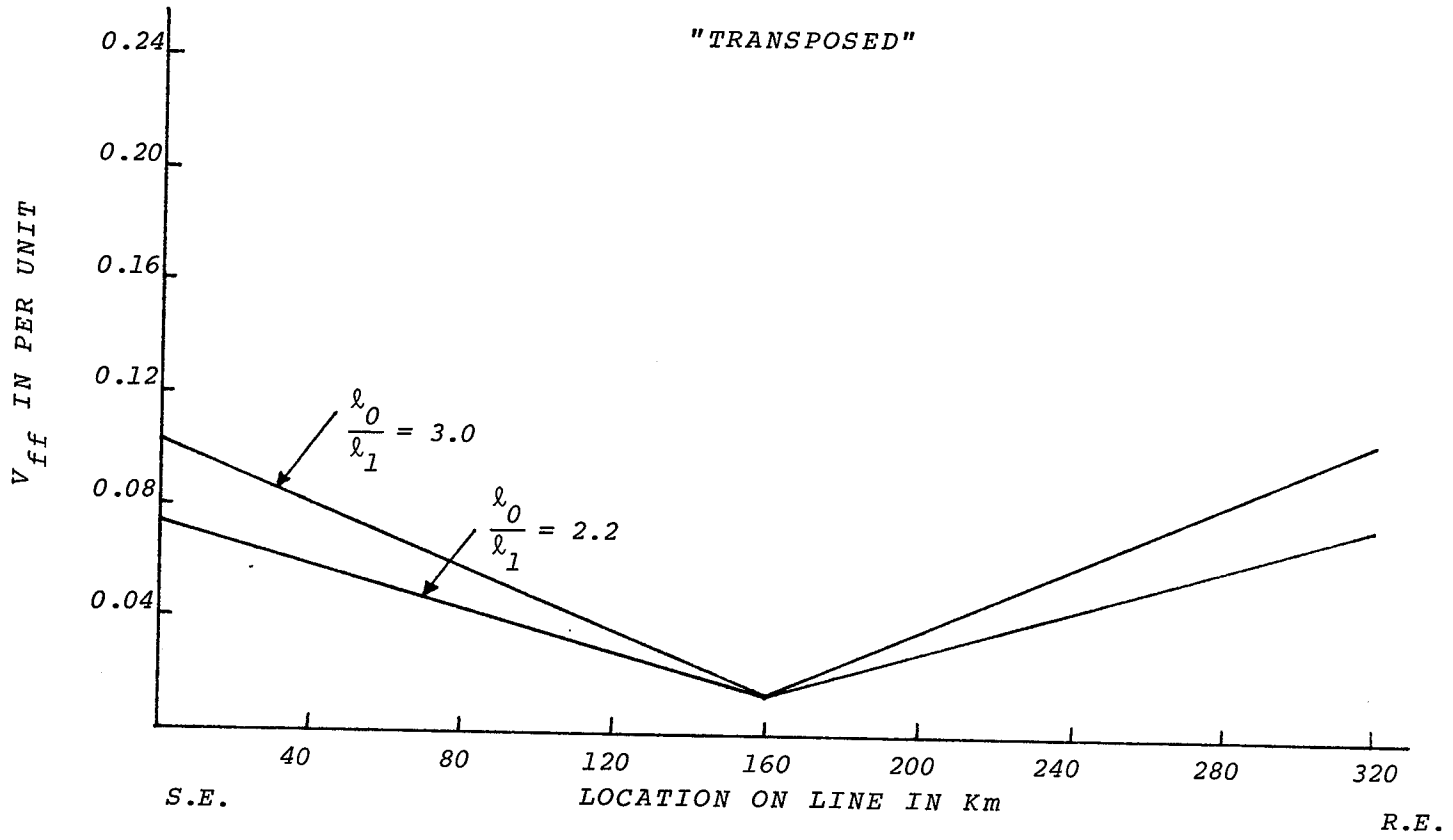


FIG. 4.2.5 - PROFILE OF  $V_{ff}$  - TWO VALUES LINE  $\frac{\lambda_0}{\lambda_1}$  RATIO

4.4 EFFECT OF COMPENSATION FACTOR

The degree of line charging KVAR compensation is also the important factor for determining the neutralization of capacitive coupling effect on single pole reclosing. In order to effectively control the secondary arc current and the recovery voltage, an optimum level of shunt compensation must be selected. The effect of compensation factor on various SPS parameters, namely, the secondary arc current,  $I_f$ , the recovery voltage,  $V_{ff}$ , on the faulted phase, and the neutral reactor voltages  $V_{SN}$  and  $V_{MN}$  were studied. All these cases are listed in Table 4.4.1.

TABLE 4.4.1

CASE NUMBER	REF. FIGURE	REMARKS
3.1	4.3.1 4.3.2 4.3.3	Compensation factor varied from 0.6 - 1.0, base case parameters used.

4.5 EFFECT OF THE DEVIATION FROM OPTIMUM VALUES OF SHUNT REACTORS - SENSITIVITY

An optimum value, in this context here, is defined as that value of the shunt reactors which results in minimum value of  $V_{ff}$  at a specified location. In section 4.2 such values were mathematically calculated for transposed and untransposed lines.

In practice, it is quite possible that the exact specified (or optimum) values may neither be available nor economi-

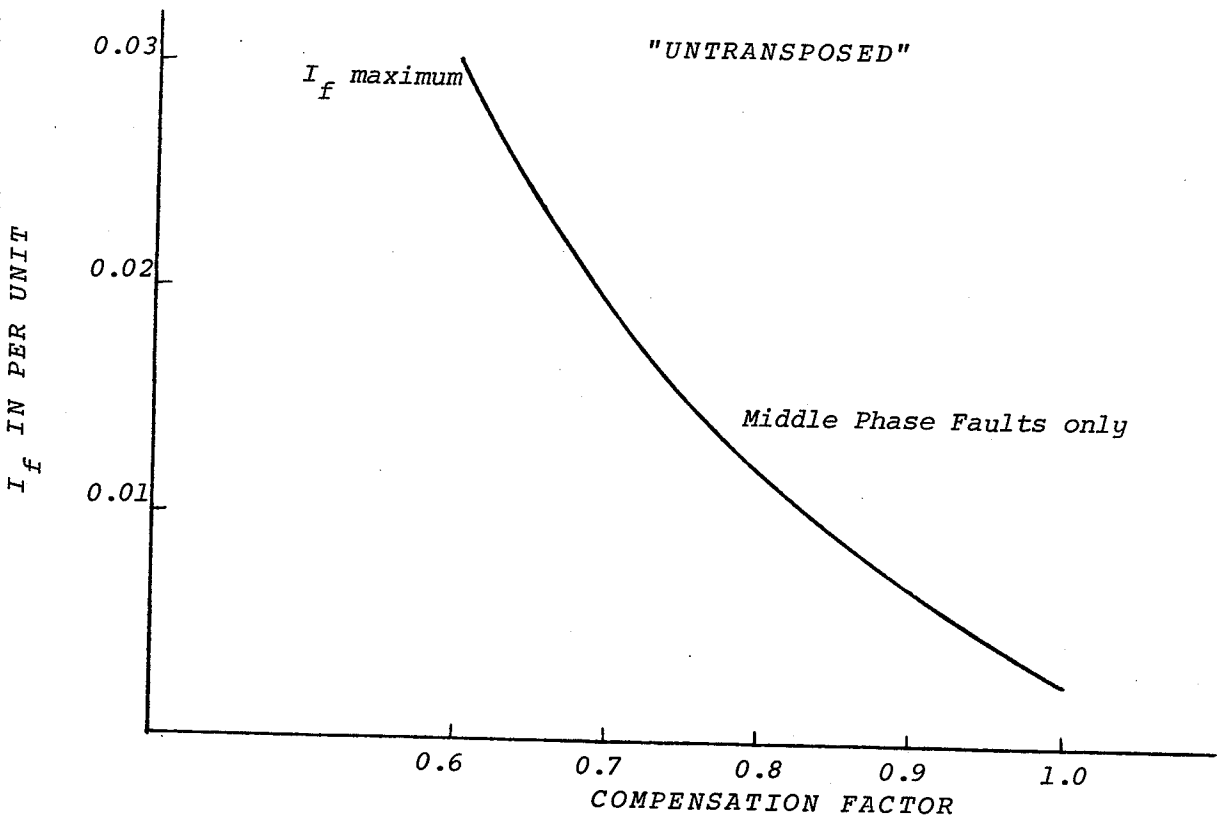
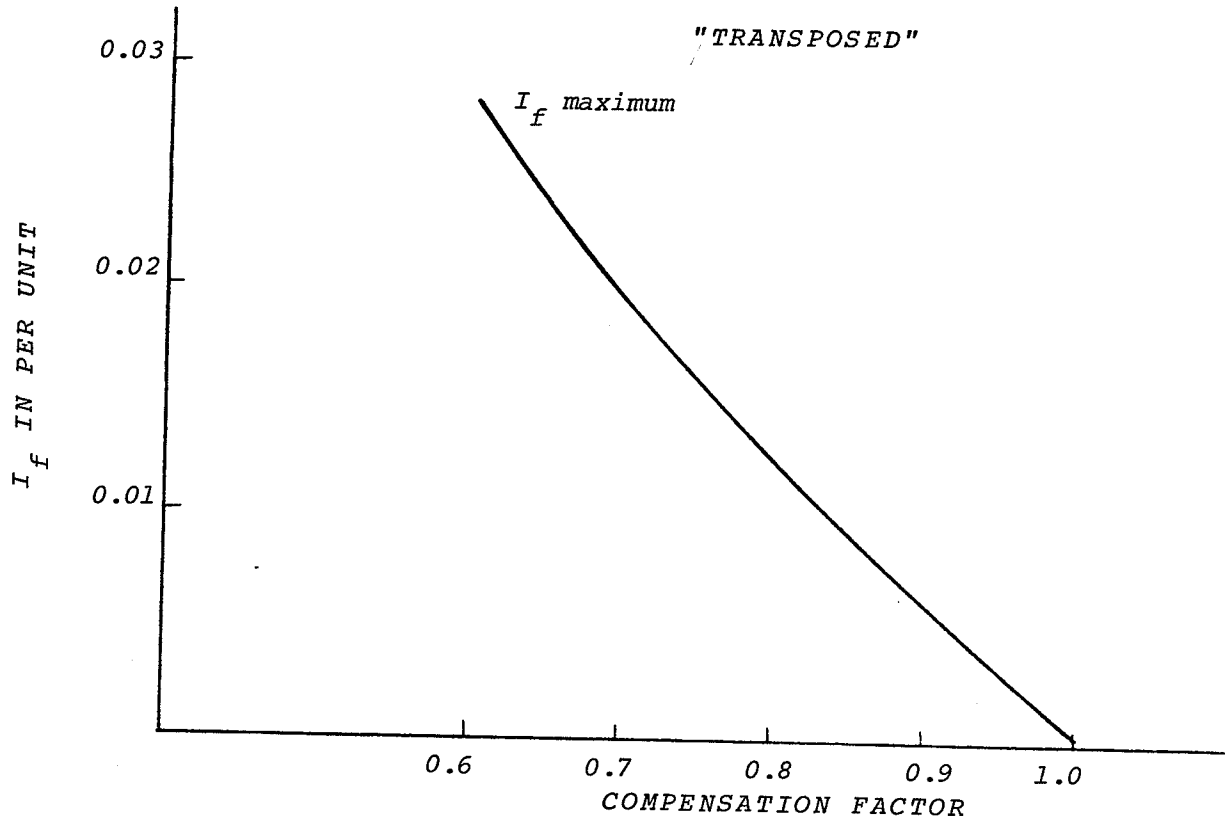


FIG. 4.3.1 - EFFECT OF COMPENSATION ON  $I_f$

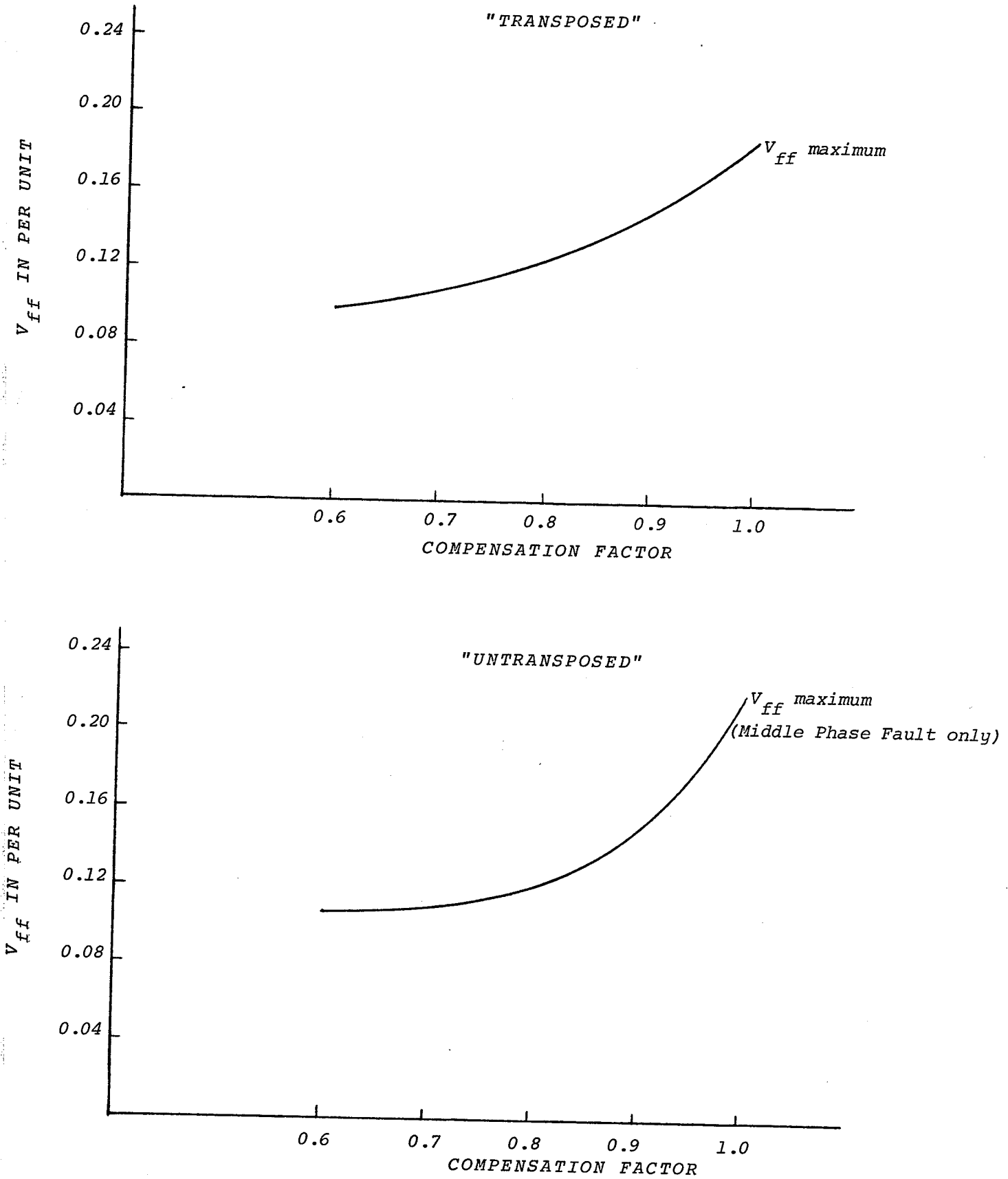


FIG. 4.3.2 - EFFECT OF VARIATION OF THE DEGREE OF KVAR COMPENSATION ON  $V_{ff}$

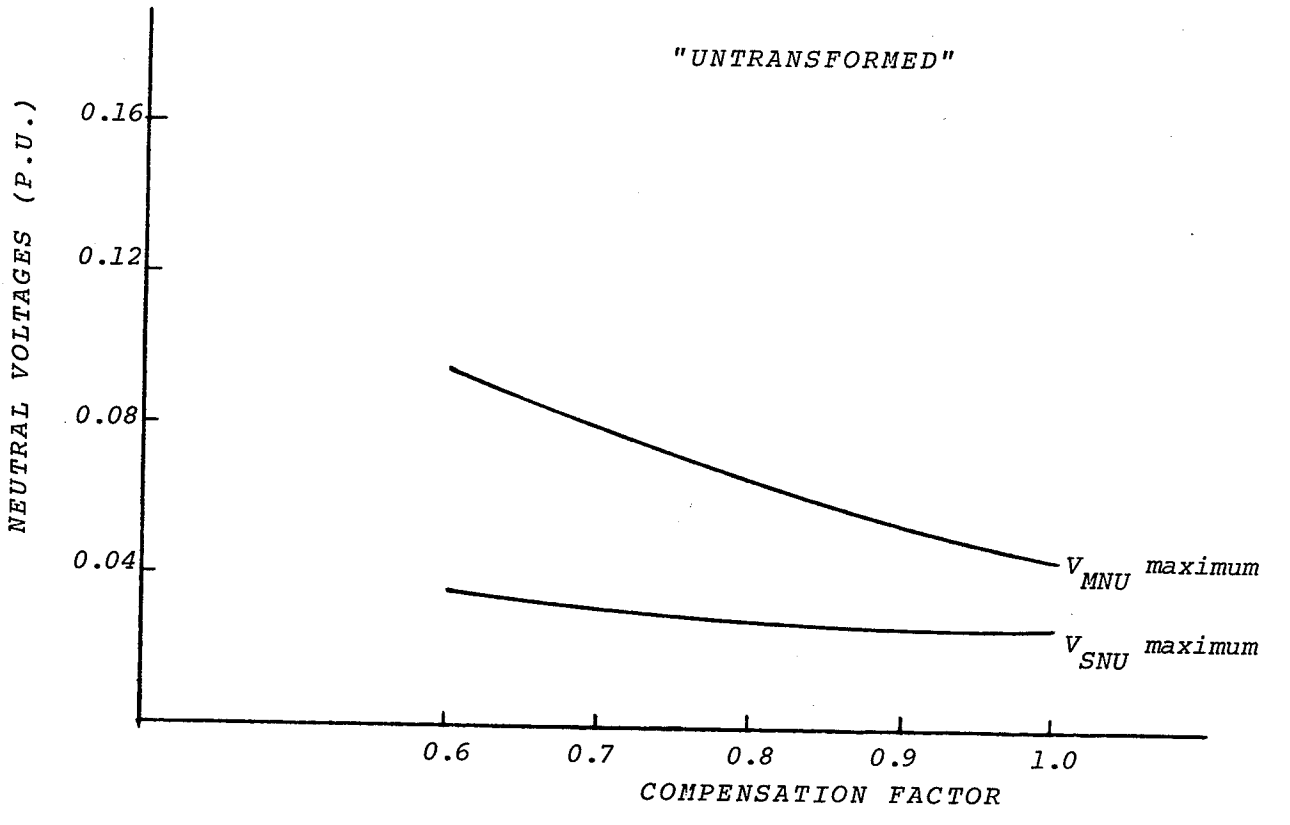
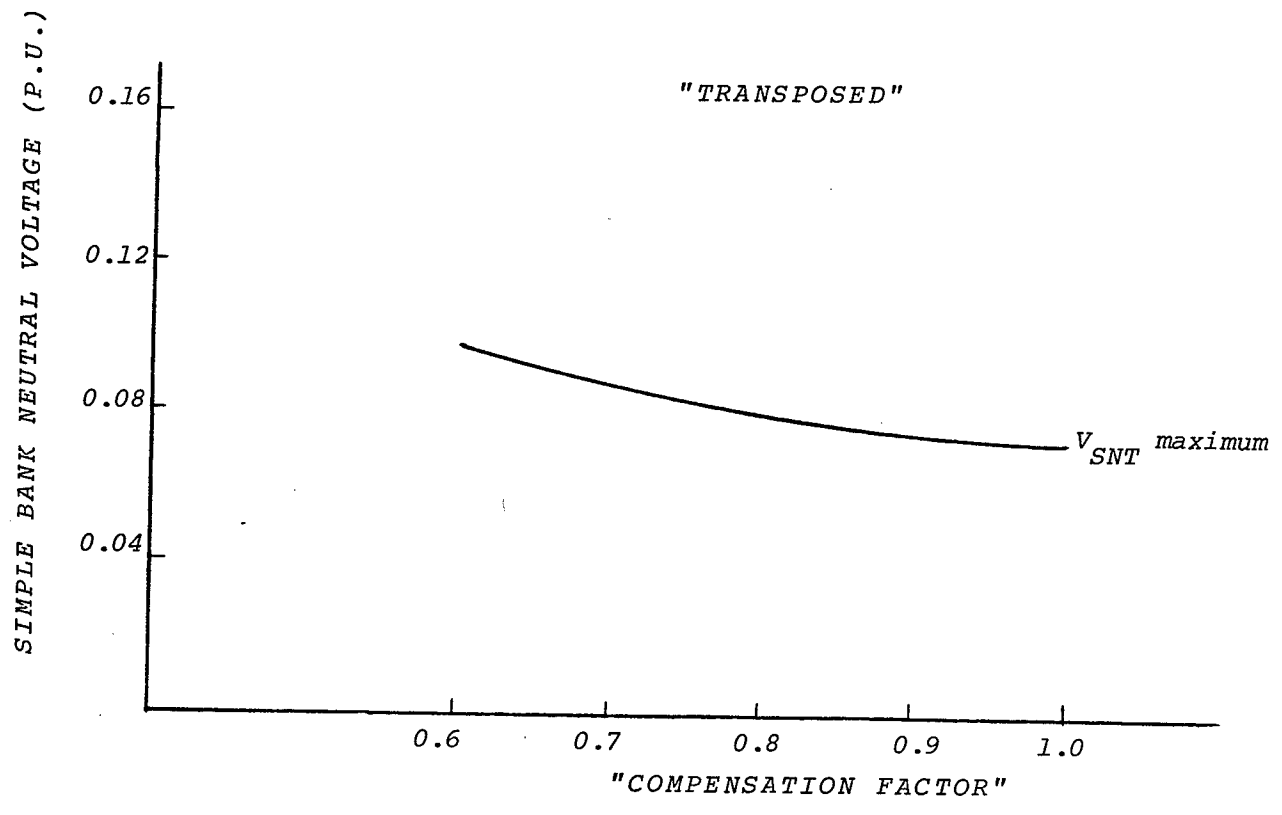


FIG. 4.3.3 - EFFECT OF COMPENSATION ON NEUTRAL VOLTAGES

cally feasible. It is, therefore, of interest to know how critical these (optimum) values are as far as their effectiveness in minimizing  $V_{ff}$  is concerned. Table 4.5 lists these cases which are a repetition of case 1.1. Values of shunt reactors and neutral reactors were varied  $\pm 10$  percent from their optimum values.

TABLE 4.5

CASE NUMBER	REF. FIGURE	REMARKS
4.1	4.4(a)	For transposed lines $X_{ST}$ , $X_{SNT}$ varied $\pm 10$ percent from the optimum value.
4.2	4.4(b)	For untransposed lines $X_{SU}$ , $X_{MU}$ , $X_{SNU}$ , $X_{MNU}$ varied $\pm 10$ percent from optimum value.

#### 4.6 USE OF DISCHARGE RESISTORS FOR MINIMIZING $V_{ff}$

It was shown in Chapter II that if the faulted phase is grounded through a suitable resistance, then the magnitude of  $V_{ff}$  can be reduced. This idea was studied for the base case, and details are given in Table 4.6.  $R_{FS}$  and  $R_{FR}$  are the resistances that are connected from the phase A conductor to ground at the sending and receiving ends, respectively. Magnitudes of these resistances used are shown on the respective graphs.

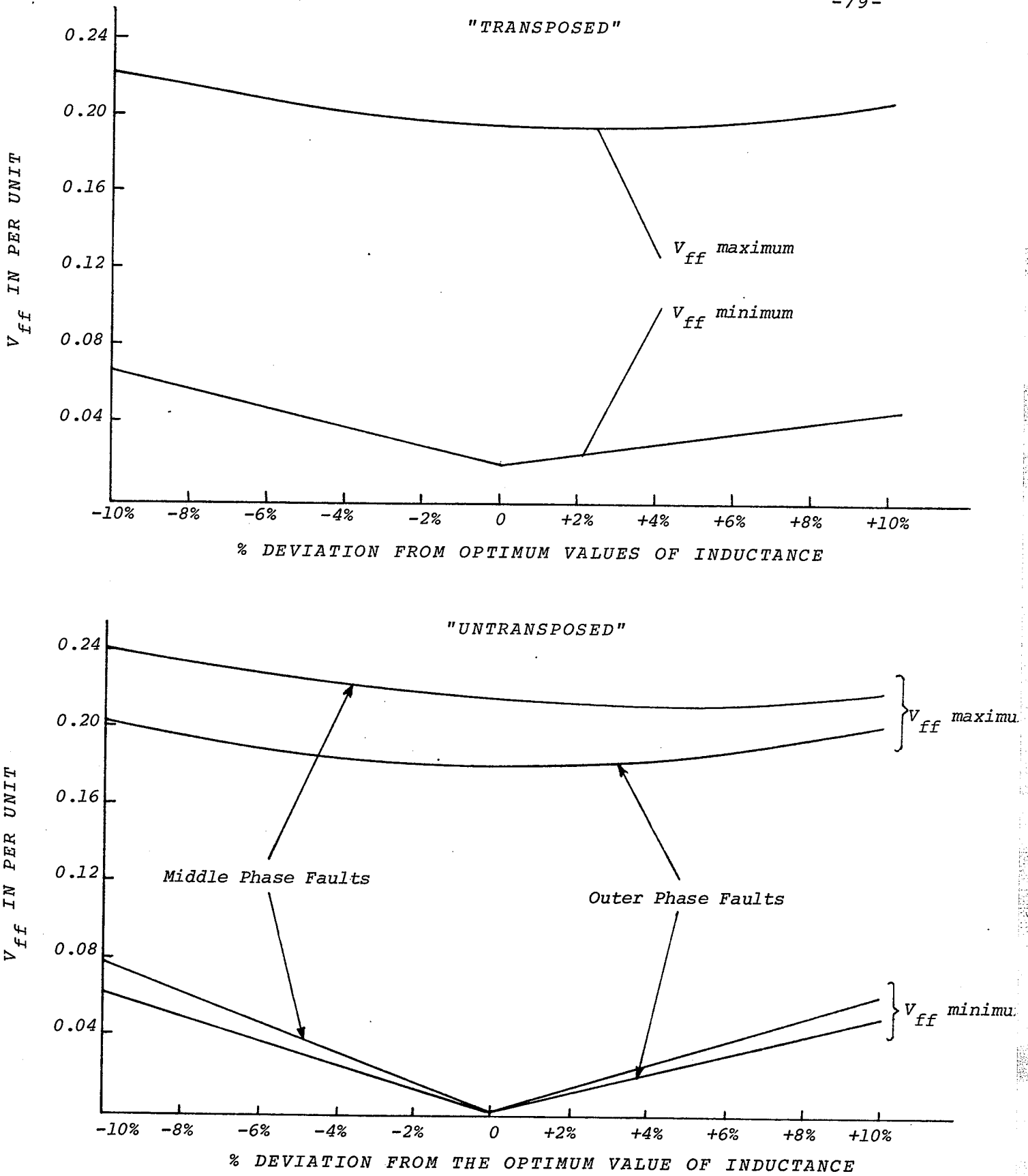


FIG. 4.4 - SENSITIVITY OF THE OPTIMUM VALUES OF SHUNT REACTORS



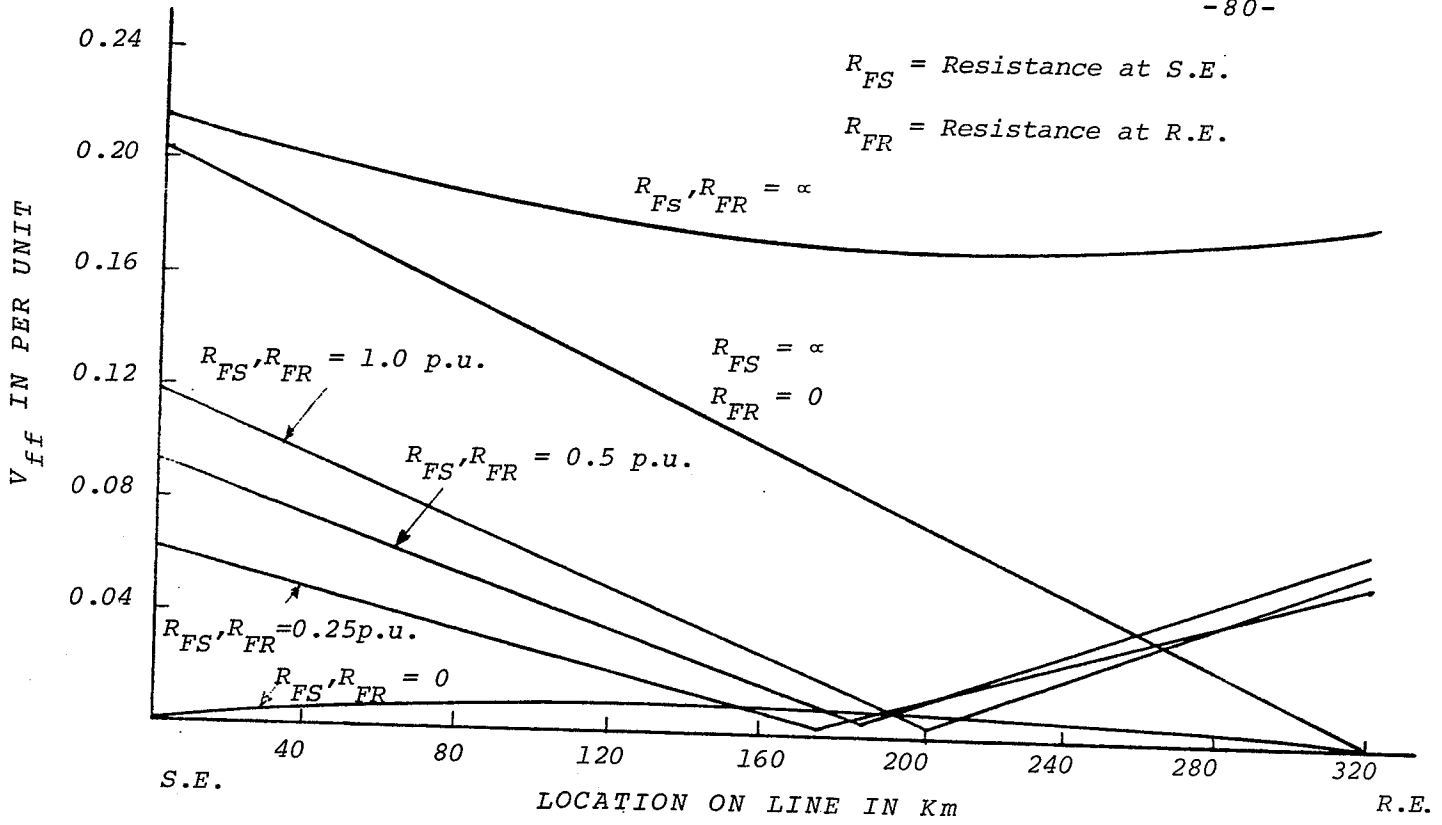


FIG. 4.5.1 - PROFILE OF  $V_{ff}$  - DISCHARGE RESISTANCE METHOD

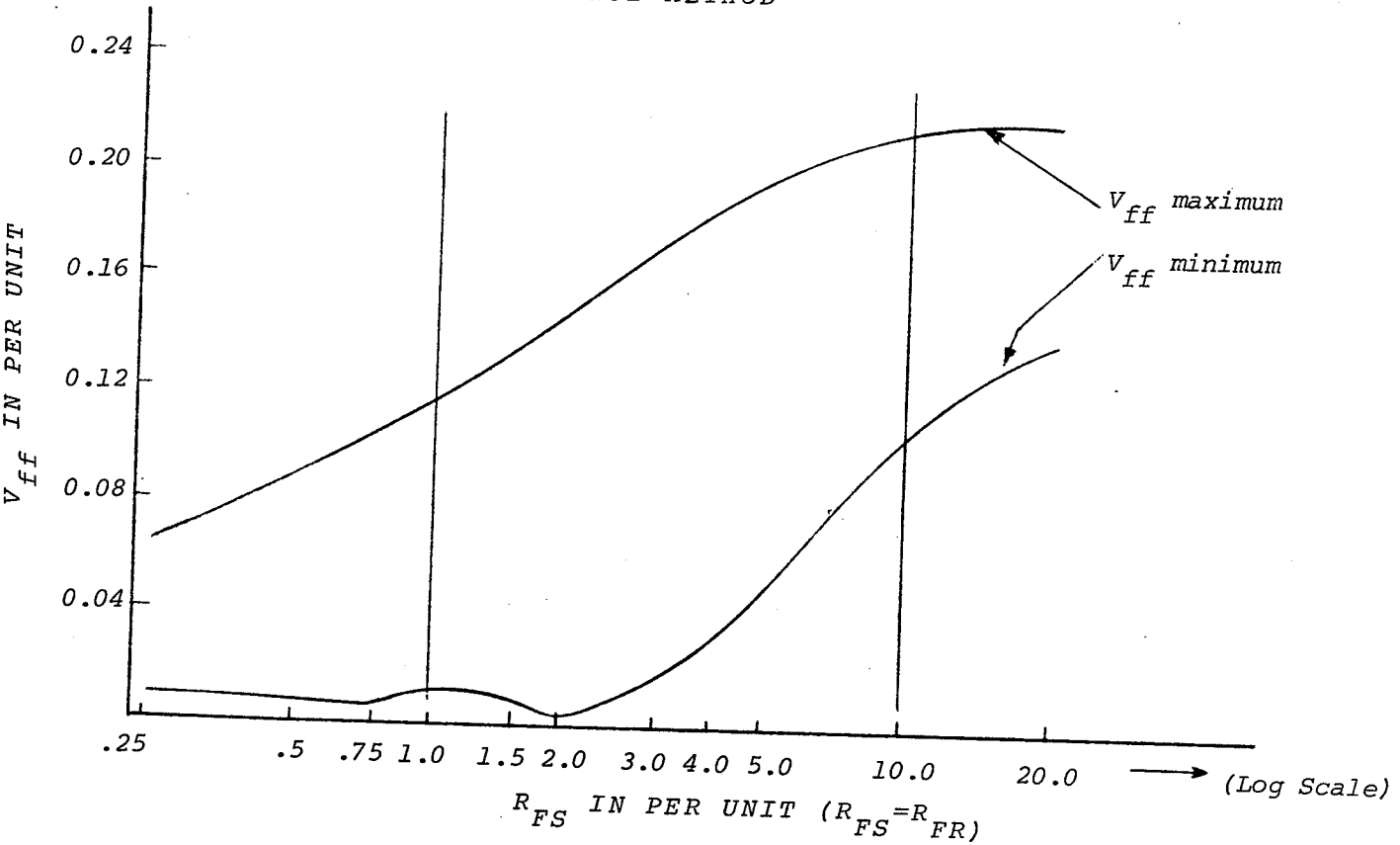


FIG. 4.5.2 - EFFECT OF VARIATION OF DISCHARGE RESISTANCE MAGNITUDE

TABLE 4.6

CASE NUMBER	REF. FIGURE	REMARKS
5	4.5.1 4.5.2	Base Case - various values of $R_{FS}$ and $R_{FR}$ .

#### 4.7 CAPACITANCE METHOD FOR MINIMIZING $V_{ff}$

This method has already been discussed in detail in Chapters II and III. Magnitude of  $V_{ff}$  can be reduced by connecting suitable values of  $C_S$  and  $C_R$  across the circuit breakers in the faulted phase. This case is listed in Table 4.7. Magnitudes of these capacitors used are listed on the respective graphs. It may be noted that no shunt reactors are used in this case.

TABLE 4.7

CASE NUMBER 5	REF. FIGURE	REMARKS
6	4.6.1 4.6.2	Base Case - various values of $C_S$ and $C_R$ .

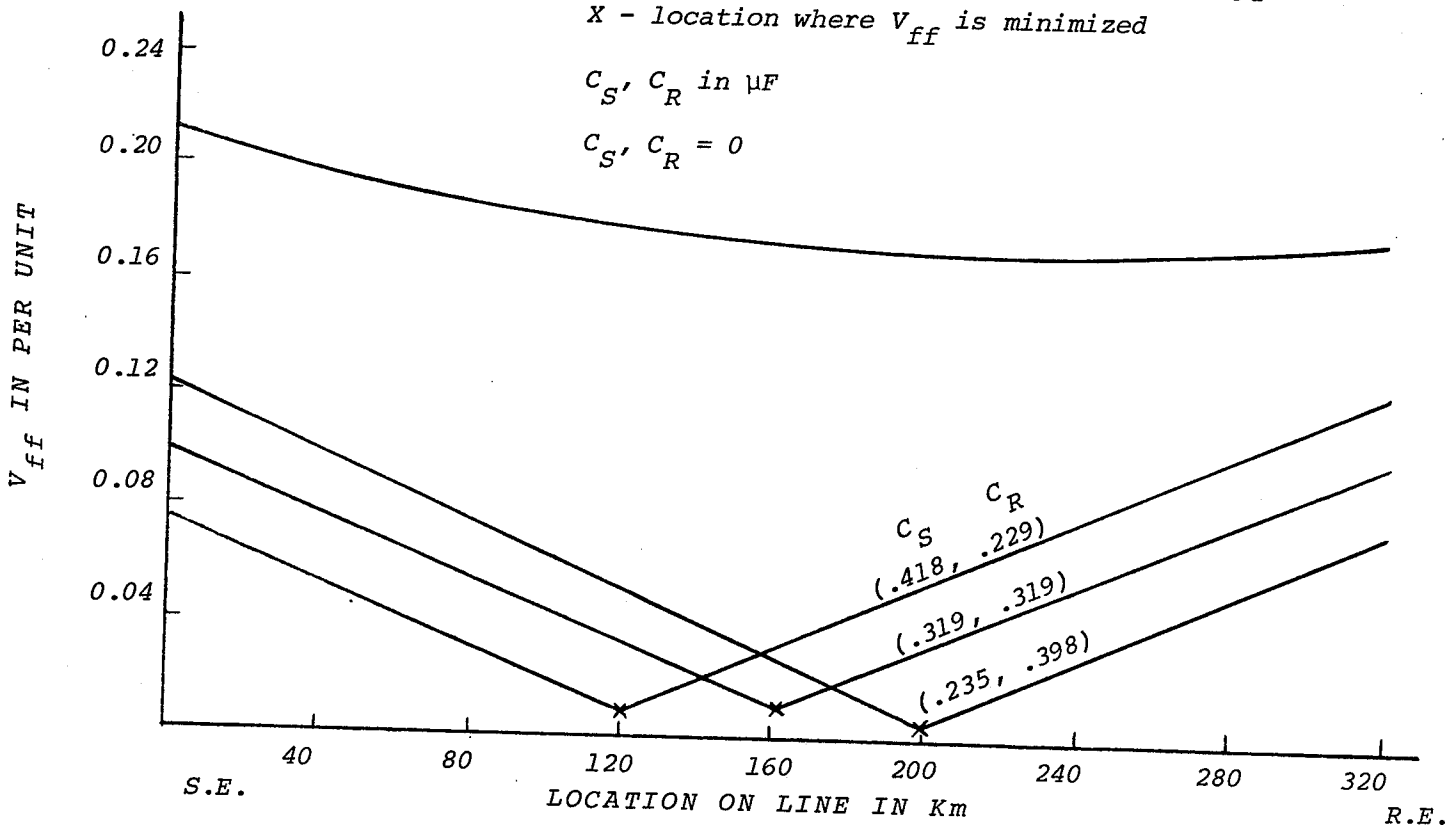


FIG. 4.6.1 - PROFILE OF  $V_{ff}$  - CAPACITANCE METHOD

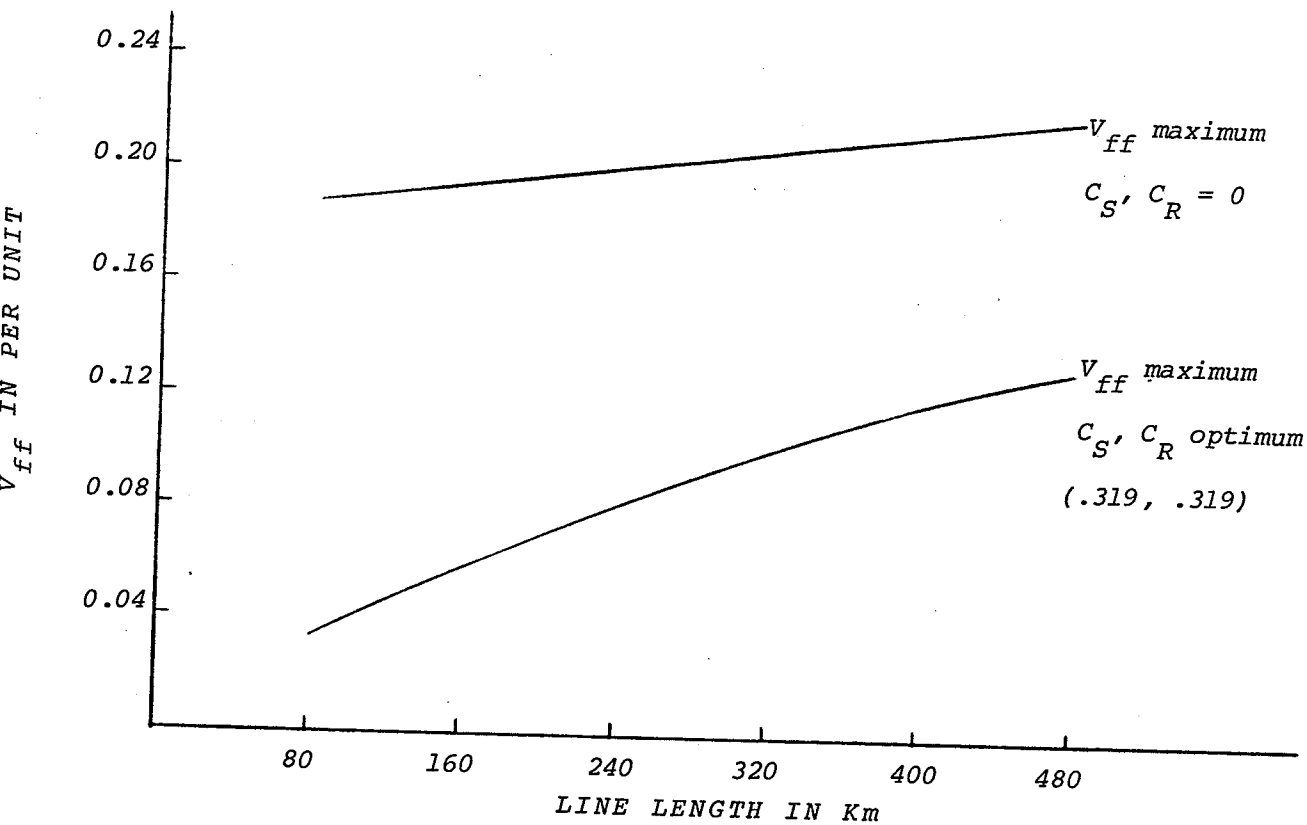


FIG. 4.6.2 - EFFECT OF THE VARIATION OF LINE LENGTH FOR SAME INITIAL LOADING

## CHAPTER V

### DISCUSSION OF RESULTS

The influence of the values of different parameters on the magnitudes of  $V_{ff}$  has been studied. The results obtained from these studies have been summarized and documented in the form of graphs. In this chapter, these results are analysed and their significance is interpreted. In all of the following discussions, it is understood that unless otherwise stated, the magnitudes of  $V_{ff}$  being referred to are those that are obtained after minimization using any one of the methods described earlier.

#### 5.1 THRESHOLD LEVEL OF SELF-SUSTAINING SECONDARY ARC CURRENT

Literature<sup>21</sup> indicates that a secondary arc current of 15-20 amperes level will extinguish itself under normal circumstances. This value has been obtained as a result of laboratory and field tests. It is, of course, understood that under given favourable atmospheric conditions, a higher amount of fault current could be self extinguishing. An arc cannot sustain itself when the rate of heat dissipation (due to convection, radiation, etc.) is greater than the rate of heat generation by the arc. The latter depends upon both the arc current and the arc resistance (a variable quantity). Estimates are given<sup>21</sup> that the magnitude of arc resistance could be

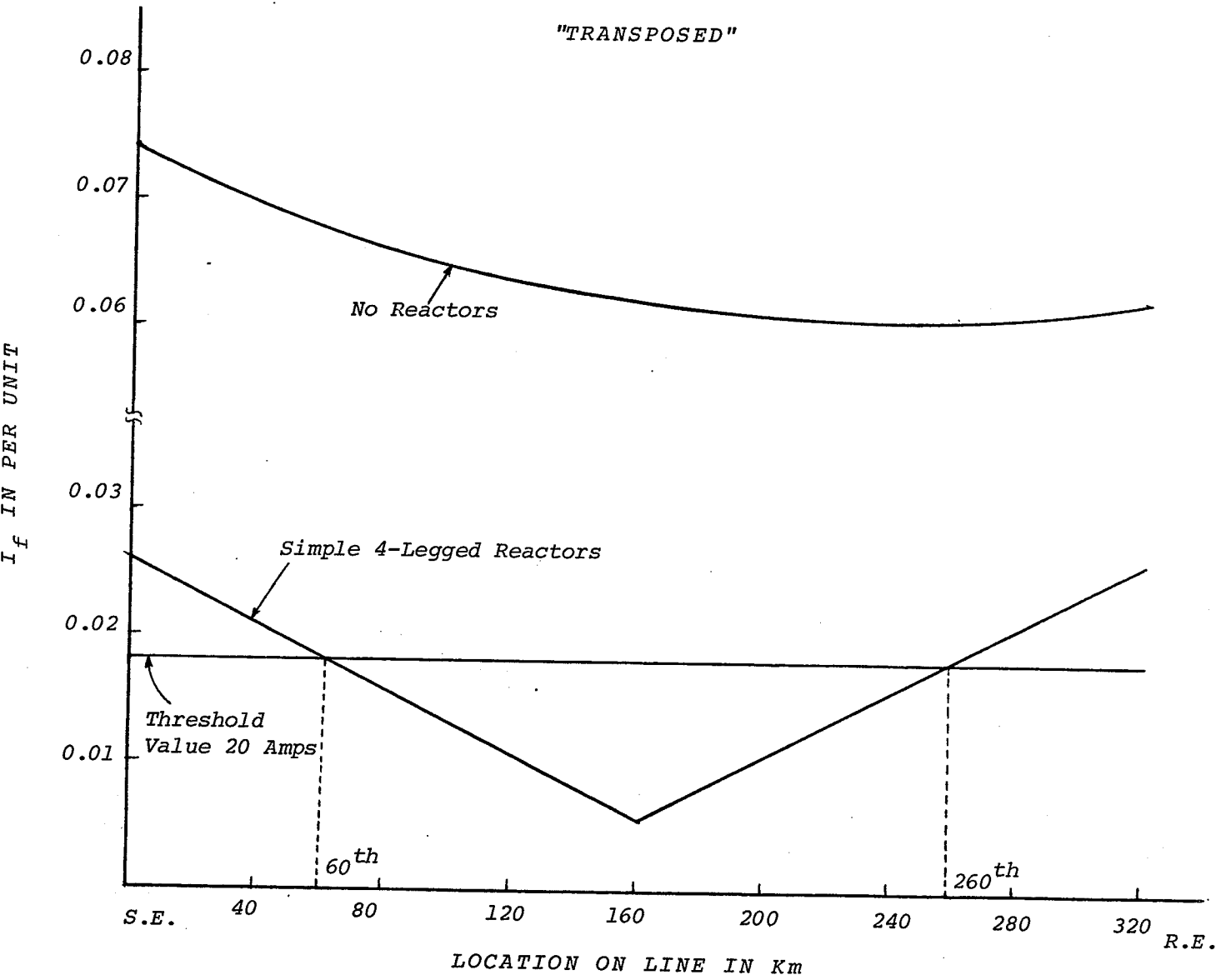


FIG. 5.1 - PROFILE OF  $I_f$ ; BASE CASE

anywhere between 200 and 500 ohms and could be as high as 1000 ohms.

Fig. 5.1 shows the magnitude of  $I_f$  as a function of fault location for the base case. Arc resistance has been assumed to be zero. A line corresponding to 20 amperes (taken as the threshold level of self-sustaining secondary arc current) is also drawn, showing that for a certain portion of the line,  $I_f$ , with optimum values of shunt reactors will be below the threshold value and the fault arc will not be self-sustaining. In this particular case of assumed loading conditions (corresponding to the base case) and other constants, the above described portion of the line lies between the 60th and the 260th kms of the 320 km line.

It may be pointed out that this estimate is on the pessimistic side because in its calculation the arc resistance is completely neglected. Inclusion of arc resistance will reduce the fault current levels everywhere on the line (as seen by the relation  $(I_f = \frac{V_{ff}}{Z_{tf} + R_{ARC}})$  and, therefore, a slightly longer portion of the line will, as a consequence, be under the threshold level for practical transitory fault cases.

#### 5.2.1 Influence of Line Length

Figs. 4.1.11 and 4.1.12 indicate the influence of line length on the maximum values of  $V_{ff}$  under two different conditions. In the first case, power transmitted was held constant at 1.0 p.u., thereby allowing the angle  $\delta$  to increase with increasing line lengths. In the second case  $\delta$  was held at  $25^\circ$

for all line lengths, allowing power transmitted to decrease with increasing line lengths.

In Fig. 4.1.11, it is noted that with 1.0 p.u. loading the maximum value of  $V_{ff}$  increases, almost linearly, as the line length for optimum values of shunt reactors. It can also be seen by relating the Fig. 4.1.1 and 5.1 that the value of  $Z_{tf}$  (fault Thevenin impedance) varies inversely as line length. Therefore, it follows that the maximum value of  $I_f$  will vary, nearly as the square of the line length.

Fig. 4.1.12 shows that after optimization the maximum value of  $V_{ff}$  is linearly constant as a function of line length.\* Once again, the value of  $Z_{tf}$  varies inversely as the line length and hence the maximum value of  $I_f$  varies as line length. In other words, the variation of the secondary arc current along the line length, measured from the minimum case, is a linear function of distance and is independent of the line length. It thus, follows that if a particular value of  $I_f$  is chosen as the threshold value, then for a given  $\delta$ , the kms of line for which  $I_f$  is less than the threshold value is a constant and is independent of total length of line (provided the line is longer than the portion considered above).

---

\* It is not so on shorter line lengths. This is so because the source reactance, which was kept constant for these cases, becomes proportionately larger as compared to the series impedance of the line. It is surmised that had the source reactance been kept at zero, the maximum value of  $V_{ff}$  would be constant for all line lengths.

### 5.2.2 Influence of Power Angle - $\delta$

Fig. 4.1.9 shows that, other parameters being constant, the maximum value of  $V_{ff}$  (under optimized conditions) increases almost linearly with  $\delta$ . As described earlier, this is due to the increasing magnetic coupling effect caused by the increasing currents in the unfaulted phases due to increasing  $\delta$ . It is obvious that, for this case also, the maximum value of  $I_f$  will vary linearly as  $\delta$ . Therefore, for a certain magnitude of  $\delta$  (or line loading),  $I_f$  at the line ends would be just below 20 amperes; and for  $\delta$  increasing beyond this value the portion of line with  $I_f$  below 20 amperes will, progressively, decrease.

Another way of looking at the magnetic coupling effect is to say that it is caused by the differences in the magnitudes of  $\ell_0$  and  $\ell_1$  as well as of  $r_0$  and  $r_1$  for the transmission line. Consider, for example, the transmission line model<sup>22</sup> of Fig. 5.2 (for transposed lines only). With one phase isolated, the currents over the remaining phases are returned via the ground return path. If  $\ell_0$  is equal to  $\ell_1$  and  $r_0$  is equal to  $r_1$  then there is no voltage drop in the return path and consequently it can not cause any voltage differential on the isolated phase conductor. If, at the same time as above,  $c_0$  for the line is equal to  $c_1$  then the isolated phase is completely decoupled from the rest of the circuit, both magnetically and electrostatically. In that case  $V_{ff}$  will be zero under any operating condition, voltage level or set of parameter



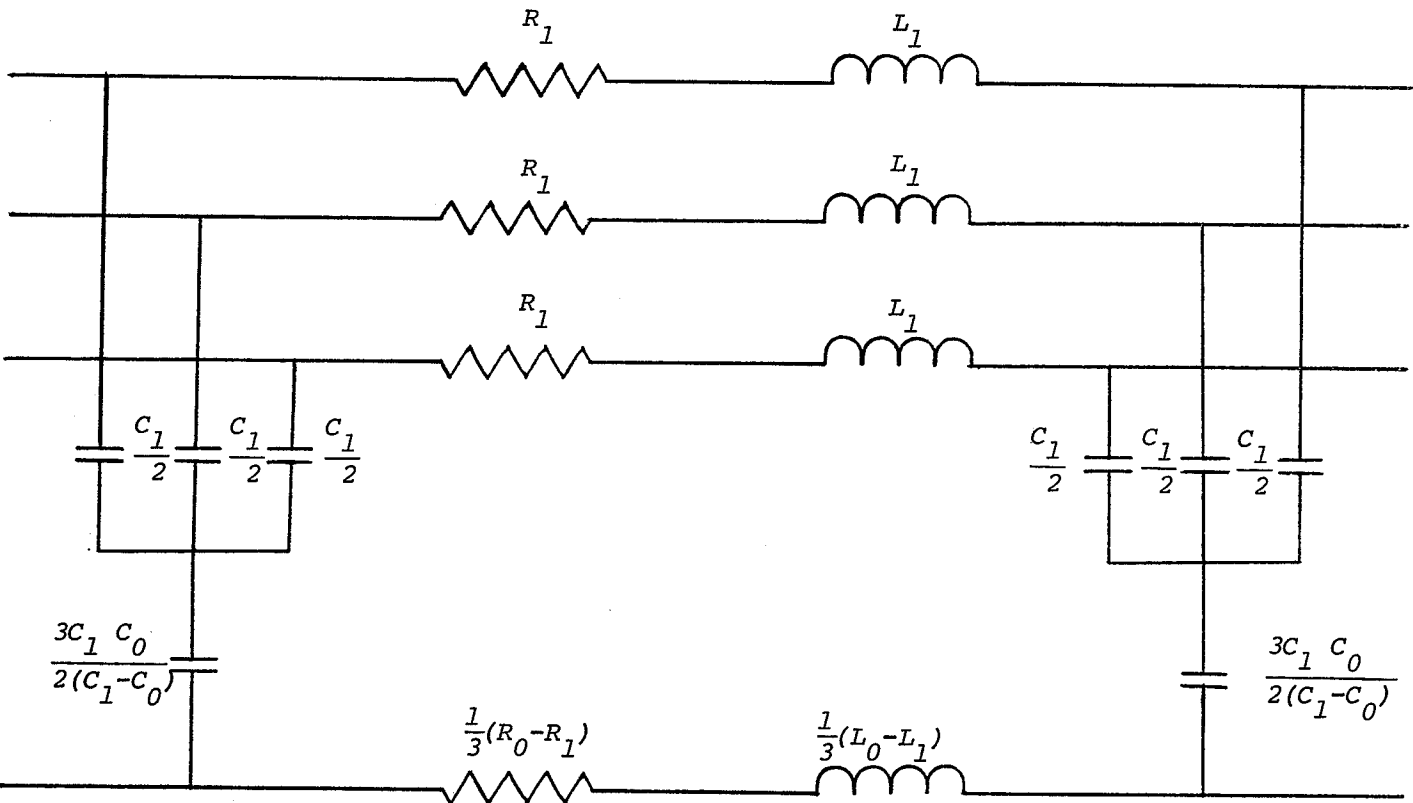


FIG. 5.2 - A  $\pi$  SECTION OF THE TRANSMISSION LINE MODEL

magnitudes. In other words the isolated phase will be really isolated.

Although in practice, it is not possible to make all the zero sequence quantities of the line equal to corresponding positive sequence quantities, any procedure which tends in this direction will reduce the magnitudes of  $V_{ff}$  for a given set of circumstances. The method suggesting the use of ground wires of good conductivity<sup>11</sup>, to reduce  $V_{ff}$ , essentially does that. Use of ground wires reduces  $\ell_0$  and increases  $c_0$  for the line. It will generally increase  $r_0$  unless the ground wires are of very low resistance. Figs. 4.2.3 and 4.2.4 indicate that  $V_{ff}$  decreases as  $\ell_0/\ell_1$  and  $r_0/r_1$  for the line are decreased.

### 5.2.3 Influence of $X_1$ and $X_0/X_1$ Ratio

-----

From Fig. 4.1.3 it is noted that, with shunt reactors (for both transposed and untransposed lines) being optimum, the maximum value of  $V_{ff}$  increases with source positive sequence reactance. Under balanced operating conditions the magnitudes of  $E_{QS}$ ,  $E_{QR}$ , and  $\delta_g$  increase with increasing magnitudes of source  $X_1$  (at constant values of  $V_S$ ,  $V_R$ , and  $\delta$ ). It may be recalled that  $E_{QS}$ ,  $E_{QR}$ , and  $\delta_g$  are assumed to remain constant during the single-phase switching operation. The increasing magnitudes of these three quantities causes the magnitude of the maximum value of  $V_{ff}$  to increase with source  $X_1$ .

The results of a variation of the above study, wherein values of source  $X_0$  are kept constant (rather than ratio  $X_0/X_1$ ), are shown in Fig. 4.2.1. It is noted that the resulting graphs are very similar to those shown in Fig. 4.1.3 (for both type of lines) and for the same reasons, namely, increasing magnitudes of  $E_{\alpha S}$ ,  $E_{\alpha R}$  and  $\delta_g$  with those of source with reactance  $X_1$ . In Fig. 4.2.1, the magnitudes of  $V_{ff}$  are slightly greater than those for the corresponding case in Fig. 4.1.3. This is explained by noting that in the latter case, the magnitudes of source  $X_0$  increases with increasing  $X_1$  while in the former it remains at a constant value.

Another variation, results of which are shown in Fig. 4.2.3, is where unequal values of  $X_1$  are selected for the two sources. Again these results show the same trend of variations which is attributed to the same cause as before.

From Fig. 4.1.5 it is observed that the maximum value of  $V_{ff}$  is linearly constant (decreased slightly) as the source  $X_0/X_1$  ratio increases. It should be noted that these results correspond to constant magnitudes of source  $X_1$  and therefore, constant magnitudes of  $E_{\alpha S}$ ,  $E_{\alpha R}$ , and  $\delta_g$ . It is, then, apparent that with these three quantities remaining constant any minor variations in the coupled zero component circuit due to variations in the magnitude of  $X_1$  will have little effect on the magnitudes of the maximum values (or any values for that matter) of  $V_{ff}$ .

#### 5.2.4 Influence of Ratio $V_S/V_R$

From Fig. 4.1.7 it is observed that the maximum value of  $V_{ff}$  varies by about 20 percent (almost equal for both types of lines) for a variation of the ratio  $V_S/V_R$  (at  $V_R = 1.0$  p.u.) of the same order. From computation, it was noted that as the ratio  $V_S/V_R$  was varied from 0.95 to 1.15,  $E_{\alpha S}$  increased and  $E_{\alpha R}$  decreased while angle  $\delta_g$  increased by less than 2 percent. These changes of voltage are in opposite directions and the relatively small variations of  $\delta_g$  should cause little variation in the magnitudes of the maximum values of  $V_{ff}$ . Variations in the ratio  $V_S/V_R$  of the order of 20 percent causes a corresponding change in the power transmitted over the line and hence the same order of change in  $V_{ff}$  magnitudes.

#### 5.2.5 Influence of Higher System Voltage

Although the entire investigation was carried out using the constants of a transmission line designed for operation at 500 kv, it will be of interest to study the influence of a higher system voltage (say 750 kv) on the magnitudes of  $V_{ff}$ . Assuming that the same system is used for both the voltage levels (500 kv and 750 kv) and that the value of  $\delta$  is unchanged, it can be easily seen that all the magnitudes of  $V_{ff}$  will increase by 50 percent. This will reduce, by one third, the portion of the line where the magnitudes of  $V_{ff}$  are below a certain threshold level. However, it must also be

noted that the amount of power transmitted will increase by 2.25 times. In other words, the increase in the amount of power transmitted, either by increasing the system voltage or by increasing  $\delta$  will be accomplished by increased magnitudes of  $V_{ff}$ . This is because the level of currents in the unfaulted phases will increase, thereby causing increased amounts of magnetic coupling effects. Any increase in the capacitive coupling effects due to an increase in system voltage is always nullified by the shunt reactors.

#### 5.2.6 Influence of Degree of Shunt Compensation

It can be seen from Fig. 4.3.2 that as the compensation factor is increased to 1, the recovery voltage,  $V_{ff}$ , increases drastically even though the secondary arc current is minimum (see Fig. 4.3.1). To compensate the line 100 percent is, therefore, undesirable for many reasons not the least of which are the expense, low voltage under normal load flow and the possibility of a potentially damaging resonance condition. Moreover, high magnitudes of  $V_{ff}$  cause reignition of secondary arc. In other words, magnitude of recovery voltage at the arc location could be quite high making it difficult for the arc to extinguish.

The dependency of maximum secondary arc current,  $I_f$ , on the compensation factor is shown in Fig. 4.3.1. Two other parameters which effect the secondary arc current  $I_f$  maximum are line length  $L$  and  $Q_R$ . Thus, for a given  $L$  and  $Q_R$ , the

the current  $I_f$  maximum decreases with reduction of  $L$ . Recovery voltage  $V_{ff}$  maximum versus  $F$  is shown in Fig. 4.3.2. This voltage correlates to the compensation factor with the trend opposite to the  $I_f$  maximum dependancy on  $F$ , namely,  $V_{ff}$  maximum increases with an increase of  $F$ . Similar to  $I_f$  maximum the recovery voltage,  $V_{ff}$ , depends on line length and  $Q_R$ . Thus for a given  $F$  and  $Q_R$ ,  $V_{ff}$  maximum increases with the line length (see Fig. 4.1.11). So by comparison, it can be concluded that  $I_f$  and  $V_{ff}$  dependencies on  $Q_R$  (for given  $F$  and  $L$ ) are similar.

The voltages, across neutral reactors of four-legged reactor banks (for both transposed and untransposed lines), dictate the insulation requirements for the shunt reactor neutrals as well as for neutral reactors. The maximum steady-state neutral voltages are presented in Fig. 4.3.3.

### 5.3 COMPARISON OF SHUNT COMPENSATION METHODS FOR TRANSPOSED AND UNTRANSPOSED LINES

As has been described earlier, simple four-legged reactors will sufficiently reduce the secondary arc current and recovery voltage on transposed lines, while this is not the case<sup>18</sup> on untransposed lines, because of unequal interphase capacitances. Therefore it was not necessary to try only simple four-legged reactor banks on untransposed lines. Instead, use of a modified four-legged reactor scheme at one end, in conjunction with a simple four-legged reactor at the other end, effectively reduces  $V_{ff}$  and  $I_f$ .

For the purpose of comparison, magnitudes of  $V_{ff}$  obtained from both the methods have been presented, in the form of graphs, in Chapter IV. The significance of the effects of different parameters on  $V_{ff}$  are well described in sections 5.1 through 5.2.6. It is noted that for the given compensation and line length, the magnitudes of  $V_{ff}$ , for the middle phase faults, for untransposed lines are slightly larger than the faults on any phase on transposed lines. It is also clear that the shunt reactor scheme, used for untransposed lines, effectively compensates the capacitive and magnetic coupling effects as compared to that for transposed lines.

#### 5.4 COMPARISON OF SHUNT REACTOR METHOD WITH OTHER METHODS

Other methods<sup>11, 14</sup> discussed for the reduction of recovery voltage are the capacitance method and the method using discharge resistors. Their effect on  $V_{ff}$  is well illustrated in Fig. 4.5.1 through 4.6.2. Referring to the Fig. 4.5.1, it is noted that grounding of the faulted phase through two zero resistances (one at each end) gives the best results as far as minimizing of  $V_{ff}$  is concerned. As the magnitudes of these resistances increase, the magnitudes of  $V_{ff}$  over the entire length of line follow patterns similar to those obtained from other methods. Fig. 4.6.1 gives the same trends for different values of capacitors to be connected across the circuit breakers at both ends of line.

Comparing the base case of the shunt reactor method (Fig. 4.11) with that of capacitance method (Fig. 4.6.1), it

is noted that the maximum  $V_{ff}$  for the latter is slightly larger than that of the first one. The capacitance method and simple four-legged reactor method, for transposed lines, fully compensates the capacitive coupling effects, but none of these neutralize the inductive coupling effects. On the other hand, switchable four-legged reactors used in conjunction with simple four-legged reactors, for untransposed lines, effectively compensates both of these coupling effects.

Above all, the shunt reactors which are, usually, required on EHV lines for the compensation of line charging current, can also be used to reduce  $V_{ff}$  and  $I_f$  in single-pole reclosing, at a additional small cost. In conclusion, the shunt reactor methods, for both transposed and untransposed lines, are very effective in reducing the dead time in single pole reclosing.



## CHAPTER VI

### CONCLUSIONS

The compensation schemes for reducing secondary arc current following single-pole switching have been studied, mainly as a steady state problem. A number of system parameters of representative magnitude were taken into account and their influence on the effectiveness of these schemes was investigated. The results obtained from this study were compared with those obtained from field tests<sup>19</sup> and other digital and transient network analyser studies<sup>17, 20</sup>. Based on the studies in this text, the following conclusions have been drawn:

1) The new scheme of using switchable four-legged reactors together with simple four-legged reactors for untransposed lines, is very effective in reducing secondary arc current and recovery voltage caused by capacitive and magnetic coupling effects.

2) The recovery voltage of a transposed and untransposed transmission system following single-pole switching has been compared. Simple four-legged reactors designed for the transposed line effectively reduce secondary arc current and recovery voltage. If the line is untransposed, only switchable four-legged reactors used in conjunction with simple four-legged reactors, result in suppression of  $V_{ff}$  and  $I_f$ .

3) Shunt reactors which are, generally, required on EHV

lines for compensation of normal charging current, can also be used for suppression of arc current at a small additional cost.

4) The secondary arc current and recovery voltage are determined to be a function of:

- a) Transmission line unbalance;
- b) Transmission line length;
- c) Circuit voltage;
- d) Fault location;
- e) Power system angle;
- f) Source impedance.

5) Successful clearing of transitory line to ground faults would greatly improve the reliability on EHV and UHV transmission lines. It would also be reasonable to rate the transmission capability of single circuit ac tie-lines by their transient stability limits for such faults.

6) Magnetic coupling of the 'two healthy phases - earth return' circuit with the faulted phase also causes voltages on the latter, if the line was loaded before the single-pole switching operation. These voltages are effectively compensated by the use of switchable four-legged reactor scheme. If simple four-legged reactors are used, these voltages still stand out as important.

7) Voltages resulting from the magnetic coupling are proportional to the currents carried by the two sound phases and earth which, in turn, are proportional to the initial

loading of the line. Any variation which tends to increase these currents will also tend to increase the voltages on the faulted phase.

8) Voltages due to capacitive coupling effect are proportional to the difference between the positive and zero sequence capacitances of the transmission line. Voltages due to magnetic coupling effect are proportional to difference between positive and zero sequence inductances of the line. The difference between the positive and zero sequence resistances of the line also produces a voltage on the affected phase if the line is initially loaded. Any method that reduces these differences, either singly or together will reduce the voltage on the faulted phase. Ideally if all these differences were zero then there will be no voltage on the faulted phase once it is disconnected from the two ends.

9) Any variation of the parameters that causes the magnitudes of the machine internal voltages of the two sources, as well as the angle between them, to increase will tend to increase the voltage on the faulted phase due to the coupling. Thus increasing source positive sequence reactance tends to increase the maximum value of the 'fundamental frequency voltage on the cleared conductor' ( $V_{ff}$ ) after minimization.

10) Increasing magnitudes of power angle between the two line ends, under balanced operation, will cause the angle between the machine internal voltages and the magnitudes of line currents to increase. Both of these will tend to increase  $V_{ff}$ .

11) Any increase in the line length, for the same initial line loadings, will cause  $V_{ff}$  to increase. On the other hand, increasing line lengths, for a constant power angle between their ends, will cause  $V_{ff}$  to remain nearly constant.

12) Variation of the source zero sequence reactance to positive sequence reactance ratio, for a constant magnitude of source reactance  $X_1$ , has relatively small effect on the magnitudes of  $V_{ff}$ . Similarly, the variation of the ratio of the sending end to the receiving end voltages of the line for a constant magnitude of the latter has relatively small effect on the magnitudes of  $V_{ff}$ .

13) A deviation of  $\pm 10$  percent from the optimum values of the reactance of the shunt reactors will have practically no effect on their usefulness in reducing  $V_{ff}$ .

14) Magnitudes of  $V_{ff}$  obtained from the shunt reactor methods are lower than those obtained from the capacitance method. Also the secondary arc currents obtained from the former are lower than those obtained from the latter.

15) The method that uses discharge (grounding) resistors is the most effective as compared with other methods when these resistors have zero magnitudes. The proposal of using such resistors, with a magnitude of the order of twice the line surge impedance, to reduce switching surge over-voltages needs examination in the transient domain. However, high magnitudes of resistance may make the extinction of secondary arc difficult.

16) The compensation method of using shunt reactors for reducing dead time is preferred to the method of using discharge resistors or capacitance method as the reactors are usually required on EHV lines.

To sum up, single-pole automatic reclosing may be a reliable technique for maintaining stability on EHV transmission lines during transient single-phase-to-ground faults. The advantage of single-pole operation lies in the fact that power can be transferred over the unfaulted phases during the period when breakers are open to clear the fault. Since most line interruptions do not permanently ground a phase conductor, successful reclosure can be obtained in majority of cases and thus restoring the system to its original condition without any time reducing the power limits to as low a value as would be the case if all three conductors were disconnected. The system can be more reliable, if the transitory SL-G faults are cleared with a dead time as minimum as possible. This dead time can be achieved by using the compensation schemes described in the text.

Obviously, the single-pole auto-reclosing scheme will be more complicated and expensive than the one where 3-pole auto-reclosing is used. However, it is possible in certain cases that the additional gain in transient stability achievable by single-pole auto-reclosing would warrant the attendant increase in the complexity of relaying.

REFERENCES

1. Sporn, P., Prince, D.C., "Ultra High-Speed Reclosing of High Voltage Transmission Lines", AIEE Trans. 1937, pp. 81-90.
2. Sporn, P., Miller, C.A., "Experience with Ultra High-Speed Reclosing of High Voltage Transmission Lines", AIEE Trans. Vol. 58, 1939, pp. 625-636.
3. Sporn, P., Miller, H.N., "Five Years Experience with Ultra High-Speed Reclosing of High Voltage Transmission Lines", AIEE Trans. Vol. 60, 1941, pp. 241-246.
4. Crary, S.B., Kennedy, L.F., Woodrow, C.A., "Analysis of the Application of High-Speed Reclosing Breakers to Transmission Systems", AIEE, Vol. 61, 1942, pp. 339-348.
5. Peterson, H.A., "Appendix III to Reference 4".
6. IEEE Working Group on Arc Deionization Times, "Arc Deionization Times on High Speed Three-Pole Reclosing", IEEE Trans. on Power Apparatus and Systems, Special Supplement, 1963, pp. 236-253.
7. Kimbark, E.W., "Chart of Three Quantities Associated with Single-Pole Switching", IEEE Trans. on Power Apparatus and Systems, Vol. PAS-94, No. 2, March/April 1975, pp. 388-395.
8. Knudsen, N., "Single-Phase Switching of Transmission Lines Using Reactors for Extinction of Secondary Arc", Paper No. 310, CIGRE, Paris, France, 1962.
9. Kimbark, E.W., "Suppression of Ground Fault Arcs on Single-Pole Switched EHV Lines by Shunt Reactors", IEEE Trans. on Power Apparatus and Systems, March 1964, p. 285.
10. Shperling, B.R., Fakheri, A., Ware, B.J., "Compensation Scheme for Single-Pole Switching on Untransposed Transmission Lines", IEEE Trans. on Power Apparatus and Systems, July/August, 1978.
11. Peterson, H.A., Dravid, N.V., "A Method for Reducing Dead Time for Single-Phase Reclosing in EHV Transmission", IEEE Trans. on Power Apparatus and Systems, Vol. PAS-88, No. 4, April 1969, pp. 286-292.
12. Jahn, D., Koettnitz, H., Schulze, H., "Earth Wires as a Means of Improving Single-Pole Rapid Reclosing of Long HV Lines", Paper No. 401, CIGRE, Paris, France, 1964.

13. Miller, M., Gygax, F., Hahn, C., Baltensperger, P., "Protection of E.H.V. Systems Taking into Account Single-Phase Automatic Reclosure on Very Long Lines", *The Brown Boveri Review*, June 1958, pp. 243-253.
14. Heinemann, T., "Single-Pole Rapid Reclosing - Effective Damping of EHV Surges Through Discharge Resistors", *Electrical Review (GB)*, 30 April, 1965, pp. 668-671.
15. Milne, K.H., "Single-Pole Reclosing Tests on Long 275 KV Transmission Lines", *IEEE Trans. on Power Apparatus and Systems*, October, 1963, pp. 658-661.
16. Clarke, Edith, "Circuit Analysis of A.C. Power Systems", Vol. I(Book), Chapter 10, John Wiley and Sons, 1943.
17. Shipley, B., Holley, H.J., Coleman, D.W., "Digital Analysis of Single-Pole Switching on EHV Lines", *IEEE Trans. on Power Apparatus and Systems*, Vol. PAS-87, No. 8, August 1968, pp. 1679-1687.
18. Balser, S.J., Krause, P.C., "Single-Pole Switching - A Study of System Transients with Transposed and Untransposed Lines", *IEEE Trans. on Power Apparatus and Systems*, July/August 1974, pp. 1208-1212.
19. Edward, L., Chadwick, Jr., J.W., Riesch, H.A., Smith, L.E., "Single-Pole Switching on TVA's Paradise-Davidson 500 KV Line Design Concepts and Staged Fault Test Results", *IEEE Trans. on Power Apparatus and Systems*, November/December 1971, pp. 2436-2450.
20. Lambert, S.R., Koschik, V., Wood, C.E., Worner, G., Rocamora, R.G., "Long Line Single-Phase Switching Transients and Their Effect on Station Equipment", *IEEE Trans. on Power Apparatus and Systems*, Vol. PAA-97, No. 3, May/June 1978, pp. 857-865.
21. Dietsch, Ch., (reporter), "Report on the work of the study group on protection and relaying", Paper. No. 327, CIGRE, Paris, France, 1962.
22. Peterson, H.A., "An Electric Circuit Transient Analyser", *General Electric Review*, September, 1939, pp. 394-400.
23. Tarnawecky, M.Z., "ELD, EHV & UHV - AC Transmission Line Design", CLASS NOTES, SEPTEMBER, 1977.
24. Shperling, B.R., Fakheri, A., "Single-Phase Switching Parameters for Untransposed EHV Transmission Lines", *IEEE Trans. on Power Apparatus and Systems*, Vol. PAS-98, No. 2, March/April 1979.

25. Rizk, A.M., "Single-Phase Autoreclosure of Extra-High-Voltage Transmission Line", Proc. IEE, Vol. 116, No. 1, January, 1969, pp. 96-100.
26. Haubrich, H.J. Hosemann, G., Thomas, R., "Single-Phase Auto Reclosing in EHV Systems", Paper No. 31-09, CIGRE, Paris, France 1974.
27. Carlsson, L., Groza, L., Cristorici, A., Necsulescu, D.S., Lonescu, A., "Single-Pole Reclosing on EHV Lines", Paper No. 31-03, CIGRE, Paris, France 1974.
28. Balser, S.J., Eaton, J.R., Krause, P.C., "Single-Pole Switching - A Comparison of Computer Studies with Field Test Results", IEEE Trans. Paper T73-406-6, 1973 Summer Power Meeting.
29. Haun, R.K., "13 Years Experience with Single-Phase Reclosing at 345 KV", IEEE Trans. on Power Apparatus and Systems, Vol. PAS-97, No. 2, March/April 1978, pp. 520-528.
30. Fukunishi, M., Anjo, K., Terase, H., Ozaki, Y., Yano, K., Kawaguchi, Y., "Laboratory Study on Dead Time of High Speed Reclosing on 500 KV Systems", Paper No. 31-03, CIGRE, Paris, France 1970.
31. Amstutz, A., "Residual Currents and Voltages with Single-Pole Rapid Reclosing", The Brown Boveri Review, July/August 1948, pp. 220-225.
32. Cabanes, Dietsch, Divan, "Does the Line Length of Line Limit the Application of Single-Phase Automatic Reclosure in Very High Voltage Transmission Systems?", Paper No. 142, CIGRE, Paris, France, 1954.
33. Maikopar, A.S., "Minimum Time of Automatic Reclosing", Electrical Technology (USSR), 1960, pp. 302-315.
34. Johnson, I.B., et al, "Fault Arc Deionization and Circuit Breaker Reclosing on EHV Lines - Field, Laboratory and Analytical Results", Paper. No. 307, CIGRE, Paris, France 1962.
35. Dommel, H.W., "Digital Computer Solution of Electromagnetic Transients in Single-and Multi-Phase Networks", IEEE Trans. on Power Apparatus and Systems, Vol. PAS-88, No. 4, April 1969, pp. 388-399.
36. Ozaki, Y., "Extinction of Secondary Arc Current in a Single Pole Reclosing Systems", J.IEE (Japan), Vol. 84, p. 909, 1964.



37. General Electric Company, "EHV Transmission Reference Book", Published (Book) in 1968 by Edison Electric Institute, 750 Third Ave., New York, N.Y. 10017.
38. GEC Measurements, "Protective Relays Application Guide", (Book) 2nd Edition, 1975, Produced by Product Support (Graphics) Limited, Derby.
39. Weedy, B.M., "Electric Power Systems", (Book) Second Edition, John Wiley & Sons, 1975.
40. Holley, H., Coleman, D., Shipley, R.B., "Untransposed EHV Line Computations", IEEE Trans. on Power Apparatus and Systems, March 1964, pp. 291-304.
41. Koschik, W., "Report on Single-pole Switching of the Manitoba Hydro to Minnesota Power and Light 500 KV Interconnection", Report No. 76-27, File No. 2-15B3-1, System Planning Division, Manitoba Hydro, Dated September 9, 1976.

APPENDIX A

The expressions for  $V_{ff}$ , under single-phase fault conditions and corresponding reclosing operations for transposed lines, are derived using  $\alpha, \beta, 0$  component representation. The derivations are based on a lumped capacitance model of the transmission line (as in section 2.1) and on the magnitude of the shunt reactors.

RECOVERY VOLTAGE ON THE OPENED PHASE

Single line to ground fault is a case of single-phase switching and reclosing. Conditions for the interconnection of component networks have already been derived for this in Chapter III and are based on Fig. 3.4.1 and Fig. 3.4.2. Using these conditions, the circuits shown in the Fig. A.1 and A.2 can be drawn. The latter is disregarded because the  $\beta$  component does not contribute to the quantities associated with phase A. Solution of the circuit in Fig. A.1. yields the following equations:

$$V_{\alpha} = \frac{\frac{B_0}{2} - \frac{B'_0}{2}}{B_1 - B'_1 + \frac{B_0}{2} - \frac{B'_0}{2}} \cdot E_{\alpha} \quad (A.1)$$

$$V_0 = -\frac{1}{2} \cdot \frac{B_1 - B'_1}{B_1 - B'_1 + \frac{B_0}{2} - \frac{B'_0}{2}} \cdot E_{\alpha} \quad (A.2)$$

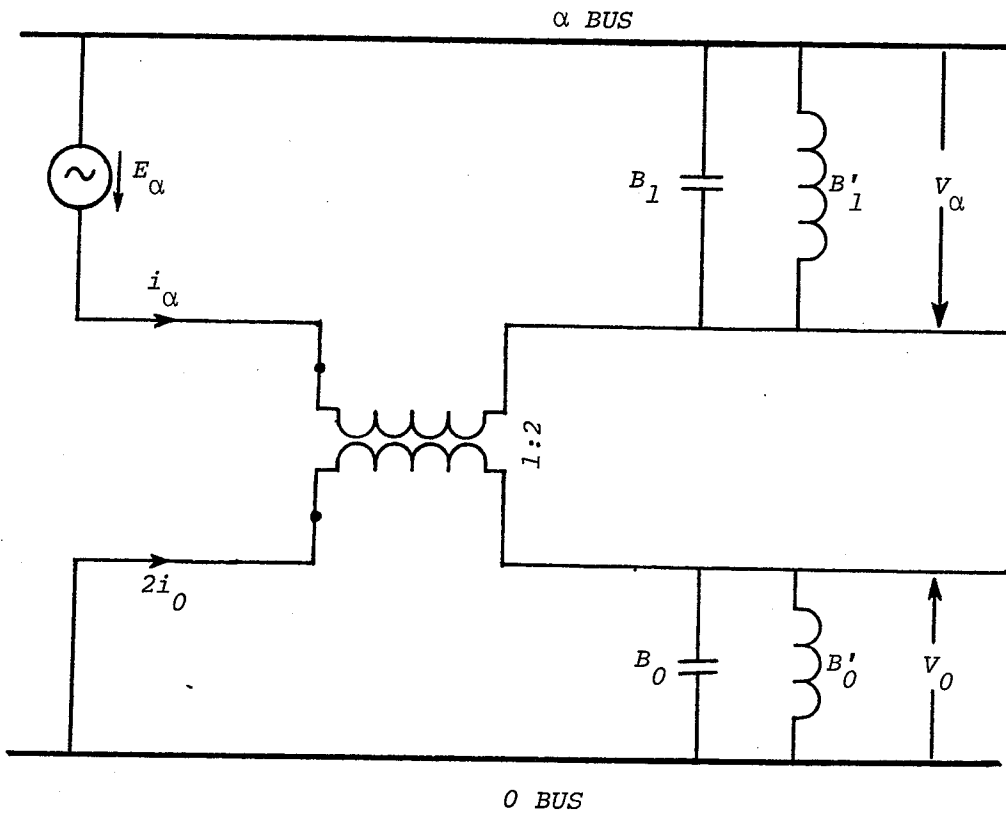


FIG. A.1

(INTERCONNECTION OF  $\alpha$  AND 0 COMPONENT NETWORKS)

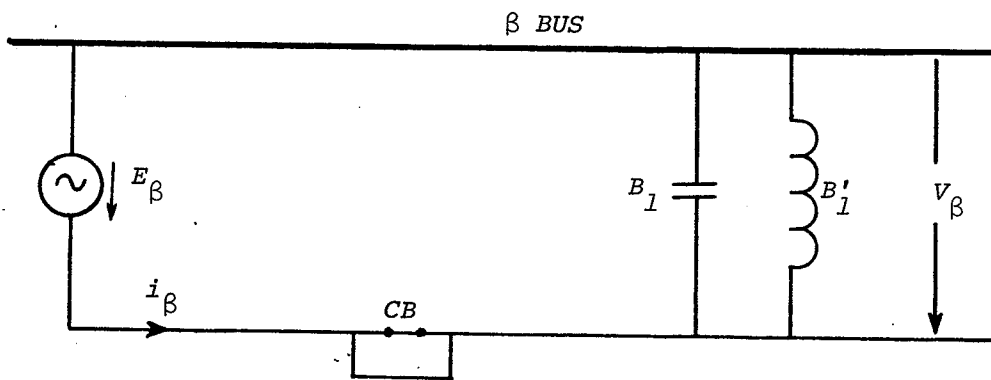


FIG. A.2

( $\beta$  COMPONENT REPRESENTATION)

Therefore,  $V_{ff} = V_{\alpha} + V_0$

$$= - \frac{(B_1 - B_0) - (B'_1 - B'_0)}{(2B_1 + B_0) - (2B'_1 + B'_0)} \cdot E_{\alpha} \quad (A.3)$$

For no shunt compensation  $B'_1 = 0, B'_0 = 0$

$$V_{ff} = - \frac{B_1 - B_0}{2B_1 + B_0} \cdot E_{\alpha}$$

$$= - \frac{C_1 - C_0}{2C_1 + C_0} \cdot E_{\alpha} \quad (A.4)$$

It may be noted that this expression is identical to the equation 2.2

for  $B_1 - B_0 = B'_1 - B'_0$

$$V_{ff} = - \frac{(B_1 - B_0) - (B_1 - B_0)}{(2B_1 + B_0) - (2B'_1 + B'_0)} \cdot E_{\alpha} = 0 \quad (A.5)$$

### Using Capacitors

The circuit of Fig. A.1 can be modified by removing the inductors and connecting the capacitors across the circuit breakers as shown in the Fig. 3.7.1 and 3.7.2. Conditions for interconnection of  $\alpha$  and 0 networks remain the same. From this circuit, following equations can be derived:

$$V_{\alpha} = \frac{\frac{3B}{2} + \frac{B_0}{2}}{B_1 + \frac{3B}{2} + \frac{B_0}{2}} \cdot E_{\alpha} \quad (A.6)$$

$$V_0 = - \frac{1}{2} \frac{B_1}{B_1 + \frac{3B}{2} + \frac{B_0}{2}} \cdot E_{\alpha} \quad (A.7)$$

Therefore

$$\begin{aligned}
 V_{ff} &= V_{\alpha} + V_o \\
 &= \frac{\frac{3B}{2} + \frac{B_0}{2} - \frac{B_1}{2}}{B_1 + \frac{3B}{2} + \frac{B_0}{2}} \cdot E_{\alpha}
 \end{aligned}
 \tag{A.8}$$

for B = 0

$$\begin{aligned}
 V_{ff} &= - \frac{B_1 - B_0}{2B_1 + B_0} \\
 &= - \frac{C_1 - C_0}{2C_1 + C_0} \cdot E_{\alpha}
 \end{aligned}
 \tag{A.9}$$

The above expression is also identical to the equation 2.2

for B =  $\frac{(B_1 - B_0)}{3}$

$$\begin{aligned}
 V_{ff} &= \frac{\frac{3}{2} \frac{B_1 - B_0}{3} + \frac{B_0}{2} - \frac{B_1}{2}}{\frac{3}{2} \frac{(B_1 - B_0)}{3} + \frac{B_0}{2} + B_1} \cdot E_{\alpha} = 0
 \end{aligned}
 \tag{A.10}$$

APPENDIX B

Appendix A deals with fully transposed lines compensated by simple four-legged reactors only. In this appendix, the expressions for  $V_{ff}$  and  $I_f$  are derived for an untransposed line interconnecting two power systems. The line is compensated by a simple four-legged reactor at the sending end, and a modified reactor bank at the receiving end. The system equivalent has been shown in Fig. 3.17.

RECOVERY VOLTAGE ON THE OPENED PHASE

The general expression for the secondary arc current has been derived in Chapter III and is given by equation 3.12.

$$I_{f(i)} = Y_{eq(i,h)} V_a(h) + Y_{eq(i,k)} V_a(k) - Y_{eq(i,g)} \left\{ I_{(h)} X_{(i,h)} + I_{(k)} X_{(i,k)} \right\} \quad (B.1)$$

where

$i$  = faulted phase;

$h$  and  $k$  = healthy phases;

$Y_{eq(i,h)}$  and  $Y_{eq(i,k)}$  = equivalent admittances between faulted and healthy phases;

$Y_{eq(i,g)}$  = equivalent phase to ground admittance at the line terminal opposite to the fault location;

$X_{(i,h)}$  and  $X_{(i,k)}$  = equivalent line mutual reactances between faulted and healthy phases;

$V_{(h)}, V_{(k)}, I_{(h)}, I_{(k)}$  = healthy phase voltage and current vectors in the middle of the line.

The values  $Y_{eq(i,h)}$  and  $Y_{eq(i,k)}$  depend on the phase which is faulted and positions of modified reactor switches. Therefore, considering the admittance matrices given by equations 3.8.1, 3.8.2, 3.8.3 and Fig. 3.17, the equivalent phase-to-phase admittances for phase one fault can be expressed as:

$$Y_{eq(1,2)} = Y'_{2m} + Y_{2s} + Y_{c(1,2)} \quad (B.2)$$

$$Y_{eq(1,3)} = Y_{2s} + Y_{c(1,3)} \quad (B.3)$$

where the subscript "c" denotes line capacitance and "m" and "s" refer to modified and simple four-legged reactor schemes respectively.

Similarly, for a mid phase fault, the equivalent admittances are

$$Y_{eq(1,2)} = Y_{2m} + Y_{2s} + Y_{c(1,2)} \quad (B.4)$$

$$Y_{eq(2,3)} = Y_{eq(1,2)} \quad (B.5)$$

The admittance  $Y_{eq(i,g)}$  for various fault locations is determined by considering equations 3.8.1, 3.8.2, 3.8.3 and Fig. 3.17. Equivalent phase to ground admittances for the faults at sending end are given as:

$$Y_{eq(1,g)} = \frac{1}{2} Y_{c(1,g)} + Y'_{1m} - Y'_{2m} \quad (B.6)$$

$$Y_{eq(2,g)} = \frac{1}{2} Y_{c(2,g)} + Y_{1m} - 2Y_{2m} \quad (B.7)$$

$$Y_{eq(3,g)} = Y_{eq(1,g)} \quad (B.8)$$

Similarly for faults at receiving end, equivalent phase-to-ground admittance are expressed as

$$Y_{eq(1,g)} = \frac{1}{2} Y_{c(1,g)} + Y_{1s} - 2Y_{2s} \quad (B.9)$$

$$Y_{eq(2,g)} = Y_{eq(1,g)} \quad (B.10)$$

$$Y_{eq(3,g)} = Y_{eq(1,g)} \quad (B.11)$$

Recovery voltage can easily be computed by considering the equations B.1 and B.6 to B.11, for different fault locations, and is given as follows:

$$V_{ff(i)} = I_{f(i)} / Y_{eq(i,g)} \quad (B.12)$$

#### LOAD CURRENTS AND LINE VOLTAGES FOR $I_f$ AND $V_{ff}$

The healthy phase currents and voltages at the middle of an untransposed line, interconnecting two systems, are obtained with the following assumptions:

- 1) Line is represented by its equivalent self and mutual impedances.
- 2) Equivalent source impedances for the sending and receiving systems are represented by their positive and zero sequence values.
- 3) The presence of shunt reactors and the opened phases are neglected.
- 4) Voltage at the line terminals are assumed equal to 1.0.



The healthy phase currents  $I_h = i_h \exp.(j\gamma_h)$  and  $I_k = i_k \exp.(j\gamma_k)$  at the middle of line, therefore can be expressed as follows:

$$I_h = \frac{(Z_1 + Z_g)E_h - Z_g E_k}{Z_1(Z_1 + 2Z_g)} ; I_k = \frac{(Z_1 + Z_g)E_k - Z_g E_h}{Z_1(Z_1 + 2Z_g)} \quad (B.13)$$

where

$$E_h = E_{Sh} - E_{Rh} ; E_k = E_{Sk} - E_{Rk}$$

$E_{Sh}$ ,  $E_{Rh}$  and  $E_{Sk}$  = sending end and receiving end system voltages.

$$Z_1 = Z_{S1} + Z_{R1} + Z_L - Z_{h,k}$$

$$Z_g = Z_{Sg} + Z_{Rg} + Z_{h,k}$$

$$Z_{Sg} = \frac{Z_{S0} - Z_{S1}}{3} ; Z_{Rg} = \frac{Z_{R0} - Z_{R1}}{3}$$

$Z_L$  and  $Z_{h,k}$  = line self and mutual impedances.

$Z_{S1}$ ,  $Z_{S0}$  and  $Z_{R1}$ ,  $Z_{R0}$  = equivalent positive and zero sequence impedances for the sending and receiving systems.

Using eq.(B.13) the healthy phase voltages

$V_h = v_h \exp.(j\beta_h)$  and  $V_k = v_k \exp.(j\beta_k)$  at the middle of the line are equal to

$$V_h = E_{Rh} + Z_{ph} I_h + Z_{\Delta} I_k ; V_k = E_{Rk} + Z_{ph} I_k + Z_{\Delta} I_h , (B.14)$$

where

$$Z_{ph} = Z_{L/2} + Z_{R1} + Z_{Rg}$$

$$Z_{\Delta} = Z_{h,k/2} + Z_{Rg}$$

Phase angle difference between healthy phase currents and voltages is given by

$$\alpha_h = \gamma_h - \beta_h$$

and  $\alpha_k = \gamma_k - \beta_k$

APPENDIX C

The digital computer programs to calculate  $V_{ff}$ , are written separately for transposed and untransposed lines. For untransposed lines, the network in the Fig. 3.17 is used. For transposed lines, the program is based on the principle of superposition and uses the network in Fig. 3.3. Input data to the program consists of transmission line constants and the values of the base case parameters (or any variations thereof) are shown in Chapter IV. The programs for transposed lines involve some complicated steps which are described briefly as follows:

STEP 1

Compute the ABCD constants for  $\alpha$  and 0 components of the line from the line constants.

STEP 2

Using  $V_S$ ,  $V_R$ ,  $\delta$ ,  $X_{\alpha S}$ ,  $X_{\alpha R}$  and the ABCD constants of the component, compute  $E_{\alpha S}$ ,  $E_{\alpha R}$ , and the angle between them. The computation assumes balance system operation and, therefore, the switches across the coupling transformers are closed.

STEP 3

Choose values of the shunt reactors (positive and zero sequence inductive reactances of the four-legged reactor scheme) and connect it as shown in Fig. A.1. Express in terms of ABCD constants, the network consisting of the transformer, and the source reactance associated with it for each end of the

line. Now the network in the Fig. 3.3 can be represented in terms of a total of four two-port networks, the other two being the  $\alpha$  and 0 equivalents as determined in Step 1.

STEP 4

For  $E_{\alpha R}$  equal to zero, computes the currents and voltages associated with this network, especially the voltages at the ends of the  $\alpha$  and 0 line components. (It is optional, in this step, to reduce the network to two or one two-port networks with respect to the active source. This will simplify the program for solving the network).

STEP 5

Using the distributed constants approach, compute the voltages  $V_{\alpha}$  at various specified location on the  $\alpha$  line component and voltages  $V_0$  at the corresponding locations on the 0 line component. Add  $V_{\alpha}$  and  $V_0$  to obtain  $V_a$  (voltage of phase A with respect to ground).

STEP 6

Repeat Step 4 for  $E_{\alpha S}$  equal to zero and repeat Step 5.

STEP 7

Add the voltages  $V_{\alpha}$  from Steps 5 and 6 to obtain the total voltage  $V_a$ . Check to see if this is minimum at a specified location on the line, e.g., midpoint. If yes, print the values of  $V_{\alpha}$  and proceed to Step 1 to accept new set data. If not, go to Step 3 and choose another set of values for shunt reactors and continue the process.

*The program for untransposed lines uses the equations derived in Appendix B and the input data is the same as above. The optimum values of simple and switchable four-legged reactor banks have been calculated mathematically and then used in the program directly.*